Mathematical Analysis of Burgers Fluid Flow Induced by an Unsteady Motion

By

Nimra Umbreen

NATIONAL UNIVERSITY OF MODERN LANGUAGES

ISLAMABAD

June, 2024

Mathematical Analysis of Burgers Fluid Flow Induced by an Unsteady Motion

By

Nimra Umbreen

MS MATH, National University of Modern Languages, Islamabad, 2024

A THESIS SUBMITTED IN PARTIAL FULFILMENT OF

THE REQUIREMENTS FOR THE DEGREE OF

MASTER OF SCIENCE

In **Mathematics**

To

FACULTY OF ENGINEERING & COMPUTING

NATIONAL UNIVERSITY OF MODERN LANGUAGES ISLAMABAD

© Nimra Umbreen, 2024

THESIS AND DEFENSE APPROVAL FORM

The undersigned certify that they have read the following thesis, examined the defense, are satisfied with overall exam performance, and recommend the thesis to the Faculty of Engineering and Computing for acceptance.

Thesis Title: Mathematical Analysis of Burgers Fluid Flow Induced by an Unsteady Motion

Submitted By: Nimra Umbreen **Registration #:** 58 MS/MATH/S22

Master of Science in Mathematics (MS)
Title of the Degree

Mathematics
Name of Discipline

Dr. Asia Anjum _____
Name of Research Supervisor Signature of Research Supervisor

Dr. Sadia Riaz _____
Name of HOD (FE&C) Signature of Dean (FE&C)

Dr. Muhammad Noman Malik. _____
Name of Dean (FE&C) Signature of Pro-Rector Academics

June 6th, 2024

AUTHOR'S DECLARATION

I Nimra Umbreen

Daughter of Muhammad Shahid Munawar

Registration # 58/MS/MATH/S22

Discipline Mathematics

Candidate of **Master of Science in Mathematics (MS)** at the National University of Modern Languages do hereby declare that the thesis **Mathematical Analysis of Burgers Fluid Flow Induced by an Unsteady Motion** submitted by me in partial fulfillment of MS degree, is my original work, and has not been submitted or published earlier. I also solemnly declare that it shall not, in future, be submitted by me for obtaining any other degree from this or any other university or institution. I also understand that if evidence of plagiarism is found in my thesis/dissertation at any stage, even after the award of a degree, the work may be cancelled and the degree revoked.

Signature of Candidate

Nimra Umbreen

Name of Candidate

6th June, 2024

Date

ABSTRACT

The aim of this work is to analyze two unsteady motions of incompressible non-Newtonian fluids through a plate channel. Exactly, we examine exact analytical expressions for unsteady, laminar flows of an incompressible Burgers fluid. The porous effects are taken into consideration. Also, we use the assumption that pressure is constant and there is no body force along the direction of the flow. The fluid motion is generated by one of the plates which is either moving in its plane or oscillates in its own plane, and the obtained solutions satisfy all imposed initial and boundary conditions. The exact analytical solutions for dimensionless velocity and associated shear stress are acquired by means of the Finite Fourier Sine Transform (FFST). The starting solutions corresponding to the oscillatory motion of the boundary are presented as a sum of permanent (steady-state) and transient components. These solutions can be useful for those who want to eliminate the transients from their experiments. For a check of the obtained results, their steady-state components are presented in different forms whose equivalence is graphically illustrated. Analytical solutions for incompressible Oldoryd-B, Maxwell and Newtonian fluids performing the same motions are recovered as limiting cases of the presented results. To shed light on some relevant physical aspects of the obtained results, the influence of the material parameters of the fluid motion as well as comparison amongst various models are underlined by graphical illustrations. It is found that the Burgers fluids flow slower as compared to Newtonian fluids. The required time to reach the steady-state is also presented. It is found that the presence of porous medium delays the appearance of the steady-state. It has been observed that the velocity is an increasing function of Burgers fluid parameter and by increasing time the magnitude of velocity is larger for both cases. Moreover, the amplitude of oscillations is larger for the velocity profile without porous medium, but we have seen the opposite effect for the steady state shear stress, for different values of Burgers parameter.

TABLE OF CONTENTS

LIST OF FIGURES

LIST OF ABBREVIATIONS

FFTF	-	Finite Fourier Transform
PDE	-	Partial Differential Equation
ODE	-	Ordinary Differential Equation
MHD	-	Magnetohydrodynamic fluid
EFDM	-	Explicit finite difference method
PINN	-	Physics-informed neutral network
CTFGB-FE	-	Solutions for Time Fractional Generalized Burgers-Fisher Equation
UCM	-	Upper Convective Maxwell
CFD	-	Computational Fluid Dynamic
FRDTM	-	Fractional Reduced Differential Transform Method
BEVC	-	Burgers equation with variable coefficients
SFSBs'E	-	Stochastic fractional-space Burgers' equation

LIST OF SYMBOLS

u , v	-	Velocity components in x and y directions
$\delta/\delta t$	-	Upper convective time derivative
d/dt		Material time derivative
∇		Gradient
ρ		Fluid density
μ	-	Coefficient of dynamic viscosity or viscosity
P	-	Pressure
A	-	Amplitude
λ	-	Maxwell parameter
τ	-	Shear stress
Re	-	Reynolds number
λ_3^*	-	Oldroyd-B parameter
λ_2^*	-	Burgers parameter
$\mathbf{T}$	-	Cauchy stress tensor
T	-	Time
We	-	Weissenberg number
K	-	Porosity parameter
I	-	Identity tensor
$\boldsymbol{V}$	-	Velocity
$\boldsymbol{S}$	-	Extra-stress tensor
U	-	Amplitude of the velocity
A	-	Acceleration
η, η_1, η_2	-	Constants
$u_{Fn}(t)$	-	Finite Fourier sine Transform of $u(y,t)$
r_{1n}, r_{2n}, r_{3n}	-	Roots
r_{4n}, r_{5n}, r_{6n}	-	Roots
r_{7n}, r_{8n}, r_{9n}	-	Roots
$r_{10n}, r_{11n}, r_{12n}$	-	Roots
$\lambda_n, , b_n$	-	Constants
a_n, d_n	-	Constants

ACKNOWLEDGMENT

In the name of the Allah who is most gracious and Merciful. I give thanks to Almighty Allah, the source of all power and knowledge, from the bottom of my heart for leading me on this scholastic path. My tenacity has been built upon his boundless favors. I would want to sincerely thank the Holy Prophet Muhammad (Peace be upon Him) for serving as a constant source of inspiration and guidance and for motivating me to pursue enlightenment and knowledge. I owe a debt of gratitude to my parents **Mr and Mrs Dr. M Shahid Munawar** and my beloved sister **Wajeha Umbreen**. for their constant love, support, and encouragement during my academic career. Being with them has brought me joy and strength, and I am fortunate to have them as my rock. I would especially want to thank my supervisor, **Dr. Asia Anjum**, for all of her help and support during the study process. The result of my thesis has been greatly influenced by her knowledge and mentoring. I would want to thank all of the instructors at NUML, Islamabad, whose expertise and understanding have helped me succeed academically. Every single one of them has been helpful in molding my comprehension. I am appreciative of my sister Wajeha's constant prayers, encouragement, and support. Her confidence in my skills has served as inspiration.

DEDICATION

This thesis work is dedicated to my parents and my teachers throughout my education career who have not only loved me unconditionally but whose good examples have taught me to work hard for the things that I aspire to achieve

CHAPTER 1

INTRODUCTION

1.1 Burgers Fluid

Fluid is a term, in physics which gas, liquid, or other material that flows through external forces or under an applied shear stress basically, these are materials that cannot sustain the impact of any shear force since they have zero shear modulus. There are two types of fluid known as Newtonian and non-Newtonian fluids. The fluid that obeys the Newton's viscosity law, or stress on fluid layers is directly proportional to the share strain rate is known as Newtonian fluid. However, fluids categorized as non-Newtonian fluids are those whose value of viscosity (μ) varies. Liquid crystals, paints, foams, lubricants, and biological fluids are a few examples for such types of fluid. Non-Newtonian fluids, like creep, shear thinning/thickening, yield stress, and relaxation time, show prominent existence from ordinary behavior of fluid. Further, non-Newtonian fluids are divided into rate type fluids which have elastic and memory effects. Here, "memory" refers to the way in which the shear stress is influenced by the relative deformation gradients. These models are employed to explain the behavior of fluids with minimal memory, like diluted polymeric solutions. The ideal model for describing the behavior of various geological materials is the rate-type fluid model, which Burgers developed to explain fluid behavior by Burgers *et al.* [1]. The Burgers model is the one that is most often used to explain how asphalt and asphalt mixtures respond by Lee *et al.* [2]. It is also frequently used to compute the earth mantle's temporary creep property; particularly the post-glacial uplift by Peltier *et al.* [3]. The study examined viscoelastic fluid behavior during accelerated flows using the fractional Burgers model. Both Newtonian and non-Newtonian fluids contributions are revealed by exact solutions, which can be expressed

using generalized Mittag-Leffler functions and applied to the range of fluid models. These discoveries provide useful applications for comprehending the dynamics of viscoelastic fluids under acceleration by Khan *et al.* [4]. The investigation uses fractional calculus and magnetohydrodynamics to examine incompressible Burgers fluid flows in a rotating frame inside porous media. Three examples examine how wall slip affects velocity evolution in various scenarios, offering information that is pertinent to MHD spinning energy producers that use rheological working fluids in real-world settings by Mqbool *et al.* [5].

1.2 Porous Medium

Porous media, like sponges, encourage the simple flow of materials from the soil into engineered structures. Proficiency in capillary action, permeation, and porosity is necessary for fluid dynamics studies, in environmental science and geology. In order to investigate relationships and apply discoveries in filtration systems, oil reservoir management, and flow of ground water, researchers employ mathematical models. Understanding fluid dynamics is crucial for many real-world applications, which requires an understanding of porous media. The later investigations in Nanofluid flow based on water in a porous medium contains particles of copper oxide across a wavy surface. Utilizing the Dupuit–Forchheimer model, showed that while nanoparticle concentration improves convection heat transfer, interactions with the porous structure led to a reduction in transfer of heat. The relationship between nanofluids, porous media, and the kinetics of heat transmission are disclosed by Hassan *et al.* [6]. The magnetohydrodynamics free convective rotating flow over an inclined, accelerated plate in a porous medium is examined in this study along with the effects of ion slip and Hall. The non-dimensional parameter effects using the Laplace transform, which is important for comprehending drag on heated and incline surfaces in seepage flows by Krishna *et al.* [7]. The pressure-driven flow of a water-alumina oxide nanofluid in a wavy path with porous media, taking radioactive electro-magnetohydrodynamics and entropy generation into account. The heat transfer, electromagnetic fields, and fluid flow interact in this channel configuration. Using the conformable derivative, the conformable Swartzendruber models for

non-Darcian flow through porous materials. These models showed good agreement when validated with data on water flow in compacted soils, and sensitivity analyses showed how parameters affect the behavior of the models by Yang *et al.* [10].

1.3 Unsteady Motion

A flow is considered non-uniform if its velocity does not always remain constant. In other words, a flow that is unsteady is one wherein the overall volume of liquid flowing varies with time. Temporary unsteady flow might eventually become zero flow or steady flow. In fluid dynamics, unstable motions introduce dynamic unpredictability that includes changes such as turbulence, periodic oscillations, and transient phenomena. These changes are important for applications in vehicle design, aerodynamics, and biological fluid dynamics. Using modified Bessel equations and Laplace transformation, the study investigates the shear stress and velocity field of a fractional Burgers fluid that oscillates within a circular cylinder. The influence of parameters is examined through numerical simulations, and the agreement between numerical and exact solutions is checked through graphical and numerical comparisons of the results by Raza *et al.* [11]. Using integral transformations and Bessel equations, Burgers fluid with fractional derivatives in a rotating annulus. Comparisons with Tzou's algorithm is used to validate the findings, which show the impact of different parameters on fluid flow patterns by Javaid *et al.* [12]. With applications to various fluid models and calculation of the amount of time required to grasp steady-state, the first steady-state exact expressions for time-dependent shear stresses producing isothermal permanent motion of Burgers fluids which is incompressible across infinite flat plate by Fetecau *et al.* [13]. Using the fractional Burgers model, the non-Newtonian MHD fluids flow (like asphalt) in porous media while taking the environment into account and examining the impact of several factors on temperature, velocity, and concentration distributions by Jiang *et al.* [14]. In convective unsteady Maxwell fluid flow around a stretchable cylinder with Lorentz force. It

finds that buoyancy, convective heat energy, and relaxation time affect fluid motion, and that relaxation phenomena affects thermal and solute energy transport by Wang *et al.* [15].

1.4 Integral Transform

A mathematical integral transform is a kind of map that uses integration to transfer a function across different function spaces, potentially making it easier to characterize and manipulate some of the original function's properties as like the initial function space. The transformed function is normally redirected using the inverse transform to the original function space. Finite Fourier transform is one of the integral transforms, which is useful in fluid dynamics. The Integral transforms to analyze flow characteristics and parameter influences to study the unsteady motion of second-grade fluid in an oscillating duct caused by rectified sine pulses by Zheng *et al.* [16]. The analytical expressions for the steady-state motions of incompressible generalized Burgers fluids with magnetic and porous effects, demonstrating the presence of these effects and the delayed attainment of steady state as well as increased flow resistance by Fetecau *et al.* [17]. Using the derivative of Caputo-Fabrizio fractional and integral transforms to obtain exact solutions, the joint effects of a magnetic field and heat transfer on magneto hydrodynamic two-phase dusty Casson fluid flow between parallel plates, revealing realistic aspects in comparison to the classical model by Ali *et al.* [18]. Using Cattaneo–Christov diffusion theory, the Buongiorno phenomenon, similarity transformations, and finite element analysis, the study creates a model for bio-convection and microorganism movement in a magnetized generalized Burgers nano liquid. The model reveals relationships between temperature, thermal Biot number, and fluid parameters with implications for nanoparticle concentration dispersion by Shahzad *et al.* [19].

1.5 Exact Solution

In fluid dynamics, exact solutions are exact mathematical solutions that satisfy governing equations exactly and provide accurate descriptions of fluid behavior. They are frequently used to validate numerical methods and comprehend basic phenomena. The nonlinear Burgers equation with flexible coefficients (BEVC) using -expansion and Jacobian elliptic functions, discovering new exact solutions with various dynamics, differing from previous studies by Qi *et al.* [23]. The solutions which is steady-state for Burgers fluids incompressible on a flat plate in a porous material with isothermal MHD movements, validating results and showing earlier attainment of steady state when a porous substance or magnetic field is present by Fetecau *et al.* [31]. In study of Burgers fluids transient electro-osmotic flow in a small tube and offers analytical and numerical insights to help solve complex problems involving transient electro-osmotic small tubes and understand its behavior in situations like blood clotting by Raza *et al.* [22]. The non-linear partial differential equations over extended period of time by approximating analytical solutions for Burgers equations using the multistage Homotopy asymptotic method. Numerical comparisons validate this methods superiority over the variational iteration method by Wang *et al.* [21].

1.6 Constantly Accelerated Flow

The fluid's acceleration is constant, which means that the change in velocity per unit of time is constant. Equations in mathematics that come from the concepts of fluid dynamics can be used to explain this phenomenon. For example, equations like Bernoulli's equation or the continuity equation can be used to evaluate the behavior of a fluid in one-dimensional steady flow with constant acceleration. These formulas describe the variations in fluid velocity, pressure, and density along the flow path. It is like realize how air accelerates in a wind tunnel or how a stream of water accelerates as it flows down a hill. Constant accelerated flow principles are fundamental to numerous scientific and engineering applications, ranging from pipeline design to the explanation of fluid behavior in various systems. Investigated accelerated flows in viscoelastic fluids using fractional Burgers' model, obtaining exact

solutions through transforms and revealing Newtonian and non-Newtonian contributions with broader applications to various fluid models by Khan *et al.* [4].

1.7 Oscillating Flow

In fluid dynamics, the term "oscillating flow" describes the recurring motion or variation of fluid particles in a system. When the fluid's velocity, pressure, and other flow characteristics change over time, it exhibits an ongoing and predictable pattern. Oscillatory pipe flow is a typical instance of oscillating flow when a fluid oscillates back and forth within a pipe or channel. External forces or mechanical vibrations applied to the fluid system frequently cause this kind of flow. Mathematical models and equations that consider the oscillation's frequency, amplitude, and phase can be used to explain the behavior of oscillating flow. The fluid particles in this instance are forming a dynamic and cyclic flow pattern by moving to the beat of oscillations. Scientists and engineers can better predict and regulate the behavior of fluids in systems that experience periodic disruptions by studying oscillating flow. For extracting experiment transients, established analytical formulations for steady-state components in oscillatory fluid motions via a rectangular channel with constant dimensionless shear stresses in power-law viscous fluids by Fetecau *et al.* [66].

1.8 Contributions to the Thesis

The review study in this thesis by Fetecau *et al.* [74] is described then the work is extended by considering the Burgers fluid flow with prescribed initial and boundary conditions when a porous material is present. Exact analytical solutions are obtained for two cases, namely, accelerating, and oscillating flow, by using integral transform. The graphical behaviors of different pertinent parameters are obtained by Mathematica and MATLAB software.

1.9 Thesis Organization

The contents of the thesis are briefly summarized in the information below:

Chapter 1 presents an introduction to the thesis and gives an overview of the main concepts and research.

Chapter 2 covers the existing literature and provides the earlier research conducted by scientists using fundamental concepts.

Chapter 3 gives some basic definitions and dimensionless parameters that are applied in the research to obtain exact the flow problem's results.

Chapter 4 provides an extensive description of the mathematical analysis of Maxwell fluid flow induced by an oscillating or continuously accelerating wall through a porous plate channel. To determine the exact solution to the governing flow problem, the finite Fourier sine transform technique is applied.

Chapter 5 expands the review work by considering the impact of Burgers fluid flowing along the direction of flow when a porous material is present between two infinite horizontal plates which are parallel in the case of isothermal flow. To convert the modeled PDE into ODE, finite FFST is employed. Exact analytical solutions are obtained for accelerated and oscillating motion of the boundary. The behavior of different parameters is discussed through graphs.

Chapter 6 gives final views on the whole investigation work and suggests possible implications for this research in the future.

The Bibliography is a list of the references that this thesis consulted.

CHAPTER 2

LITERATURE REVIEW

2.1 Overview

The rate types are those fluids that believe the elastic and memory effects among them. Rate type models are employed to explain the behavior of fluids with minimal memory, like diluted polymeric solutions. Here, "memory" refers to the way in which the shear stress is influenced by the relative deformation gradient's past. The ideal model for describing the behavior of various geological materials is the rate-type fluid model, which Burgers developed to explain fluid behavior by Burgers *et al.* [1]. The Burgers model is the one that is most often used to explain how asphalt and asphalt mixtures respond by Lee *et al.* [2]. It is also frequently used to compute the earth mantle's temporary creep property, particularly the post-glacial uplift by Peltier *et al.* [3].

The study examines viscoelastic fluid behavior during accelerated flows using the fractional Burgers' model. Both Newtonian and non-Newtonian contributions are revealed by exact solutions, which can be expressed using generalized Mittag-Leffler functions and applied to a range of fluid models. These discoveries provided useful applications for comprehending the dynamics of viscoelastic fluids under acceleration by Khan *et al.* [4]. The investigation was made fractional calculus and magnetohydrodynamics to examine incompressible Burgers' fluid flows in a rotating frame inside porous media. Three examples examined how wall slip affects velocity evolution in various scenarios, offering information that is pertinent to MHD spinning energy producers that use rheological working fluids in real-world by Maqbool *et al.* [5]. The later investigated water-based nanofluid movement in a porous medium across a wavy surface with copper oxide particles. Utilizing the Dupuit–Forchheimer model, it showed that while nanoparticle concentration improves convection heat transfer, interactions with the porous structure cause the transmission of heat to decrease. This reveals the nuanced

relationship between nanofluids, porous media, and the dynamics of heat transfer by Hassan *et al.* [6].

The magnetohydrodynamics free convective rotating flow over an inclined, accelerated plate is investigated in a porous media in this research along with the effects of Hall and ion slip. It investigated non-dimensional parameter effects using the Laplace transform, which are important for comprehending drag on heated and incline surfaces in seepage flows by Krishna *et al.* [7]. This research examined the pressure-driven flow of a water-alumina oxide nanofluid in a wavy channel with porous media, taking radiative electro-magnetohydrodynamics and entropy generation into account. The goal of the research is to better understand how heat transfer, electromagnetic fields, and fluid flow interact in this channel configuration. Its research enhanced our comprehension of these phenomena in real-world contexts by Ellahi *et al.* [8].

Using the time-fractional Caputo-Fabrizio derivatives, the research examined incompressible viscous fluid flow while considering the motion of a plane wall in a porous medium under a magnetic field. Laplace and Fourier transforms are used to obtain solutions to the fractional differential equation, which showed the sum of the transient and steady components for sinusoidal oscillations of the plane wall. The research enhances our knowledge of fractional derivative fluid dynamics in intricate situations involving porous media and magnetic fields by Haq *et al.* [9]. Using the conformable derivative, the study showed conformable Swartzendruber models for non-Darcian flow in porous media. The models showed good agreement when validated with data on water flow in compacted soils, and sensitivity analyses show how parameters affect the behavior of the models by Yang *et al.* [10]. Using modified Bessel equations and Laplace transformation, the study investigated the shear stress and the velocity field of a fractional Burgers fluid oscillating in a circular cylinder. The influence of parameters is examined through numerical simulations, and the agreement between numerical and exact solutions is checked through graphical and numerical comparisons of the results by Raza *at al.* [11].

Using integral transformations and Bessel equations, the study examined a Burgers fluid with fractional derivatives in a rotating annulus. Comparisons with Tzou's algorithm is used to validate the findings, which show the impact of different parameters on fluid flow patterns by Javaid *et al.* [12]. With applications to various fluid models and the amount of time to attain

stable condition estimation, the study presented for time-dependent shear stresses the first exact steady-state solutions producing isothermal permanent movements of incompressible Burgers fluids across an infinite flat plate by Fetecau *et al.* [13]. Using the fractional Burgers model, the research investigated the MHD non-Newtonian fluids flow (like asphalt) in porous media while taking the environment into account and examining the impact of several factors on temperature, velocity, and concentration distributions by Jiang *et al.* [14].

The flow of mixed convective unsteady Maxwell fluid flow around a stretchable cylinder with Lorentz force was examined that buoyancy, convective heat energy, and relaxation time affect fluid motion, and that relaxation phenomena affects thermal and solutal energy transport by Wang *et al.* [15]. The study of Fourier sine and Laplace transforms to analyze flow characteristics and parameter influences to investigate the second-grade fluid's unsteady motion in an oscillating duct caused by rectified sine pulses by Zheng *et al.* [16]. The research examined precise analytical solutions for the steady-state incompressible motions of generalized Burgers fluids with porous and magnetic effects, demonstrating the presence of these effects and the delayed attainment of steady state as well as increased flow resistance by Fetecau *et al*. [17].

Using the Caputo-Fabrizio fractional derivative and transforms to obtain exact solutions, the research investigated heat transfer's combined effects and a magnetic field on magnetohydrodynamics two-phase dusty Casson fluid flow between parallel plates, revealing realistic aspects in comparison to the classical model by Ali *et al.* [18]. Using Cattaneo–Christov diffusion theory, the Buongiorno phenomenon, similarity transformations, and finite element analysis, the study investigated a model for bio-convection and microorganism movement in a magnetized generalized Burgers nano liquid. The model revealed relationships between temperature, thermal Biot number, and fluid parameters with implications for nanoparticle concentration dispersion by Shahzad *et al.* [19].

The study inspected Burgers' steady-state solutions for incompressible fluids moving in an isothermal MHD manner in a porous material on a flat plate, verifying results and showing earlier attainment of steady state when a magnetic field is present or porous medium by Fetecau *et al.* [20]. Moreover, the non-linear partial differential equations over extended periods of time by approximating analytical solutions for Burgers equations using the multistage Homotopy asymptotic method. Numerical comparisons validate this method's

superiority over the variational iteration method compute by Wang *et al.* [21]. The research explores Burgers fluids transient electro-osmotic flow in a small tube and offers analytical and numerical solution to solve complex problems involving transient electro-osmotic small tubes and understand its behavior in situations like blood clotting by Raza *et al.* [22].

The (BEVC) using expansion and Jacobian elliptic functions, discovering new exact solutions with various dynamics, differing from previous studies performed by Qi *et al.* [23]. By transforming the PDE into an ODE and contrasting the outcomes with alternative solution techniques, the Power Index Method is used to present new, exact solutions for Burger's equation in this research by Amad *et al.* [24]. The KdV–Burgers equation and Lie group analysis are used in this article to derive new and more general exact solutions, including arbitrary functions and constants, for the investigation of ion acoustic waves in a plasma. Their physical implications are discussed, and numerical simulations are included by Tanwar *et al.* [25].

Through theoretical and numerical analyses, the accuracy and stability of the upwind, Lax–Friedrichs, and Lax–Wendroff schemes in solving the inviscid Burgers equation were examind by Koroch *et al.* [26]. The study examined the $(1 + 1)$-dimension Lie symmetry analysis and the modified Kudryashov method applied to the Boussinesq–Burgers system to extract different wave solutions for describing shallow water waves with physical interpretations by Kumar *et al.* [27]. With consideration for shear stress along the boundary, the study offers precise analytical solutions for the magnetohydrodynamic incompressible motions over an infinite plate of generalized Burgers fluids. Numerical and graphical analyses are used to verify the findings by Fetecau *et al.* [28]. Burgers equation is used to investigate longitudinal dispersion in porous media; new integral transform and Homotopy perturbation technique are used for analytical solutions. The longitudinal dispersion phenomenon shows that concentration drops with distance at fixed times and somewhat rises with time inspected by Kunjan Shah *et al.* [29]. The extended generalized–expansion method uncovers new exact solutions for the modified Korteweg–de Vries and Burgers equations, providing insights into diverse applications and dynamic behaviors by Mohanty *et al.* [30]. By modifying Darcy's rule, the research investigates the unsteady MHD rotational flow of a generalized Burgers' fluid pass through moving plate through a porous media. The fluid decelerates as the porosity parameter (K) grows, and Hartmann number (M) according to the results. In contrast, a large Hall parameter (m) modifies the velocity profile by increasing the imaginary component and

decreasing the real part by Khan *et al*. [31]. Computational fluid dynamics (CFD) for aeronautical design could be revolutionized by quantum computing, which overcomes the limitations of classical computing and demonstrates efficiency and accuracy in simulations, especially for the complex Burgers equation by Oz *et al.* [32]. To provide unconditional convergence and stability in a semi-discrete scheme, this study presented the two-dimensional Burgers-type equation numerically a localized mesh less collocation method. This is followed by a spatial approximation using a local radial basis function partition of unity (LRBF-PU) by Li *et al.* [33].

Adem *et al.* [34] examined a coupled Burgers system in fluid mechanics that is extended (2 + 1)-dimensional. It finds new exact solutions using the Kurdyshov and Lie symmetry techniques, which have wide-ranging applications in science. Biesek *et al.* [35] studied the Burgers equation effectively using Physics-Informed Neural Networks (PINNs) with implicit Euler transfer learning, showing accuracy with lower computational costs thanks to smaller neural network architecture. A general semi-analytical solution for the non-integrable damped KdV-Burgers-Kuramoto equation is achieved, providing insight into the propagation of non-stationary dissipative waves in a variety of natural phenomena by Aljahdaly *et al.* [36].

FRDTM is utilized to investigate The Burger-Fisher equation with time fractional modifications. Its validity and accuracy are established by means of a comparison with exact solutions for varying fractional order values by Tamboli *et al.* [37]. Complex singularities are found developing the shape of an eye around the origin in the temporal domain of the in viscid Burgers equation, indicating their relevance well in advance of the pre shock time; singularity theory and an asymptotic analysis are used to address the observed tyger phenomenon, and two strategies are proposed to mitigate its effects: iterative UV and tyger purging completion by Rampf *et al.* [38].

Using various fractional derivatives and an implicit upwind scheme, Doley *et al.* [39] investigated the time-fractional Burgers equation numerically. It compared with exact solutions and other fractional models and validates against stability and convergence. With consideration for magnetohydrodynamics and radiation the Caputo-Fabrizio fractional derivative to analyze the heat transformation in second-grade unsteady incompressible fluid. Accurate analytical solutions were obtained, and the effects of different physical parameters are explored through graphical illustrations investigated by Sehra *et al.* [40].

The nonlinear forced Zakharov-Kuznetsov equation is derived in the paper using perturbation expansion and multiple scales methods. Multiple kink solutions are then obtained using a variety of mathematical techniques, and their features—such as interaction behavior and external source influence—were examined by Yin *et al.* [41]. In the context of the 1D viscous Burgers' equation, the study suggested a Neural Network-based method to accelerate high order discontinuous Galerkin methods. By applying corrective forcing terms to low order solutions, the method achieves high accuracy with reduced computational costs. Error bounds are analyzed for various scenarios, meshes, polynomial orders, and viscosity values by de Lara. *et al.* [42].

Using the -expansion method, the study investigated the stochastic fractional-space Burgers' equation (SFSBs'E) with noise with multiplicative properties. It has provided analytical solutions and, through graphical representations, sheds light on the influence of stochastic terms on solution stability by Al-Askar *et al.* [43]. Explicit finite difference method (EFDM) and physics-informed neural networks (PINN) are used to solve the Burgers equation; the results are compared with analytical solutions. Both approaches demonstrate good agreement, but EFDM aligns more closely with analytical solutions, suggested that it is a competitive method for simulating nonlinear phenomena in a variety of fields, including gas dynamics, flood waves, chromatography, and traffic flow. According to the research, these methods were useful for creating numerical models of various nonlinear partial differential equations by Savović *et al.* [44].

Different unidirectional kink and peakon-like solutions are found when analytical solutions for the Time Fractional Generalized Burgers–Fisher Equation (CTFGB-FE) are investigated using the Exponential Function and Exponential Rational Function methods. Visual representations shed light on how these solutions behave by Ramya *et al.* [45]. The study analyzed the analysis is to combine Newtonian and non-Newtonian forms to find analytical solutions for magnetohydrodynamics (MHD) of a generalized Burger's fluid in a porous media. The paper offers compact series solutions for the velocity field and shear stress using integral transforms and uses graphical examples to analyze the effects of permeability, magnetism, and rheological factors inspected by Alotaibi *et al*. [46] and Abro *et al.* [47].

Using the generalized-improved and generalized approaches, exact solutions for the Schamel Burgers equation that produce shock-type waves are obtained, examined using Mathematica-12, and visually displayed by Mohanty *et al.* [48]. Due to numerous applications in science and engineering, there have been numerous studies on the flow of viscous fluids among parallel plates investigated. Exact results for these motions are having in book by Schlichting *et al.* [49] and Wang *et al*. [50, 51]. Exciting solutions for Couette flow which is unsteady, the unsteady generalized flow which is Couette and the unsteady flow of Poiseuille of the viscous, incompressible fluids (a Poiseuille flow layered on the simple Couette flow) has also been established by Erdogan *et al*. [52].

Still, for the velocity field the initial exact solutions that corresponds to the non-Newtonian incompressible fluids' motions, or second-grade fluids, lies between two parallel plates appear by Rajagopal *et al*, [53] and Siddiqui *et al.* [54], when a plate moves or oscillates inside its plane. Wang *et al.* [55] and Sun *et al.* [56] has established systematic formulations for the two oscillatory motions of incompressible Maxwell fluids' steady-state solutions via a tube has a right triangular cross section that is rectangular/ isosceles Wenchang *et al.* [57], and Qi *et al.* [58] has made numerous modifications of earlier Maxwell fluid fractional solutions.

The study focuses on how velocity in the MHD flow of a Burgers' fluid through a porous material in a circular channel is affected by the time-dependent pressure gradient. Bessel and modified Bessel functions are used to construct analytical solutions, and the research examines the impacts of various factors using visual aids and discussions of specific instances by Safdar *et al*. [59]. However, research on these flows through porous surfaces is crucial in a variety of fields, including technology and the natural sciences. Al-Hadhrami *et al.* [60], has presented a numerous investigation of viscous fluid flow via plate channels of porous medium, although flow in steady convection between parallel surfaces that are inclined has been examined by Cimpean *et al.* [61].

The effects of porous on some incompressible viscous fluids' unstable simple Couette flow have been estimated by Kesavaiah *et al.* [62]. A numerical representation has been made of the impact of imperfections at the border on non-isothermal flow of fluid in a narrow media-filled channel by Maruši´c-Paloka *et al.* [63]. In a recent study, Ehlers *et al.* [64] proved that, although all situations in their field can be solved using the expanded equations, the classical equations were only valid under specific limits, even though the classical equations are

essential for motions across porous media. Fetecau *et al.* [65] has published on an extensive investigation of the unstable Viscose fluids move hydromagnetically via a porous medium between endless plates which is horizontal parallel. Further exact solutions have been found for the identical fluids' oscillatory movements among two infinite plates that are parallel to each other by Fetecau *et al.* [66] and Danish *et al.* [67] as limited examples of certain outcomes for fluids whose viscosity is depending on pressure. This study investigated unstable movements of incompressible UCM fluids across a plate channel, including porous effects. Shear stress and dimensionless velocity fields have analytical solutions established, and they are compared to incompressible Newtonian fluids. The findings demonstrate that a permeable media's presence postpones the achievement of steady-state and that flow of Maxwell fluids more slowly by Fetecau *et al.* [74].

CHAPTER 3

Fundamental and Basic Definitions

3.1 Fluid

A substance is referred to as fluid if it can flow and take on the shape of its container. It is described as a condition of matter that is different from gases and solids. Liquids like water, milk, or oil as well as gases like air or helium, can be considered fluids. One of the special qualities of fluids is their hydrostatic pressure, which is the capacity to apply pressure uniformly in all directions. Additionally, they display viscosity, or flow resistance. There are nineteen distinct fluids with varying viscosities; some are more "thick" or high viscosity, while others are more "thin" or low viscosity. Fluids react and interact with forces as they pass through objects or pipelines, for example, according to fluid dynamics. This area of research includes the conservation of mass, energy, and momentum, Bernoulli's, and turbulence principle. Fluids are used in many aspects of daily life and many different businesses, such as engineering, transportation, weather forecasting, and medical. Besides numerous other processes, they are essential to blood circulation, hydraulic systems, cooling systems, and weather patterns. Liquids are a common type of fluid that lacks an ongoing shape but has a certain volume. They flow smoothly and are nearly incompressible, taking the shape of the container. Examples are oil, liquids, and blood. Another kind of fluid that has both a defined shape and volume is a gas. They may expand to fill their vessel and are incredibly compressible. Examples of gases are air, carbon dioxide, and helium. Interesting behaviors of fluids include viscosity, surface tension, and fluid flow. These characteristics are essential in many fields of research and engineering, such as materials science, thermodynamics, and fluid dynamics science [49].

3.2 Fluid statics

The well-known area of fluid mechanics that deals with fluids that are not moving but is instead at rest. Another name for it is pressures and hydrostatics while stationary. The hydrostatic equation, which connects a fluid's pressure at a given depth to its weight above that depth, is another crucial idea in fluid statics. The formula, which derives from the mass conservation law, can be used to determine the pressure in a fluid at any depth. There are numerous real-world uses for fluid statics, including the design of water tanks, dams, and other structures that store or move fluids. In the medical field, it is also employed for tasks like blood pressure monitoring and IV fluid infusion rate monitoring [49].

3.3 Fluid kinematics

A vital area of fluid mechanics, which examines fluid motion unaffected by external factors. Its focus is on characterizing and evaluating fluid flow properties like acceleration, deformation, and velocity. The motion of a fluid particle is one of the main ideas in fluid kinematics. A tiny amount of fluid that flows with the fluid flow is called a fluid particle. Understanding the features of the fluid flow such as its acceleration and velocity, can be obtained by monitoring the motion of the fluid's constituent particles. The description of fluid flow geometry, such as the size and form of fluid elements as they pass through a flow field, is also related to fluid kinematics. This is crucial for examining the actions of fluids in many applications, including hydraulic system design and ocean current research [49].

3.4 Fluid dynamics

The study of fluids in motion or at rest is known as fluid dynamics. This important area of study has applications in many different industries, including for example, mechanical, chemical, environmental, and aeronautical engineering, meteorology, and geophysics. The

aim of the goal of fluid dynamics research is to clarify the characteristics of fluids, including their pressure, viscosity, and density, as well as how they respond to external forces like gravity or fluid flow. Important ideas related to fluid dynamics include the Reynolds number, turbulence, boundary layers, and the Navier-Stokes equations. Fluid dynamics is used in everything from spacecraft and airplane design to weather patterns and ocean current research. The movement of water and blood through the human body via channels and pipes, and the movement of fluids in turbines and engines are a few typical instances of fluid dynamics at action [49].

3.5 Types of Flow

3.5.1 Steady Flow

When the fluid characteristics in the system are constant across time at any given place, it is referred to as steady flow. In other words, the flow parameters, such as velocity, pressure, and temperature, remain constant at a particular location over time. Imagine a river with a constant, unchanging flow rate. If you pick a specific point in the river and observe the water properties over time, you'll find that they don't vary.

3.5.2 Unsteady Flow

Unsteady flow, on the other hand, is when the fluid properties at a given point change with time. The flow parameters are not constant, and there are variations over time. Picture a sudden surge of water in a river, causing the velocity and pressure at a particular spot to change rapidly. This dynamic behavior characterizes unsteady flow.

3.5.3 Laminar flow

The term "laminar flow" describes the orderly, smooth travel of fluid molecules that follow parallel, straight streamlines. It is sometimes referred to as streamline or viscous flow and is usually seen in thin pipelines with minor fluid velocity and high viscosity. Laminar flow comes with various forms, such as pulsatile, unidirectional, and oscillatory flow. Some instances of this kind of flow include the flow of blood through capillaries, the flow of oil via thin tubes, and the upward, straight-line passage of smoke from a stick. But as the smoke reaches a particular altitude and starts to deviate from its intended course, it turns into a turbulent flow.

3.5.4 Turbulent Flow

The irregular movement of the fluid particles in this kind of flow leads to the production of waves, which significantly waste energy. Large-diameter pipes with high fluid velocities of thirty are usually the sites of this type of flow, which is characterized by continuously shifting fluid speeds and directions. Turbulent flow analysis is frequently done using fluid dynamics (FD) analysis. CFD, or FD, is a subfield of fluid dynamics that addresses problems involving turbulent fluid flows using numerical analysis and algorithms. The non-dimensional Reynolds number is used to identify the kind of flow in pipes.

3.5.5 Incompressible Flow

The density of the fluid remains constant regardless of changes in pressure for incompressible flow. This means that the volume of the fluid elements doesn't change significantly, even when subjected to variations in pressure or temperature. Liquids like water are often considered incompressible under normal conditions. In scenarios where the flow speeds are relatively low, and the pressure changes are not extreme, the density remains nearly constant, simplifying the fluid dynamics equations.

3.5.6 Compressible Flow

The density of the fluid can change in response to variations in pressure and temperature for compressible flow. This usually occurs at high speeds or in situations where there are significant changes in pressure. As an example, when an aircraft moves at high speeds, the air around it experiences changes in pressure and temperature, leading to variations in density. Compressibility effects become important in such scenarios. Compressible flow is crucial in aerodynamics, supersonic and hypersonic flows, and other applications where the speed and pressure changes are significant.

3.5.7 Transient Flow

Transient flow in fluid dynamics refers to fluid motion where the properties like velocity and pressure vary with time at a specific location within a system. Unlike steady flow, which implies constancy, transient flow captures the dynamic changes occurring, such as during start-ups or abrupt alterations in system conditions. Picture turning on a tap—initially, the water flow isn't immediately constant, but undergoes adjustments until it stabilizes. Understanding transient flow is pivotal in engineering for predicting fluid behavior during dynamic events and ensuring system stability under changing conditions.

3.6 Stress

The pressure or internal forces that are applied within an object or material are referred to as stress in relation to mechanics and physics. It measures the body's resistance to deformation or shape change. Both internal forces within the material itself and external forces applied to an object can generate stress. Usually, stress is expressed in terms of its direction and amplitude. The orientation of the internal forces within the material is indicated by the direction of stress. Stress can take many different forms, such as shear, compressive, and tensile stress. In

disciplines like engineering, materials science, and structural analysis, stress is an important idea. The concept of stress management in materials and structures is essential to the design of dependable and safe systems. Stress in mathematics is shown by

$$\sigma = \frac{Force(F)}{\text{Area(A)}}, \tag{3.1}$$

where A, σ, and F are the area of the force application, stress applied and force applied, respectively. The stress units in SI units are N/m^2 [49].

3.6.1 Tangential and Normal Stress

Tangential stress is the force that is parallel to or operating along a surface. The best illustration of tangential stress is shear stress operating on the fluid. When a force acts perpendicular (or "normal") to the surface of an object is known as normal stresses [72].

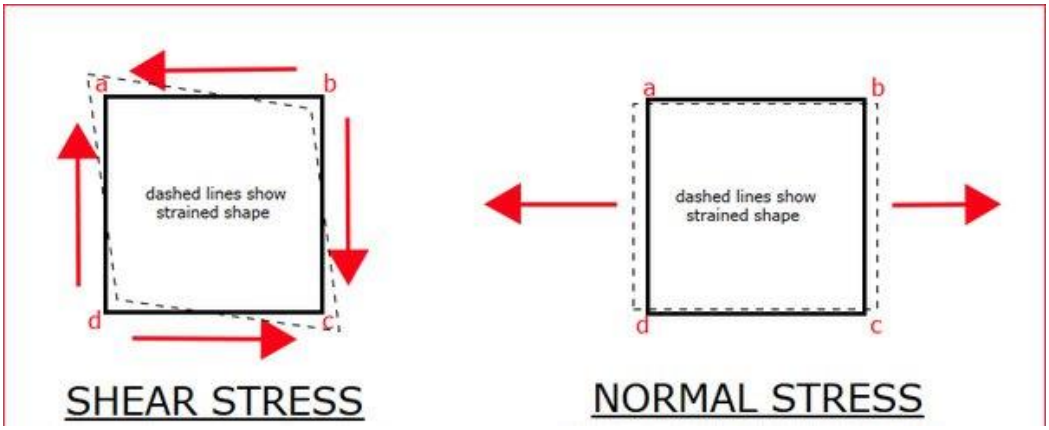

Figure 3.1: Normal and shear stresses

3.6.2 Strain

Measured as the proportion of the body's deformation to its original size, strain represents the amount that a force applied causes a body to deform in that direction.

$$Strain\ (\epsilon) = \frac{\text{Change in length}(\delta l)}{\text{Original length}(L)}, \tag{3.2}$$

where ϵ, L and δl is the strain produced on by the applied tension, the material's original length, and its length change, respectively [49].

3.7 Viscosity

A fluid's (gas or liquid) resistance to shape change or the relative movement of neighboring parts is known as viscosity. There are two ways to relate viscosity follows:

3.7.1 Dynamic viscosity

When an external force is applied the fluid's resistance to flow is known as its dynamic viscosity.

$$\mu = \frac{\text{shear stress}}{\text{velocity gradient}}. \tag{3.3}$$

The SI unit for dynamic viscosity is Ns/m^2 or can be stated as kg/ms [49].

3.7.2 Kinematic viscosity

Kinematic viscosity is defined as a liquid's absolute viscosity divided by its density at the same temperature, i.e.,

$$\nu = \frac{\mu}{\rho}. \tag{3.4}$$

The unit of measurement for kinematic viscosity in SI is m^2/s [49].

3.8 Types of Fluid

3.8.1 Newtonian Fluid

According to Newton's law of viscosity, shear stress, "is linearly proportional to the rate of angular deformation velocity gradient." Fluids that follow Newton's law of viscosity are referred to as Newtonian fluids. In mathematics,

$$\tau \propto \frac{du}{dy} \quad \text{or} \quad \tau = \mu \frac{du}{dy}, \tag{3.5}$$

where τ denote applied shear stress to a fluid element, μ is called absolute or dynamic viscosity known as proportionality constant. The motion of fluid is represented by Navier-Stokes equations. For Newtonian fluids, the Cauchy stress tensor $\boldsymbol{T}$ meets the following relationship,

$$\boldsymbol{T} = -p\,\boldsymbol{I} + \boldsymbol{A_1}, \tag{3.6}$$

where, I is identity tensor, p is hydrostatic pressure, $\boldsymbol{A_1}$ is first Rivlin-Ericksen tensor and μ is fluid dynamic viscosity defined by

$$\boldsymbol{A_1} = \text{grad}\,\boldsymbol{V} + (\text{grad}\,\boldsymbol{V})^{\intercal}, \tag{3.7}$$

where ⊺ denotes the transpose and **V** is the velocity vector**.**

3.8.2 Non-Newtonian Fluid

Any fluid that defies Newton's law of viscosity is considered a non-Newtonian fluid. When the connection between the applied shear stress and the rate of shear strain is nonlinear, the fluid is referred to be non-Newtonian. Mathematically,

$$\text{Shear Stress} = k\left(\frac{dV}{dy}\right)^{n}, \qquad n \neq 1 \tag{3.8}$$

where k is the consistency index and n is the flow behavior index.

3.8.2.1 Classification of non-Newtonian Fluids

3.8.2.1.1 Time Independent

A non-Newtonian time-independent fluid's viscosity depends on both temperature and shear rate. The following explanations of the flow behavior are based on how viscosity varies with shear rate:

Shear thinning: as shear rate increases, viscosity drops like paint, shampoo, slurries, fruit juice concentrates, ketchup etc.

Shear thickening: when the shear rate is raised, the viscosity rises like wet sand, concentrated starch suspensions.

3.8.2.1.2 Time Dependent

Fluids whose behavior may change over time are known as time dependent non-Newtonian fluids. If the rate of shear strain remains at the same level, shear stress may vary., and vice versa. The fluid is referred to as thixotropic if when the fluid is sheared, the shear stress gradually decreases, and rheopectic if the opposite effect occurs. For example,

Thixotropic: yoghurt, paint

Rheopectic: gypsum paste

Figure 3.2: Paint

Figure 3.3: Yoghurt

Figure 3.4: Gypsum paste

3.8.2.1.3 Viscoelastic Fluids

A viscous and an elastic component interact to generate a type of non-Newtonian fluid known as viscoelastic fluid. Metals at very high temperatures, biopolymers, semi-crystalline

polymers, and amorphous polymers, and bitumen materials are a few instances of viscoelastic materials.

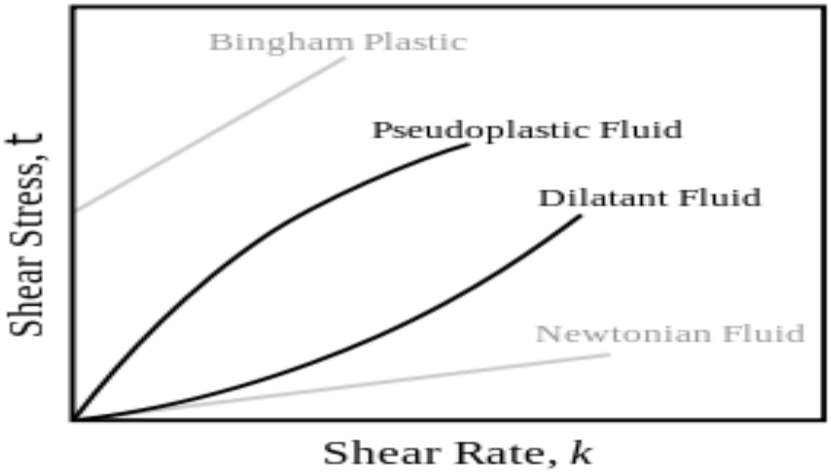

Figure 3.5: Behavior of the different types of Fluids.

3.9 Porous Medium

A porous medium is a substance that consists of a solid matrix and numerous interconnected pores. The fluid can flow out of the material because the pores are filled with it. In a indeed porous medium, the pores are dispersed in a variety of shapes and sizes. The porosity of a medium identifies it as being porous like Sandstone, beach sand, wood, dry bread.

3.9.1 Porosity

The proportion ratio the material's total area to the associated void area is known as the medium porosity. It is defined by φ. As a result, the fraction that the substance. Porosity is described as the connected void to total volume ratio. and is called effective porosity if all pore space is not connected like Sponges, wood, rubber, and some rock.

Figure 3.6: Sponges with pore space

3.9.2 Permeability

The capacity of a porous material to permit fluids to pass through it is known as its permeability like The permeability of a highly porous rock with disconnected pores is minimal or nonexistent.

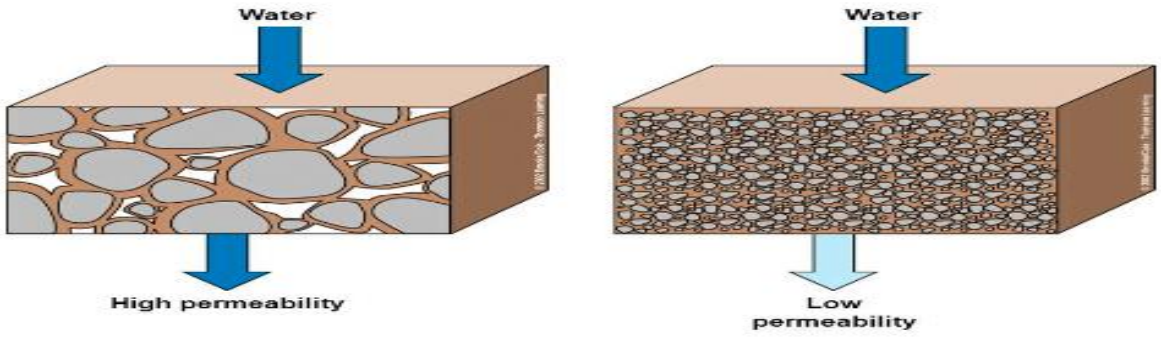

Figure 3.7: Shows permeability of rock

3.9.3 Darcy's Law

The Darcy Law refers to the constitutive formula that provides an explanation of a fluid's flow in a porous medium. It serves as an example of how water, oil, and gas flow through petroleum reservoirs. The proportionality relationship between the flow rate q of a uniform medium and the pressure and water difference, i.e

$$q = \frac{K}{\mu} \nabla p, \tag{3.9}$$

where K is permeability, q denotes the instantaneous flow rate, ∇p is pressure drop and μ dynamic viscosity of fluid.

3.10 Continuity Equation

A system's entry mass is equal to its exit mass plus its entry mass developing produced inside the system, according to the continuity equation, which is the law of conservation of mass. The expression for the equation of continuity is:

$$\frac{\partial \rho}{\partial t} + \boldsymbol{\nabla}.(\rho\, \boldsymbol{V}) = 0. \tag{3.10}$$

Where ρ the density of fluid and $\boldsymbol{V}$ is the velocity. When a fluid is incompressible, its density (ρ) stays constant over its whole length, and the continuity equation becomes

$$\boldsymbol{\nabla}.\boldsymbol{V} = 0. \tag{3.11}$$

3.11 Momentum Equation

The momentum equation, which derives from Newton's second Law of motion, relates the total force applied on a fluid element to its acceleration or momentum change rate. The equation of motion for an incompressible fluid is:

$$\rho \frac{d\boldsymbol{V}}{dt} = \nabla.\boldsymbol{T} + \boldsymbol{R}\,, \tag{3.12}$$

where p is pressure, $\boldsymbol{T}$ is Cauchy stress tensor, ρ is density, d/dt the upper convective derivative and $\boldsymbol{R}$ is Darcy resistance.

3.12 Reynolds Number

The Reynolds number is defined as the ratio of dynamic forces to shearing forces, and it is a dimensionless number represented by Re. Mathematically, it is defined as,

$$\text{Re} = \frac{\text{intertial force}}{\text{viscous force}}, \qquad \text{or} \qquad \text{Re} = \frac{\rho \boldsymbol{V} L}{\mu} = \frac{\boldsymbol{V} L}{\nu}, \tag{3.13}$$

where density is denoted by ρ, velocity by $\boldsymbol{V}$, characteristic length by L, kinematic viscosity by ν. and dynamic viscosity as μ. While low Reynolds numbers suggest high viscous forces and laminar flow, significant Reynolds numbers also indicate turbulent flow where inertial forces predominate [49].

3.13 Integral Transform

The Fourier integral formula was often used to develop the origin of an integral transform. Numerous issues in applied mathematics and engineering research have been solved using integral transforms. A unique mathematical procedure for a real or complex-valued function that creates a new function is called an integral transform. The main objective of the integral transform is to simplify a challenging mathematical issue so that it may be addressed quickly and readily without the need for laborious and time-consuming computations. Like this, integral transformations have been shown to be effective operational techniques for solving initial boundary value issues, initial value problems of integral, and linear differential equations. These issues typically come up while simulating fluid mechanics issues. The following standard definition provides an overview of the fundamental ideas and definition of integral transform [49].

3.13.1 Finite Fourier Sine Transform

There is no dispute about the effectiveness of using the finite Fourier sine and inverse finite Fourier sine transforms to address linear initial value and boundary value issues resulting from fluid mechanics phenomena. For the following reasons, this transform is crucial to the general solution of integral and differential equations:

- The differential and integral equations are translated into simple algebraic equations, allowing us to investigate the modified function's solution.
- Boundary value problem solutions are then inverted to return to the original variable format.
- An attractive compact version of the solutions is produced by connecting the convolution theorem with the FFST.

Consider a function $u(y,t)$ which is piecewise continuous and absolutely integrable over $[0,d]$ the FFST and inverse FFST operators are defined below

$$U_{Fn}(t) = \int_0^d \mathrm{u(y,t)}\ \mathrm{Sin}(\lambda_n y)\, dy, \tag{3.14}$$

and

$$u(y,t) = \frac{2}{L}\sum_{n=1}^{\infty} U_{Fn}(t)\, Sin(\lambda_n y)\,. \tag{3.15}$$

CHAPTER 4

Mathematical Analysis of Maxwell Fluid Flow through a Porous Plate Channel Induced by Constantly Accelerating or Oscillating Wall

4.1 Introduction

In this chapter, an examination is carried out for laminar, unsteady, incompressible and one dimensional upper-covected Maxwell fluid that lies between two horizontal parallel plates along x-axis. The effects of porosity are taken into account. One of the plates is accelerating or oscillating in its own plane, producing the fluid motion, and the solutions satisfy all boundary and initial conditions. Unsteady motions through channel are analyzed in an analytical manner. The solutions obtained for sinusoidal motion are presented as the sum of transient and steady-state components. The exact analytical solution for the dimensionless velocity field and shear stress are obtained by means of FFST. The solutions of viscous fluid are obtained as limiting case. A discussion and graphical representation are provided for the impact of physical characteristics of fluid movement.

4.2 Mathematical Formulation

Incompressible, unsteady, one dimensional, upper covected Maxwell fluid lies between two infinite horizontal parallel plates at a distance d apart is considered. Moreover, effects of porous medium are also taken into account. The flow is governed by profile of velocity and stress field of the form

$$\boldsymbol{V} = (u(y,t), 0, 0) \quad \text{and} \quad \boldsymbol{S} = \boldsymbol{S}(y,t), \tag{4.1}$$

and constitutive equations for the unsteady flow are given by:

$$\boldsymbol{\nabla}.\mathbf{V} = 0, \tag{4.2}$$

and

$$\rho \frac{d\boldsymbol{V}}{dt} = \nabla.\boldsymbol{T} + \boldsymbol{R}, \tag{4.3}$$

where the stress tensor for the Maxwell fluid is given below:

$$\boldsymbol{T} = -p\,\boldsymbol{I} + \boldsymbol{S}, \qquad \text{and} \qquad \boldsymbol{S} + \lambda \frac{\delta \boldsymbol{S}}{\delta t} = \mu\, \boldsymbol{A_1}, \tag{4.4}$$

in which

$$\frac{\delta(.)}{\delta t} = \frac{d(.)}{dt} - (\text{grad}\,\boldsymbol{V})(.) - (.)(\text{grad}\,\boldsymbol{V})^{\intercal}, \tag{4.5}$$

where $\boldsymbol{V}$ is the velocity, $\boldsymbol{A_1}$ is first Rivlin-Ericksen tensor**,** $\boldsymbol{S}$ is the extra-stress tensor, $\boldsymbol{T}$ is the Cauchy stress tensor, $-p\,\boldsymbol{I}$ is the constitutively uncertain portion of the stress imposed on by the

incompressibility constraint, $\boldsymbol{L}$ is the velocity gradient, λ is the relaxation time, μ is the dynamic viscosity, d/dt is the material time derivative, $\delta/\delta t$ is upper convective time derivative, $^{\intercal}$ denotes the transpose and $\boldsymbol{R}$ is the Darcy resistant.

Using Eq. (4.1), we have

$$\mathbf{A_1} = \begin{bmatrix} 0 & \frac{\partial u}{\partial y} & 0 \\ \frac{\partial u}{\partial y} & 0 & 0 \\ 0 & 0 & 0 \end{bmatrix}, \tag{4.6}$$

$$\frac{\delta \boldsymbol{S}}{\delta t} = \begin{bmatrix} \frac{\partial}{\partial t}S_{xx} - 2\,S_{yx}\frac{\partial u}{\partial y} & \frac{\partial}{\partial t}S_{xy} - S_{yy}\frac{\partial u}{\partial y} & \frac{\partial}{\partial t}S_{xz} - S_{yz}\frac{\partial u}{\partial y} \\ \frac{\partial}{\partial t}S_{yx} - S_{yy}\frac{\partial u}{\partial y} & \frac{\partial}{\partial t}S_{yy} & \frac{\partial}{\partial t}S_{yz} \\ \frac{\partial}{\partial t}S_{zx} - S_{zy}\frac{\partial u}{\partial y} & \frac{\partial}{\partial t}S_{zy} & \frac{\partial}{\partial t}S_{zz} \end{bmatrix}. \tag{4.7}$$

Substitution of Eqs. (4.6) and (4.7) into Eq. $(4.4)_b$ one can write Eq. $(4.4)_b$ in the component form as

$$S_{xx} + \lambda\left(\frac{\partial S_{xx}}{\partial t} - 2\lambda S_{yx}\frac{\partial u}{\partial y}\right) = 0, \tag{4.8}$$

$$S_{xy} + \lambda\left(\frac{\partial S_{xy}}{\partial t} - S_{yy}\frac{\partial u}{\partial y}\right) = \mu\frac{\partial u}{\partial y}, \tag{4.9}$$

$$S_{xz} - \lambda\left(\frac{\partial S_{xx}}{\partial t} - S_{yz}\frac{\partial u}{\partial y}\right) = 0, \tag{4.10}$$

$$S_{yy} + \lambda\left(\frac{\partial S_{yy}}{\partial t}\right) = 0, \tag{4.11}$$

$$S_{yz} + \lambda\left(\frac{\partial S_{yz}}{\partial t}\right) = 0, \tag{4.12}$$

and

$$S_{zz} + \lambda\left(\frac{\partial S_{zz}}{\partial t}\right) = 0. \tag{4.13}$$

Having in mind the initial conditions of the form

$$S(y,0) = \frac{\partial S(y,0)}{\partial t} = 0, \tag{4.14}$$

Eqs. (4.10)-(4.13) becomes

$$S_{yy} = S_{yz} = S_{zz} = S_{xz} = 0. \tag{4.15}$$

4.3 Statement of Problem

At t = 0^+, the lower plate start to move in its own plane with the velocity At or to oscillate with the velocity $Usin(\omega t)$. The fluid moves gradually due to the shear and the equation of continuity (4.2) is satisfied identically. Introducing the velocity field given by Eq. $(4.1)_a$ in the constitutive Eqs. (4.8) and (4.9) and since:

$$\boldsymbol{V}(y,0) = 0,\ \boldsymbol{S}(y,0) = 0;\ 0 \le y \le d, \tag{4.16}$$

therefore, we get the following equations

$$\left(1 + \lambda\frac{\partial}{\partial t}\right)\tau(y,t) = \mu\frac{\partial u(y,t)}{\partial y}\ , \tag{4.17}$$

and

$$\left(1 + \lambda\frac{\partial}{\partial t}\right)\sigma_x(y,t) = 2\lambda\,\tau(y,t)\frac{\partial u(y,t)}{\partial y}, \tag{4.18}$$

where $\tau(y,t) = S_{xy}(y,t)$ and $\sigma_x(y,t) = S_{xx}(y,t)$ are the non-trivial component of $\boldsymbol{S}$. In flow direction, pressure gradient is absent, so the balance of linear momentum (4.3) reduces to

$$\rho \frac{\partial u(y,t)}{\partial t} = \frac{\partial \tau(y,t)}{\partial y} + R_x(y,t); \qquad 0 < y < d, t > 0, \tag{4.19}$$

$$0 = -\frac{\partial p}{\partial y}, \tag{4.19a}$$

and

$$0 = -\frac{\partial p}{\partial z}, \tag{4.19b}$$

where $R_x(y,t)$ is the Darcy resistance along $x-$axis and ρ is the fluid density for which such fluids have to satisfy the in relation [69]:

$$\left(1 + \lambda \frac{\partial}{\partial t}\right) R_x(y,t) = -\frac{\mu\phi}{k} u(y,t), \tag{4.20}$$

where, k is the porosity parameter and ϕ is the permeability of the porous medium. Eqs. (4.19a) and (4.19b) shows that ρ is not a function of y and z. Eliminating $\tau(y,t)$ from Eqs. (4.17) and (4.19) and bearing in mind Eq. (4.20), the resultant equation takes the following form

$$\left(1 + \lambda \frac{\partial}{\partial t}\right) \frac{\partial u(y,t)}{\partial t} = \nu \frac{\partial^2 u(y,t)}{\partial y^2} - \frac{\nu\phi}{k} u(y,t), \qquad 0 < y < d, \quad t > 0, \tag{4.21}$$

where $\nu = \mu/\rho$ is the kinematic viscosity of the fluid. The appropriate initial and boundary conditions are defined below:

I.C $$u(y,0) = 0, \quad \left.\frac{\partial u(y,t)}{\partial t}\right|_{t=0} = 0; \quad 0 \le y \le d, \tag{4.22}$$

and

B.C $$u(0,t) = At, \; u(d,t) = 0; \quad t > 0, \tag{4.23}$$

for the motion generated by the bottom plate's steady acceleration, and:

B.C $$u(0,t) = U\,sin(\omega t), \quad u(d,t) = 0;\ t > 0, \tag{4.24}$$

where A is the acceleration, U is the amplitude of the velocity, and ω the frequency of oscillations.

4.4 Solution of the Problem

4.4.1 Case I: Flow due to a constantly accelerating bottom plate

Consider the following dimensionless parameters of the form:

$$y^* = \frac{y}{d}, \quad t^* = \frac{t}{\sqrt[3]{A^2/\nu}}, \quad u^* = \frac{u}{\sqrt[3]{A\nu}}, \quad \tau^* = \frac{\tau}{\rho dA}, \quad \sigma_x^* = \frac{\sigma_x}{\rho dA}. \tag{4.25}$$

Substituting Eq. (4.25) into Eqs. (4.21)–(4.23), the following dimensionless problem is obtained after removing the star notation

$$\left(1 + \mathrm{We}\frac{\partial}{\partial t}\right)\frac{\partial u(y,t)}{\partial t} = \frac{1}{Re}\frac{\partial^2 u(y,t)}{\partial y^2} - Ku(y,t);\ 0 < y < 1,\ t > 0, \tag{4.26}$$

$$u(y,0) = \frac{\partial u(y,t)}{\partial t}\Big|_{t=0} = 0, \text{ for } 0 \le y \le 1, \tag{4.27}$$

and

$$u(0,t) = t, \text{ and } u(1,t) = 0 \quad \text{if} \quad t > 0, \tag{4.28}$$

where the Reynold number (Re), the Weissenberg number (We), and the dimensionless porosity parameter (K) are defined below:

$$Re = \frac{\eta d}{v}, \quad We = \lambda \frac{\eta}{d}, \text{ and } \quad K = \frac{\phi v \sqrt[3]{v}}{k \sqrt[3]{A^2}}, \tag{4.29}$$

where $\eta = d \sqrt[3]{A^2/v}$ is the characteristic velocity. Additionally, it is important to note that, in contrast to the Weissenberg number, whose values are sufficiently small the illustrations of Karra [68] and Housiadas [70] there is a notable range of fluctuation in the Reynolds number (Re) within the Weissenberg number range of 0.06 to 10 [71] (for internal flows, this range is as low as 2.000 in the laminar regime, as high as 4.000 in the transition phase, and as greater as 4.000 in the turbulent regime).

Dimensionless forms of the Eqs. (4.17) and (4.18) are given below:

$$\left(1 + We \frac{\partial}{\partial t}\right) \tau(y,t) = \frac{1}{Re} \frac{\partial u(y,t)}{\partial y}, \tag{4.30}$$

and

$$\left(1 + We \frac{\partial}{\partial t}\right) \sigma_x(y,t) = 2\beta \, \tau(y,t) \frac{\partial u(y,t)}{\partial y}, \tag{4.31}$$

where $\beta = \lambda \sqrt[3]{Av}/d$. The corresponding initial conditions are:

$$\tau(y,0) = 0; \qquad 0 \leq y \leq 1, \tag{4.32}$$

and

$$\sigma_x(y,0) = 0; \qquad 0 \leq y \leq 1, \tag{4.33}$$

Multiplying Eq. (4.26) by $sin(\lambda_n y)$, and the result is integrated with respect to y from zero to one keeping in mind the condition (4.28), it results that:

$$Re\left(1 + We\frac{\partial}{\partial t}\right)\frac{du_{Fn}(t)}{dt} + (\lambda_n^2 + KRe)u_{Fn}(t) = \lambda_n t;\ t > 0, \qquad (4.34)$$

with the initial conditions:

$$u_{Fn}(0) = 0, \qquad \left.\frac{du_{Fn}(t)}{dt}\right|_{t=0} = 0; \qquad n\ 1, 2, 3\ .. \qquad (4.35)$$

where $u_{Fn}(t)$ is the finite Fourier sine transform of $u(y,t)$, and $\lambda_n = n\pi$. The solution of Eq. (4.34) with the initial conditions (4.35), is given by

$$u_{Fn}(t) = \frac{(\mu^2 + Re\ \mathrm{r}_{1n})}{(\mathrm{r}_{2n} + \mathrm{r}_{1n})}\ e^{r_{2n}t} - \frac{(\mu^2 + Re\ \mathrm{r}_{2n})}{(\mathrm{r}_{2n} + \mathrm{r}_{1n})}\ e^{r_{1n}t} + \frac{\lambda_n}{\mu_n^2}\left(t - \frac{Re}{\mu_n^2}\right), \qquad (4.36)$$

where $r_{1n}, r_{2n} = [-1 \pm \sqrt{1 - 4We\mu_n^2/Re}]\ /(2We)$ are the roots and $\mu_n^2 = \lambda_n^2 + KRe$.

By applying the inverse FFST to Eq. (4.36), the following velocity profile is obtained:

$$u(y,t) = \sum_{n=1}^{\infty}\left\{t - \frac{Re}{\mu_n^2} - \frac{(\mu_n^2 + Re\ r_{1n})e^{r_{2n}t} + (\mu_n^2 + Re\ r_{2n})e^{r_{1n}t}}{(r_{2n} - r_{1n})\mu_n^4}\right\}\frac{\lambda_n \sin(\lambda_n y)}{\mu_n^2}, \qquad (4.37)$$

or equivalently (see the Table IX entry three in [73])

$$u(y,t) = (1 - y)t - 2tKRe\ \sum_{n=1}^{\infty}\frac{\sin(\lambda n y)}{\lambda_n \mu_n^2} - 2Re\sum_{n=1}^{\infty}\{1$$

$$+\frac{(\mu_n^2 + Re\ r_{1n})\,e^{r_{2n}t} + (\mu_n^2 + Re\ r_{2n})\,e^{r_{1n}t}}{Re(r_{2n} - r_{1n})}\Big\}\ \frac{\lambda_n\ \sin\ (\lambda_n\, y)}{\mu_n^4}. \qquad (4.38)$$

Introducing $u(y,t)$ from Eq. (4.38) into Eq. (4.30) and integrating the result by keeping in mind the initial condition (4.32), it results that:

$$\tau(y,t) = -\frac{t}{Re} + \frac{We}{Re}\left[1 - \exp\left(-\frac{t}{We}\right)\right] - 2\mathrm{K}\sum_{n=1}^{\infty}\left\{t - \left(We - \frac{\lambda_n^2}{K\mu_n^2}\right)\right.$$

$$\left.\times\left(1 - \exp\left(-\frac{t}{We}\right)\right)\right\}\frac{\cos(\lambda_n y)}{\mu_n^2} - \frac{2}{We}\sum_{n=1}^{\infty}\left\{\frac{(\mu_n^2 + Rer_{1n})}{(Wer_{2n}+1)}e^{\,r_{2n}t}\right.$$

$$\left.-\frac{(\mu_n^2 + Re\ r_{2n})}{(We\ r_{1n}+1)}e^{r_{1n}t}\right\}\frac{\lambda_n^2\cos(\lambda_n y)}{(r_{2n}-r_{1n})\mu_n^4} + \frac{2}{Re}\exp\left(-\frac{t}{We}\right)$$

$$\times\sum_{n=1}^{\infty}\left\{\frac{(\mu_n^2 + Rer_{1n})(Wer_{1n+1}) - (\mu_n^2 + Rer_{2n})(Wer_{2n}+1)}{(r_{2n}-r_{1n})(Wer_{2n}+1)\,(Wer_{1n}+1)}\right\}\frac{\lambda_n^2\cos(\lambda_n y)}{\mu_n^4}. \qquad (4.39)$$

4.4.2 Special cases

(i) Taking K →0, into Eq. (4.38) the solution in the absence of porous medium is obtained in the following form:

$$u(y,t) = (1-y)t - 2Re\sum_{n=1}^{\infty}\left\{1 + \frac{(\lambda_n^2 + Re\,r_{3n})e^{r_{4n}t} + (\lambda_n^2 + Re\,r_{4n})e^{r_{3n}t}}{(r_{4n}-r_{3n})Re}\right\}\frac{\sin(\lambda_n y)}{\lambda_n^3}, \qquad (4.40)$$

where $r_{3n}, r_{4n} = [-1 \pm \sqrt{1 - 4We\lambda_n^2/Re}]\,/(2We)$ are the roots of above equation.

(ii) Making $We \to 0$ into Eqs. (4.38) and (4.39), we recover the similar solutions corresponding to incompressible Newtonian fluids performing the same motion. For instance,

$$u_N(y,t) = (1-y)t - 2tKRe\sum_{n=1}^{\infty}\frac{\sin(\lambda_n y)}{\lambda_n\mu_n^2} - 2Re\sum_{n=1}^{\infty}\left\{\frac{\lambda_n\sin(\lambda_n y)}{\mu_n^2}\left[1 - \exp\left(-\frac{\mu_n^2}{Re}t\right)\right]\right\}. \qquad (4.41)$$

and

$$\tau_N(y,t) = -\frac{t}{Re} - 2tK\ \sum_{n=1}^{\infty}\frac{\cos(\lambda_n y)}{\mu_n^2} - 2\ \sum_{n=1}^{\infty}\left\{\frac{\cos(\lambda_n y)}{\mu_n^4}\right\}[1-\exp\left(\frac{\mu_n^2}{Re}t\right)]. \qquad (4.42)$$

(iii) Moreover, the motion under study is irregular and will continue to be inconsistent. Therefore, long-time solutions can sufficiently explain the fluid motion at large values of time t in the following expressions

$$\mathrm{u_{Lt}(y,t)} = (1-\mathrm{y})\mathrm{t} - 2\mathrm{Re}\sum_{n=1}^{\infty}\left(t\ K + \frac{\lambda_n^2}{\mu_n^2}\right)\frac{\sin(\lambda_n y)}{\lambda n \mu_n^2}, \qquad (4.43)$$

and

$$\mathrm{\tau_{Lt}(y,t)} = -\frac{(-t+We)}{Re} - 2K\sum_{n=1}^{\infty}\left(t - We + \frac{\lambda_n^2}{\mu_n^2}\right)\frac{\cos(\lambda_n y)}{\mu_n^2}. \qquad (4.44)$$

4.4.3 Case II: Flow due to oscillatory motion of the bottom plate

Consider the following non-dimensional variables of the form

$$y^* = \frac{y}{d}, \quad t^* = \frac{tU}{d}, \quad u^* = \frac{u}{U}, \quad \tau^* = \frac{\tau}{\rho U^2}, \quad \sigma_x^* = \frac{\sigma_x}{\rho U^2}, \quad \omega^* = \frac{\omega d}{U}, \qquad (4.45)$$

Introducing Eq. (4.45), into Eq. (4.21)-(4.22) and Eq. (4.24), we obtain the same Eq. (4.26) and (4.27), in which

$$Re = \frac{Ud}{\nu}, \quad We = \frac{\lambda U}{d}, \quad \text{and} \quad K = \frac{\nu\varphi d}{kU}, \qquad (4.46)$$

whereas the Eq. (4.24) takes the following form

$$u(0,t) = sin(\omega t);\ t > 0, \qquad (4.47)$$

and

$$u(1,t) = 0; \quad t > 0. \tag{4.48}$$

Applying again the FFST to Eq. (4.26) and keep in mind the boundary conditions (4.47) and (4.48), we obtain

$$Re\, We \frac{d^2 u_{Fn}(t)}{dt^2} + Re\, \frac{du_{Fn}(t)}{dt} + \mu_n^2 u_{Fn}(t) = \lambda_n \sin(\omega t)\,; t > 0. \tag{4.49}$$

The solution of the Eq. (4.49) by using initial conditions (4.35) is given in the following equation

$$u_{Fn}(t) = \frac{a_n \sin(\omega t) - \omega Re \cos(\omega t)}{a_n^2 + (\omega Re)^2} \lambda_n + \frac{(a_n + Re\, r_{1n}) e^{r_{2n} t} - (a_n + Re\, r_{2n}) e^{r_{1n} t}}{(r_{2n} - r_{1n}) \mu_n^4} \omega \lambda_n\,, \tag{4.50}$$

where $a_n = \mu_n^2 - ReWe\omega^2$.

Now by applying the inverse FFST to Eq. (4.50), the result is that the dimensionless velocity field $u_s(y,t)$ can be written as

$$u_s(y,t) = u_{sp}(y,t) + u_{st}(y,t), \tag{4.51}$$

where

$$u_{sp}(y,t) = 2 \sum_{n=1}^{\infty} \left\{ \frac{(a_n \sin(\omega t) - \omega\, Re \cos(\omega t))}{(a_n^2 + (\omega\, Re)^2)} \right\} \lambda_n Sin(\lambda_n y), \tag{4.52}$$

and

$$u_{st}(y,t) = 2\omega \sum_{n=1}^{\infty} \left\{ \frac{\left((a_n + Re\, r_{1n}) e^{r_{2n} t} - (a_n + Re\, r_{2n}) e^{r_{1n} t} \right)}{(r_{2n} - r_{1n}) \mu_n^4} \right\} \lambda_n Sin(\lambda_n y), \tag{4.53}$$

in which $u_{sp}(y,t)$ is the permanent and $u_{st}(y,t)$ is the transient solution.

Moreover, Eq. (4.52) can also be written as

$$u_{sp}\,(y,t) = (1-y)\sin(\omega t) + 2Re\sum_{n=1}^{\infty}\{\,((a_n(\mathrm{We}\omega^2 - \mathrm{K}) - \mathrm{Re}\omega^2 \times \sin(\omega t) - \omega\lambda_n^2\cos(\omega t))\,Sin(\lambda_n y)/\,\lambda_n)/(a_n^2 + (\omega Re)^2)\}. \tag{4.54}$$

Generalized form of $u_{sp}\,(y,t)$ can be written as

$$u_{sp}\,(y,t) = \mathrm{Im}\left\{\frac{sh[(1-y)\sqrt{\psi}]}{sh(\sqrt{\psi})}\right\};\;\; \psi = \mathrm{Re}(\mathrm{K} - \mathrm{We}\omega^2 + \mathrm{i}\omega), \tag{4.55}$$

where "Im" stands for imaginary component.

Also, the expression for shear stress $\tau_s(y,t)$ can be obtained in the following form

$$\tau_s(y,t) = \tau_{sp}(y,t) + \tau_{st}(y,t), \tag{4.56}$$

where

$$\tau_{sp}(y,t) = \frac{(\omega We\,cos(\omega t) - \sin(\omega t))}{[(\omega Re)^2+1]Re} + 2\sum_{n=1}^{\infty}\left\{\frac{(b_n - We\omega^2\lambda_n^2)\sin(\omega t) - \omega(b_n We + \lambda_n^2)\cos(\omega t)}{[a_n^2+(\omega Re)^2][(\omega We)^2+1]}\right\}\cos(\lambda_n y), \tag{4.57}$$

and

$$\tau_{st}(y,t) = \frac{2\omega}{We}\sum_{n=1}^{\infty}\left\{\frac{(a_n + Rer_{2n})(Wer_{2n}+1)e^{\,r_{1n}t} - (a_n + Rer_{1n})(Wer_{1n}+1)e^{\,r_{2n}t}}{(Wer_{2n}+1)(r_{2n} - r_{1n})(Wer_{1n}+1)[a_n^2 + (\omega Re)^2]}\right\}\lambda_n^2\cos(\lambda_n y)$$

$$-\frac{2\omega}{We}e^{\left(-\frac{t}{We}\right)}\sum_{n=1}^{\infty}\left\{\frac{(a_n + Rer_{2n})\;(Wer_{2n}+1)e^{\,r_{1n}t} - \;(a_n + Rer_{1n})\;(Wer_{1n}+1)\;e^{\,r_{2n}t}}{(Wer_{2n}+1)(r_{2n} - r_{1n})(Wer_{1n}+1)(a_n^2 + \;(\omega Re)^2)}\right\}$$

$$\times\ \lambda_n^2 \cos(\lambda_n y) - e^{\left(-\frac{t}{We}\right)}\left\{\frac{\omega\, We}{(\omega\, We)^2+1)Re} - 2\omega\sum_{n=1}^{\infty}\frac{\left(\lambda_n^2+Web_n\right)}{((\omega\, We)^2+1)[a_n^2+(\omega\, Re)^2]}\right\}\cos(\lambda_n y), \tag{4.58}$$

where b_n = (μ_n^2 $- ReWe\omega^2$)(Weω^2 − K) − Re ω^2. Taking y = 1 into Eqs. (4.57) and (4.58), for instance the associated dimensionless transient and steady-state shear stress

$$\tau_{sp}(y,t) = -\frac{1}{Re} Im\left\{\frac{\sqrt{\psi}}{(1+i\omega We)}\frac{ch[(1-y)\sqrt{\psi}}{sh(\sqrt{\gamma})}e^{i\omega t}\right\}, \tag{4.59}$$

can be easily obtained in the same way as for $u_{sp}(y,t)$.

4.4.4 Special Cases

(i) In the absence of porous medium, Eqs. (4.54) and (4.53) take the simpler form as define below

$$u_{sp}(y,t) = (1-y)\sin(\omega t) + 2Re\omega\sum_{n=1}^{\infty}\left\{\frac{\omega(a_n \mathrm{We} - \mathrm{Re})\sin(\omega t) - \omega\lambda_n^2\cos(\omega t)}{a_n^2+(\omega Re)^2}\right\}\frac{Sin(\lambda_n y)}{\lambda_n}, \tag{4.60}$$

and

$$u_{st}(y,t) = 2\omega\sum_{n=1}^{\infty}\left\{\frac{\left(\mu_n^2 - ReWe\omega^2\right) + Rer_{1n})e^{r_{2n}t} - ((\mu_n^2 - Re\, We\, \omega^2) + Re\, r_{2n})e^{r_{1n}t}}{(r_{2n}-r_{1n})[a_n^2+(\omega Re)^2]}\right\}\lambda_n Sin(\lambda_n y), \tag{4.61}$$

Eq. (4.55) becomes identical to the solution obtained in ([75] Eq. (56)).

(ii) Taking $We \rightarrow 0$ into Eqs. (4.53), (4.54) and (4.57), (4.58) we get similar solution for Newtonian fluid in the following form.

$$u_{Nsp}(y,t) = (1-y)\sin(\omega t) - 2Re\sum_{n=1}^{\infty}\left\{\frac{(K\mu_n^2 + Re\omega^2)\sin(\omega t)+\omega\lambda_n^2\cos(\omega t)}{(\lambda_n^2+KRe)^2+(\omega Re)^2}\right\}\frac{\sin(\lambda_n y)}{\lambda_n}, \tag{4.62}$$

$$u_{Nst}(y,t) = 2\omega Re\ \sum_{n=1}^{\infty}\left\{\frac{\lambda_n\sin(\omega t)}{(\lambda_n^2+KRe)^2+(\omega Re)^2}e^{\left[-\left(\frac{\lambda_n^2}{Re}+K\right)t\right]}\right\}, \tag{4.63}$$

$$\tau_{Nsp}(y,t) = -\frac{t}{Re}\sin(\omega t) - 2\sum_{n=1}^{\infty}\left\{\frac{(K\mu_n^2 + Re\omega^2)\sin(\omega t)+\omega\lambda_n^2\cos(\omega t)}{(\lambda_n^2+KRe)^2+(\omega Re)^2}\right\}\cos(\lambda_n y), \tag{4.64}$$

and

$$\tau_{Nst}(y,t) = 2\omega\sum_{n=1}^{\infty}\left\{\frac{\lambda_n\cos(\omega t)}{(\lambda_n^2+KRe)^2+(\omega Re)^2}e^{\left[-\left(\frac{\lambda_n^2}{Re}+K\right)t\right]}\right\}. \tag{4.65}$$

The expressions of $u_{Nsp}(y,t)$ and $u_{Nst}(y,t)$ given by Eqs. (4.62) and (4.63) are identical for those of $u_{sp}(y,t)$ and $u_{st}(y,t)$ from [66] of its Eqs. (41) and (42).

4.5 Results and Discussion

In this chapter we give the solutions for constantly accelerating and oscillating flows of an incompressible Maxwell fluid in the presence of porous medium that lies between two parallel plates. Due to constant pressure, acceleration or plate oscillation causes the motion in the fluid. Integral transforms are used to provide the analytical solutions for the velocity field and the corresponding shear stress. The solutions obtained for sine oscillation of the boundary are presented as the sum of the steady-state and transient solutions, depending on the initial and boundary conditions. To bring light on certain physical aspects of the attained results, the graphical representation of velocity and associated shear stress fields only for the flow caused by a constantly accelerating and sine oscillation of the lower plate illustrate the impact of the material characteristics on the fluid motion. We discuss the problem of constantly accelerating and oscillating motion of the plate with porous medium. Furthermore, to see the effect of porosity, a comparison of the velocity and shear stress for the flow in the with and without porous medium is provided. In the limiting instance when $We \to 0$, the solutions for Newtonian fluid are recovered. The numerical results for the velocity profile are plotted in Figures 4.1-4.5. Also, graphical depiction for tangential stress is given in Figures 4.6 and 4.7. We discuss these results with respect to the variations of the Weissenberg number (We), porosity parameter (K), Reynolds number (Re), and different values of the time t.

Figure 4.1 shows the influence of different values of Weissenberg number (We) i.e $We = 0.002, 1$ and 6 for $t = 1$ and $t = 2$ on velocity profile obtained in Eq. (4.38) and (4.41), respectively. In both cases, velocity profile decreases from maximum values to zero values and clearly satisfy the boundary condition. Moreover, velocity is an increasing function of time, and it reduces for increasing values of the Weissenberg number (We). Also, due to the physical expectation of We i.e ratio between elastic and viscous forces, the viscous fluid flows faster in comparison with incompressible upper covected Maxwell fluids. Further, when Weissenberg number $We \to 0$, the convergence of velocity field $u(y,t)$ given by Eq. (4.38) to $u_N(y,t)$ given by Eq. (4.41) is also illustrated graphically.

Figure 4.2 depicts the equivalence graphically for the time on different forms of steady-state component of the velocity $u_{sp}(y,t)$ given by Eqs. (4.54) and (4.55) for $\omega = \pi/12$, $K = 1$

$Re = 100$ and $We = 0.7$, respectively. Figures 4.3 and 4.4 represent the required time to reach the steady-state for oscillatory motion given by Eqs. (4.51) and (4.54) due to upper convective Maxwell (UCM) fluids caused by the sinusoidal boundary velocity for $K = 1, Re = 100, \omega = \pi/12$ and $We = 0.7$ or 1.5, respectively $\omega = \pi/12$, $We = 0.7$, $Re = 100$ and $K = 1$ or 2. At this stage, the fluid flows in accordance with permanent solutions and the figures of starting solution $u_s(y,t)$, exactly superimpose over those of its steady-state component $u_{sp}(y,t)$. It can be observed that the time required to reach the steady-state flow of UCM fluids endures an increasing function with respect to We while it decreases for rise in porosity parameter (K). Thus, the steady-state is alternatively acquired for oscillating motions of viscous fluids in contrast to incompressible UCM fluid. Simultaneously, the steady-state takes larger to smallest in the presence of porous medium.

Figure 4.5 presents the time variation of mid plane for the steady-state component of the velocity related to the sine oscillation of the boundary for $K = 0$ and 0.8, and various values of We. It is found that the convergence to general solutions $u_{sp}(0.5,t)$ to the viscous fluid when $We = 0$ and the oscillating aspects of the velocity are clearly depicted. The amplitude of oscillation increases with increase in We and generally decreases as value of K rises when $\omega = \pi/6$, and $Re = 100$.

In Figures 4.6 and 4.7, the steady-state shear stress profile $\tau_{sp}(y,t)$ are plotted for sine oscillation of the boundary. Figure 4.6 shows the influence two different values of time t on shear stress given by Eqs. (4.58) and (4.59) for $\omega = \pi/6$, $K = 1$, $Re = 100$ and $We = 0.7$. It can be seen that both solutions give the same behavior. Figure 4.7 describes the time variation of mid plane of the steady-state (permanent) component of shear stress related to sinusoidal motion of the boundary for $K = 0$ and 0.8 and different values of We. It is clearly seen that the convergence to general solution $\tau_{sp}(0.5,t)$ to the incompressible Newtonian fluid corresponding to $We = 0$ and the oscillatory aspects of the shear stress. Hence, amplitude of the shear stress $\tau_{sp}(y,t)$ is rising regarding We and decrease for increase in value of K.

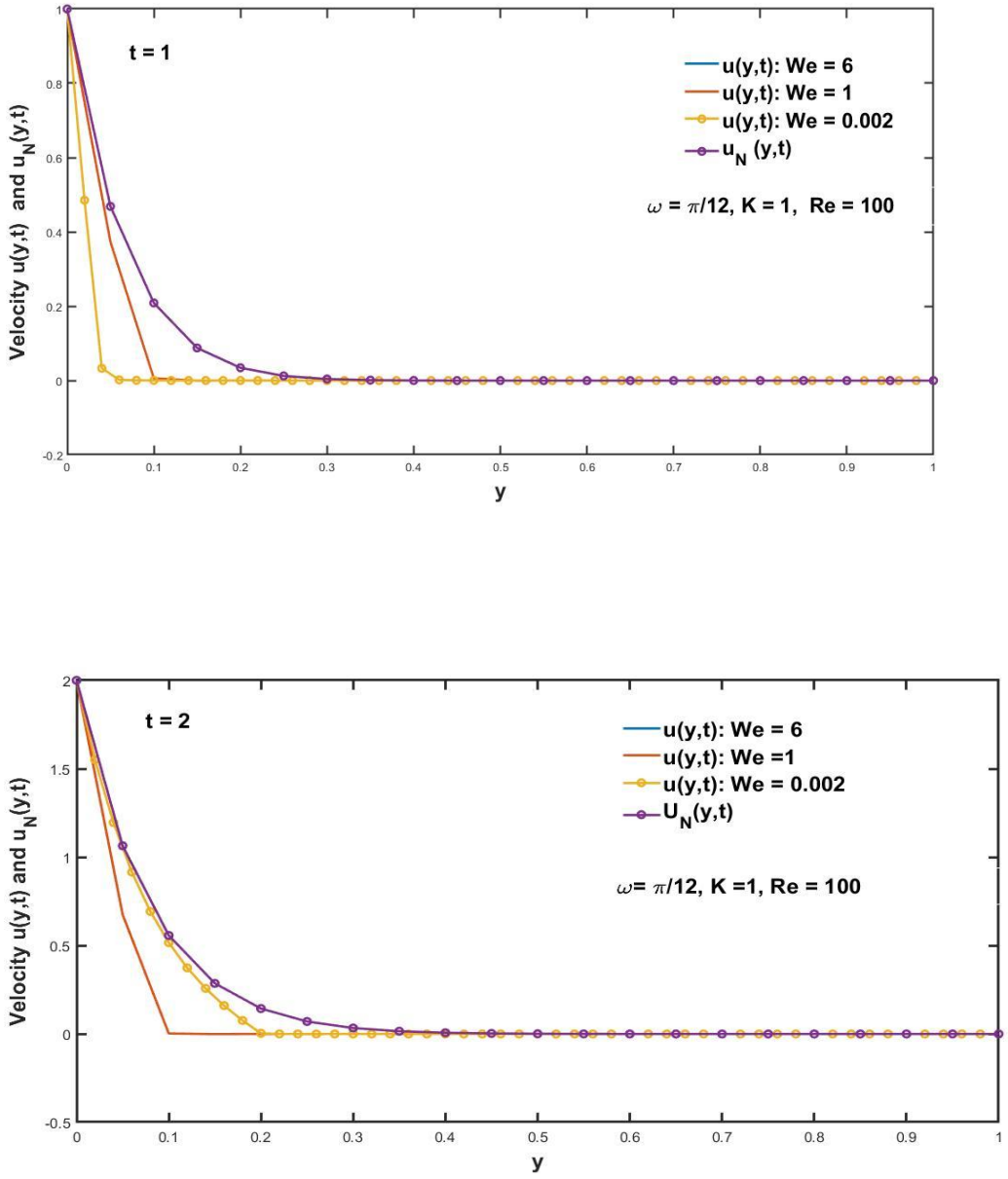

Figure 4.1: The velocity field profiles of $u(y,t)$ and $u_N(y,t)$, respectively.

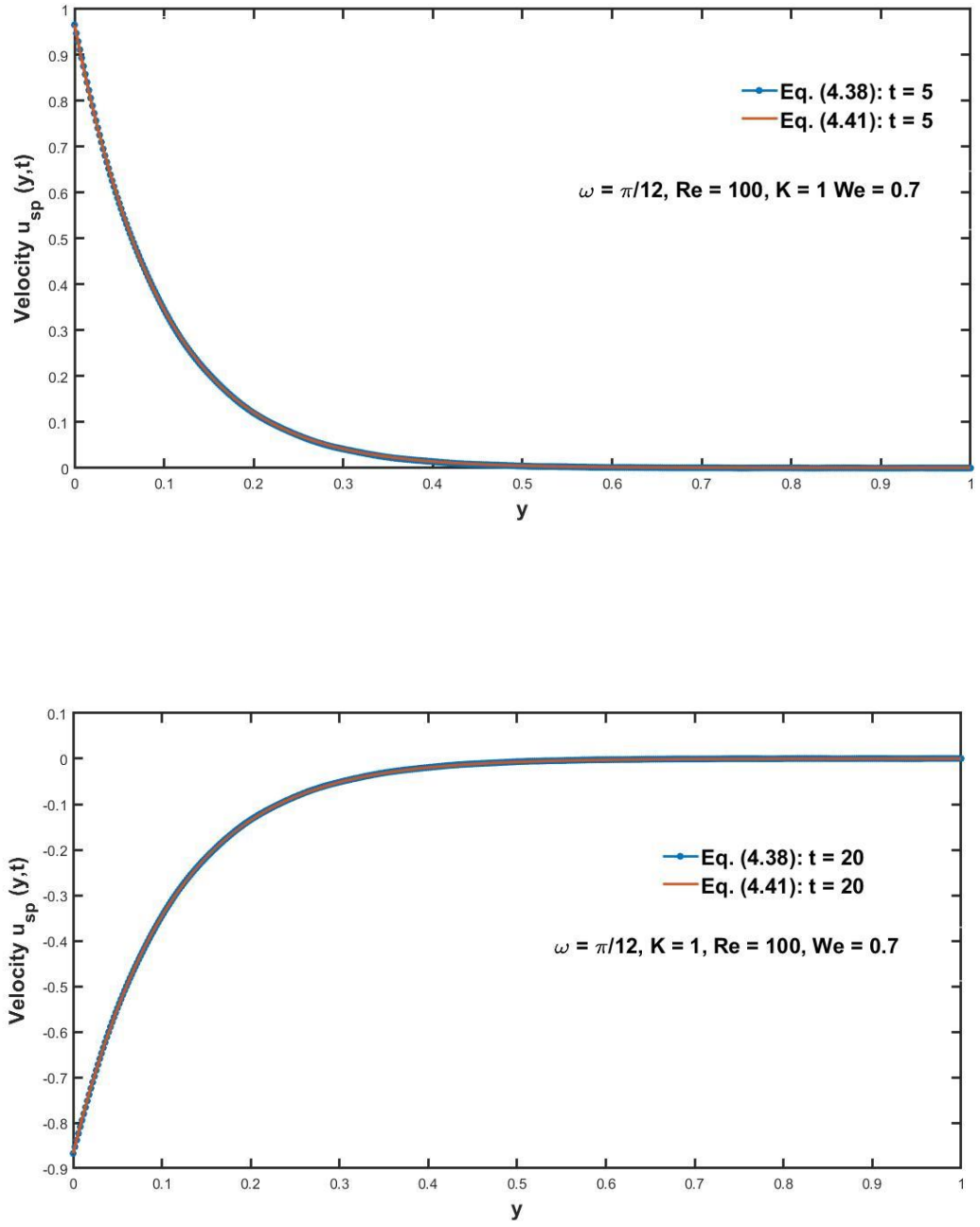

Figure 4.2: The steady-state component's profiles $u_{sp}(y,t)$.

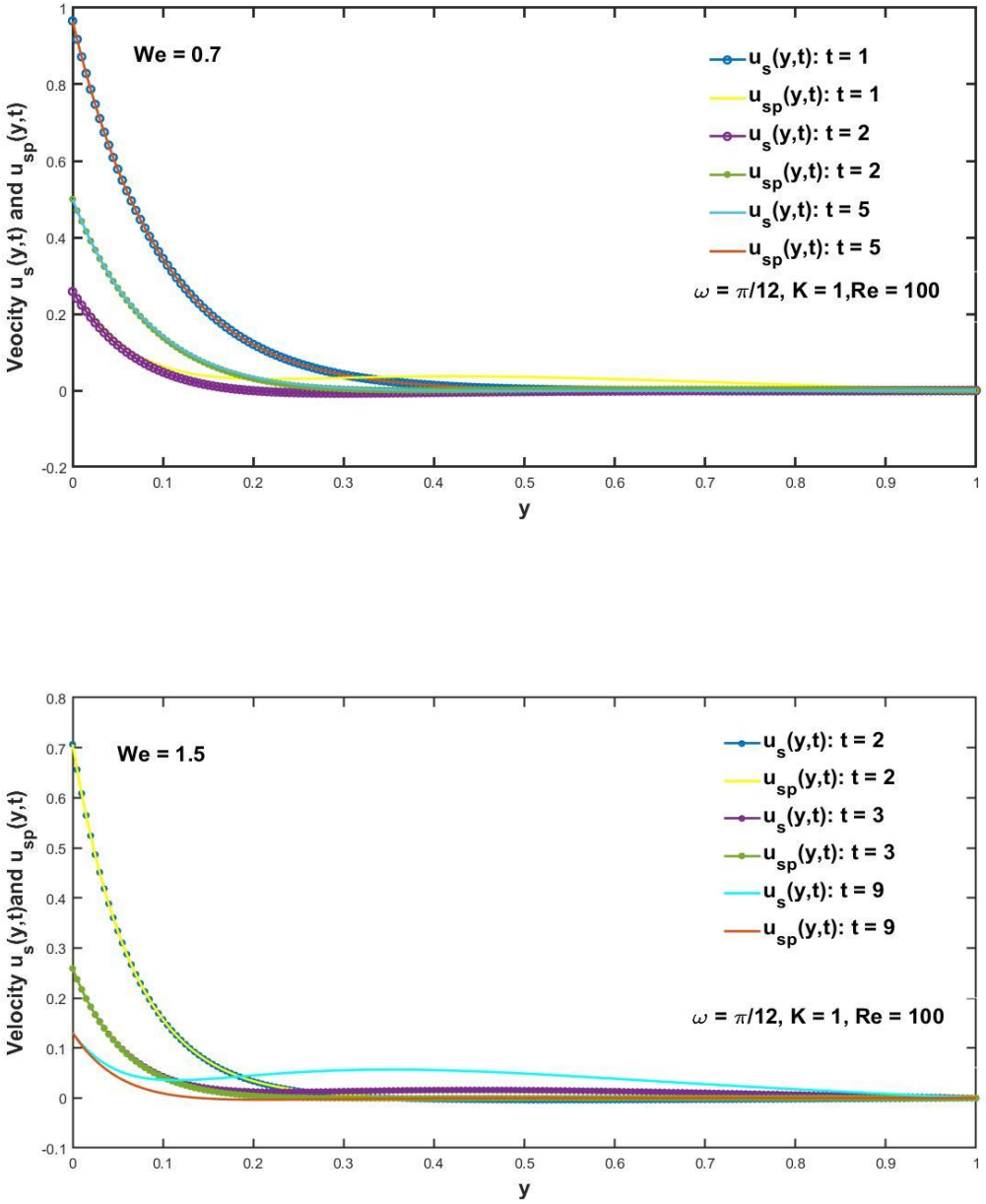

Figure 4.3: Required time to reach the steady-state velocity due to sine oscillation of the boundary.

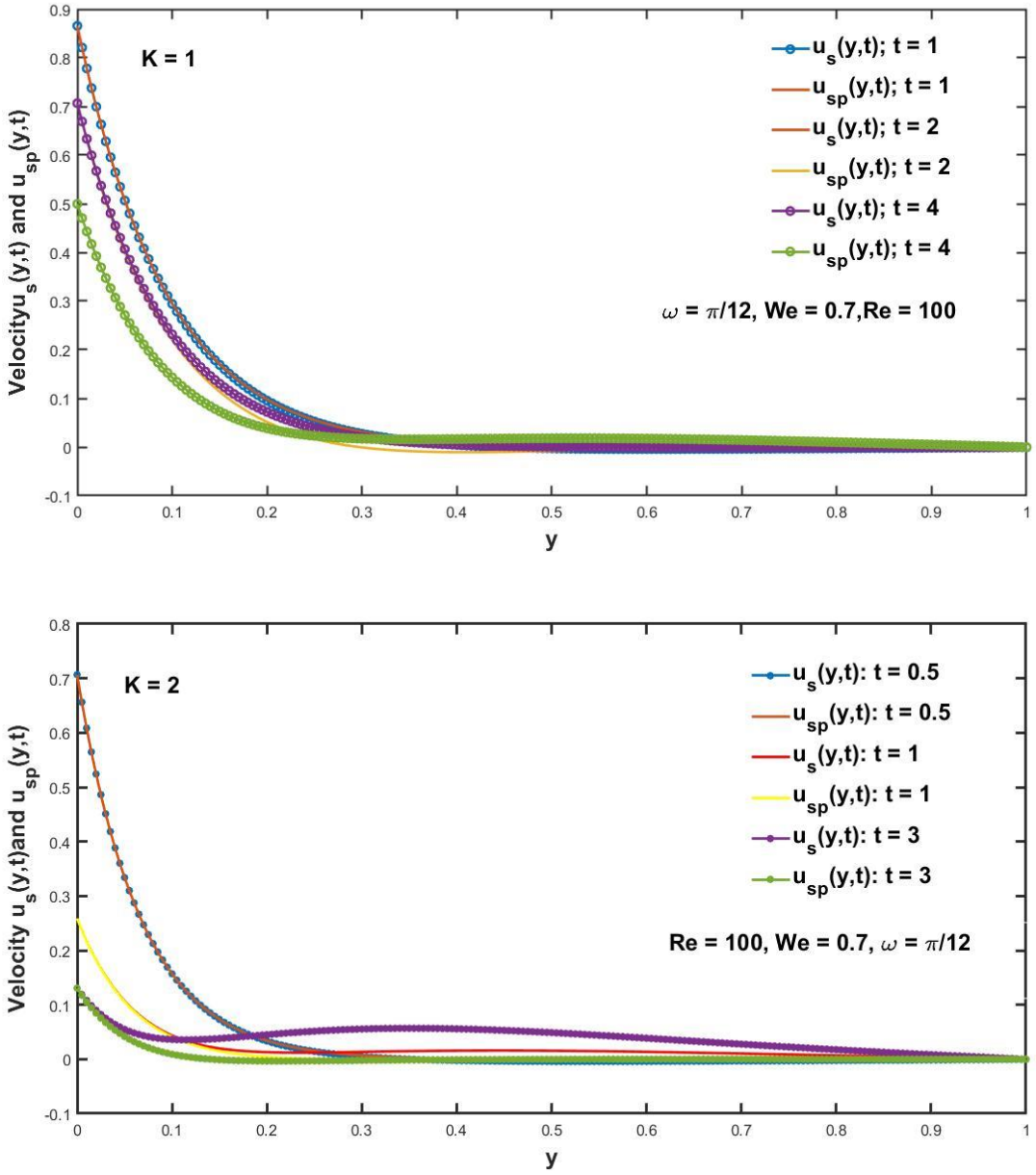

Figure 4.4: Required time to reach the steady-state velocity due to sine oscillation of the boundary.

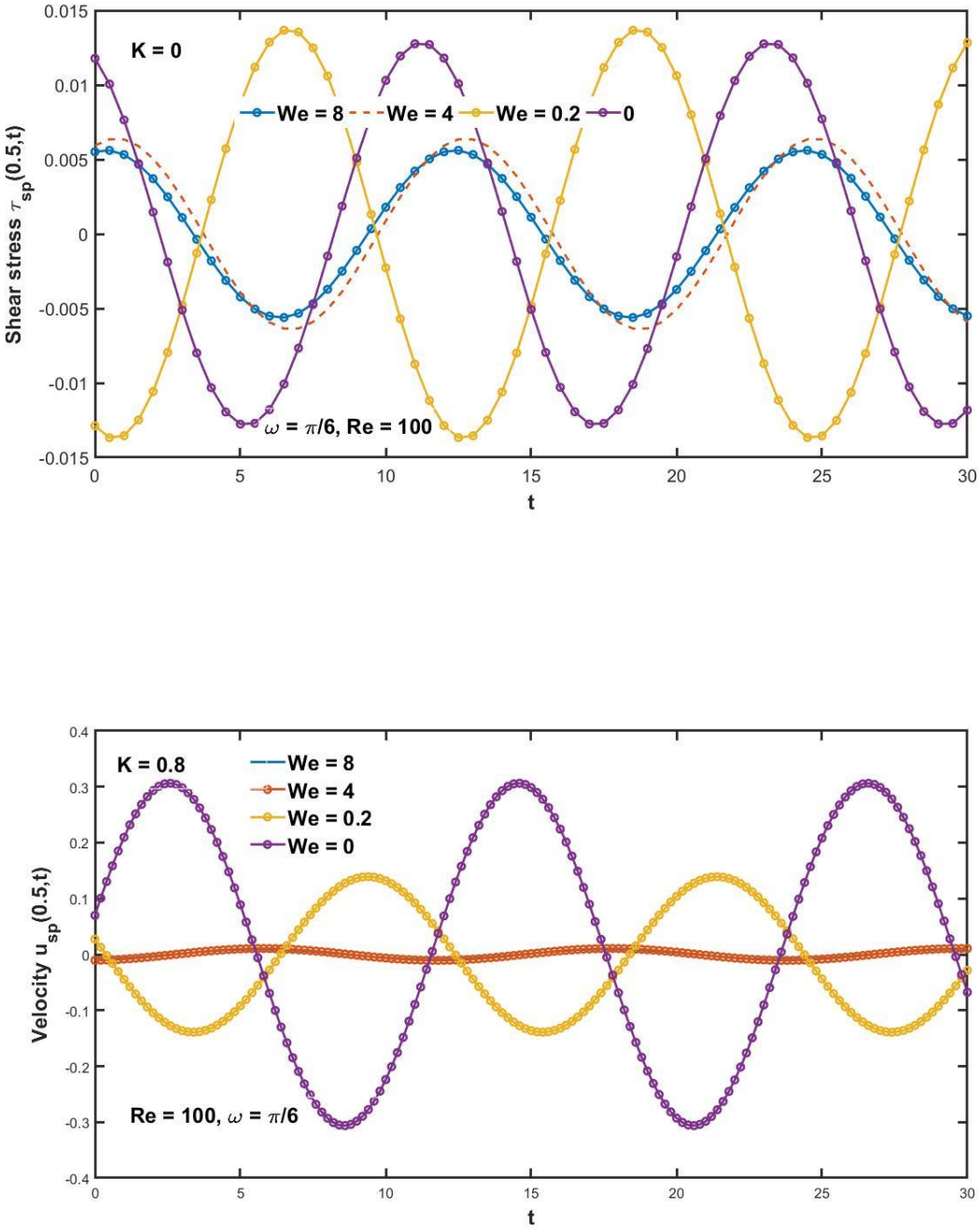

Figure 4.5: Time series of steady-state $u_{sp}(0.5, t)$ due to sine oscillation of the boundary.

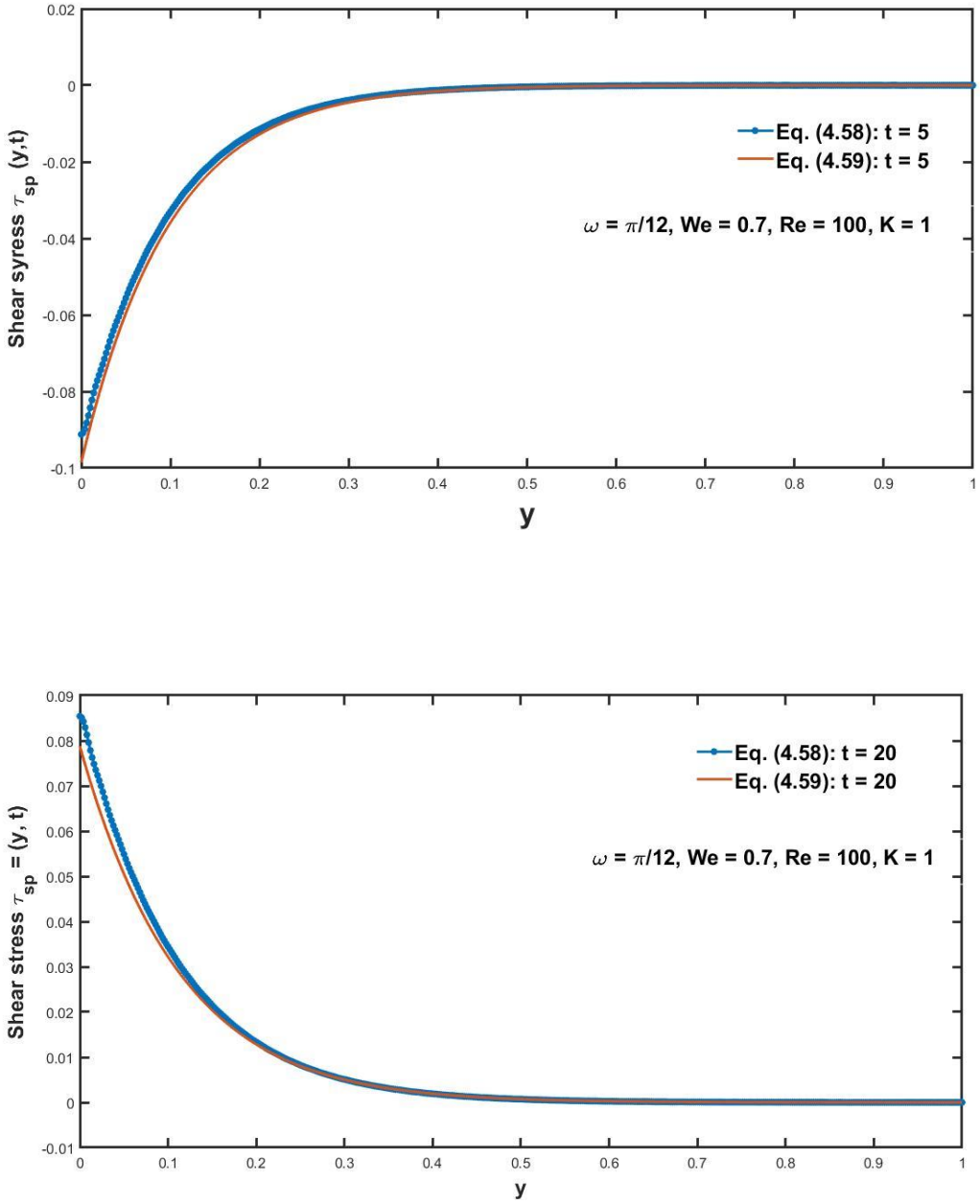

Figure 4.6: The steady-state component's profiles $\tau_{sp}(y,t)$ of shear stress.

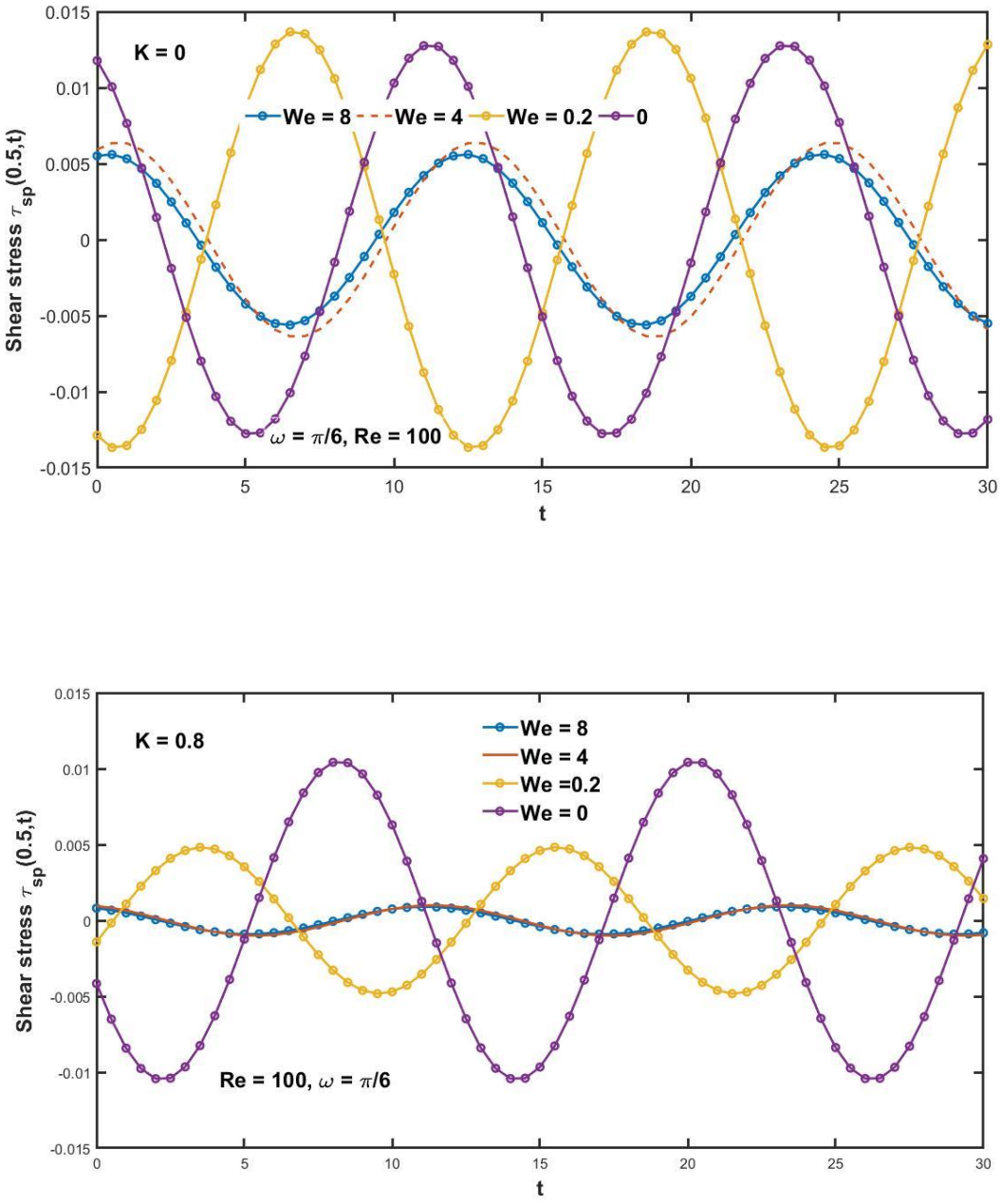

Figure 4.7: Time series of steady-state $\tau_{sp}(0.5, t)$ due to sine oscillation of the boundary.

CHAPTER 5

Mathematical Analysis of Burgers Fluid Flow Induced by an Unsteady Motion

5.1 Introduction

In this chapter, an examination is carried out for laminar, unsteady, incompressible and one-dimensional Burgers fluid that lies among two parallel, horizontal plates at a distance $\boldsymbol{d}$ apart along $\boldsymbol{x}$-axis. The medium is considered to be porous. One of the plates is accelerating or oscillating in its own plane, producing fluid motion, and the solutions satisfy all boundary and initial conditions. Unsteady motions through channel are analyzed in an analytical manner. The starting solutions for the oscillating motion can be seen as the sum of their steady-state and transient components.. The exact analytical solution for the dimensionless velocity and shear stress are obtained by means of FFST. Similar solutions for Oldoryd-B fluid, Maxwell fluid and Newtonian fluid are obtained as limiting case of presented results. The effects of pertinent parameters are discussed through graphical illustration to show interesting aspects of the solutions.

5.2 Geometry of the Problem

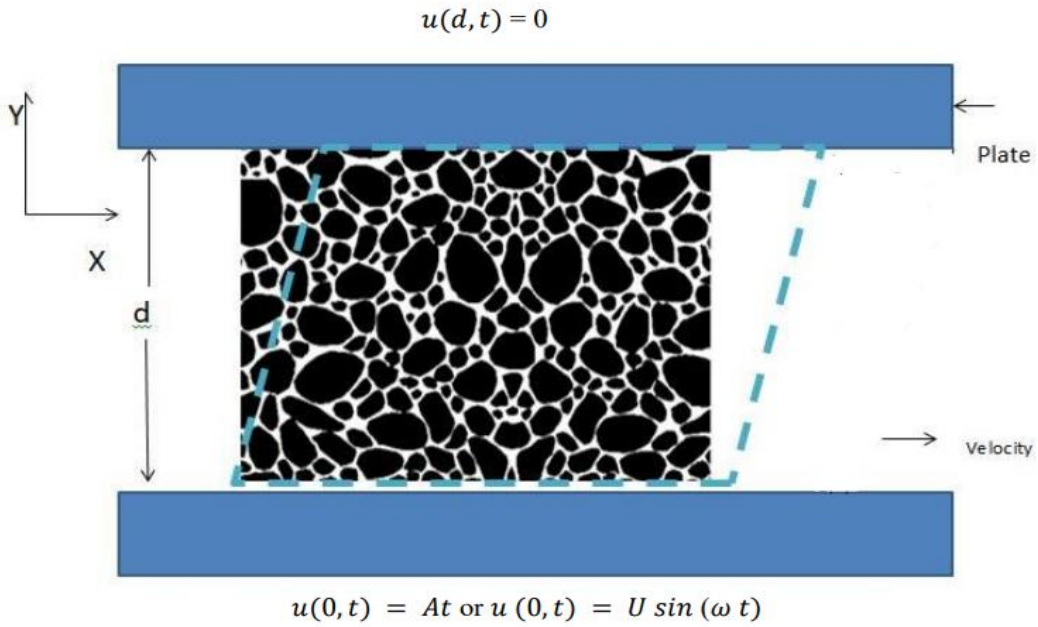

Figure 5.1: Geometry of the Problem

5.3 Mathematical Modeling

Consider the flow of laminar, unsteady, incompressible Burgers fluid occupying the space above the $x-axis$, and bounded by two horizontal plates situated at $y = 0$ and $y = d$. Moreover, the effect of porous medium is also taken into account. The flow is governed by the following fundamental laws i.e.

- Law of conservation of mass

$$\text{div}\,\boldsymbol{V} = 0. \tag{5.1}$$

- Law of conservation of momentum in the absence of body force

$$\rho \frac{d\boldsymbol{V}}{dt} = -\text{grad}\, p + \text{div}\boldsymbol{S} + \boldsymbol{R}, \tag{5.2}$$

in which

$$\boldsymbol{R} = (R_x, R_y, R_z), \tag{5.3}$$

where ρ the density of the fluid, $\boldsymbol{V}$ is the velocity field, p is the pressure, $\frac{d}{dt} = \left(\frac{\partial}{\partial t} + (\boldsymbol{V}.\boldsymbol{\nabla})\right)$ is the material time derivative, $\boldsymbol{R}$ the Darcy resistance and $\boldsymbol{S}$ is the extra stress tensor for Burgers fluid [36] denoted as

$$\boldsymbol{S} + \lambda_1 \frac{\delta \boldsymbol{S}}{\delta t} + \lambda_2 \frac{\delta^2 \boldsymbol{S}}{\delta t^2} = \mu \boldsymbol{A_1} + \mu\lambda_3 \frac{\delta \boldsymbol{A_1}}{\delta t}, \tag{5.4}$$

in which μ the dynamic viscosity, $\boldsymbol{A_1} = \text{grad}\,\boldsymbol{V} + (\text{grad}\,\boldsymbol{V})^T$ is the first Rivlin-Ericksen tensor, λ_1 and λ_3 ($< \lambda_1$) are the relaxation time and retardation time, respectively, λ_2 the material parameter of non-Newtonian Burgers fluid, d/dt is the substantial time derivative and $\delta/\delta t$ is the upper convected time derivative and denoted by

$$\frac{\delta(.)}{\delta t} = \frac{d(.)}{dt} - (\text{grad}\boldsymbol{V})(.) - (.)(\text{grad}\boldsymbol{V})^{\intercal}, \tag{5.5}$$

where $^{\intercal}$ represents the transpose. It is important to note that the following are included as special instances in the Burgers fluid model:

- The Oldroyd-B model (when $\lambda_2 = 0$)
- The Maxwell model (when $\lambda_2 = \lambda_3 = 0$)
- The second-grade model (when $\lambda_2 = \lambda_1 = 0$; $\mu\lambda_3 = \alpha_1$)
- The Newtonian model (when $\lambda_1 = 0$; $\lambda_2 = 0$; $\lambda_3 = 0$).

For 1-dimensional flow, we consider the velocity and corresponding stress fields of the form

$$\boldsymbol{V}(y,t) = (u(y,t),0,0) \text{ and } \boldsymbol{S} = \boldsymbol{S}(y,t). \tag{5.6}$$

The incompressibility constraint (5.1) is automatically satisfied for such flows. Now, in view of Eq. $(5.6)_a$ we have

$$\boldsymbol{A}=\begin{bmatrix}0 & \frac{\partial u}{\partial y} & 0\\ \frac{\partial u}{\partial y} & 0 & 0\\ 0 & 0 & 0\end{bmatrix},\ \frac{\delta \boldsymbol{A_1}}{\delta t}=\begin{bmatrix}-2\left(\frac{\partial u}{\partial y}\right)^2 & \frac{\partial^2 u}{\partial y \partial t} & 0\\ \frac{\partial^2 u}{\partial y \partial t} & 0 & 0\\ 0 & 0 & 0\end{bmatrix}, \tag{5.7}$$

$$\frac{\delta \boldsymbol{S}}{\delta t}=\begin{bmatrix}\frac{\partial}{\partial t}S_{xx}-2S_{yx}\frac{\partial u}{\partial y} & \frac{\partial}{\partial t}S_{xy}-S_{yy}\frac{\partial u}{\partial y} & \frac{\partial}{\partial t}S_{xz}-S_{yz}\frac{\partial u}{\partial y}\\ \frac{\partial}{\partial t}S_{yx}-S_{yy}\frac{\partial u}{\partial y} & \frac{\partial}{\partial t}y & \frac{\partial}{\partial t}S_{yz}\\ \frac{\partial}{\partial t}S_{zx}-S_{zy}\frac{\partial u}{\partial y} & \frac{\partial}{\partial t}S_{zy} & \frac{\partial}{\partial t}S_{zz}\end{bmatrix}, \tag{5.8}$$

and

$$\frac{\delta^2 \boldsymbol{S}}{\delta t^2}=\begin{bmatrix}\frac{\partial^2 S_{yx}}{\partial t^2}-2\left(\frac{\partial S_{yx}}{\partial t}\frac{\partial u}{\partial y}+S_{yy}\left(\frac{\partial u}{\partial y}\right)^2\right) & \frac{\partial^2 S_{xy}}{\partial t^2}-2\frac{\partial S_{yy}}{\partial t}\frac{\partial u}{\partial y}-S_{yy}\frac{\partial^2 u}{\partial y \partial t} & \frac{\partial^2 S_{xz}}{\partial t^2}-2\frac{\partial S_{yz}}{\partial t}\frac{\partial u}{\partial y}-S_{yz}\frac{\partial^2 u}{\partial y \partial t}\\ \frac{\partial^2 S_{yx}}{\partial t^2}-2\frac{\partial S_{yy}}{\partial t}\frac{\partial u}{\partial y}-S_{yy}\frac{\partial^2 u}{\partial y \partial t} & \frac{\partial^2 S_{yy}}{\partial t^2} & \frac{\partial^2 S_{yz}}{\partial t^2}\\ \frac{\partial^2 S_{zx}}{\partial t^2}-2\frac{\partial S_{zy}}{\partial t}\frac{\partial u}{\partial y}-S_{zy}\frac{\partial^2 u}{\partial y \partial t} & \frac{\partial^2 S_{zy}}{\partial t^2} & \frac{\partial^2 S_{zz}}{\partial t^2}\end{bmatrix}. \tag{5.9}$$

Substitution of Eqs. (5.7)-(5.9), into Eq. (5.4) gives the component form as follows

$$\left(1+\lambda_1\frac{\partial}{\partial t}+\lambda_2\frac{\partial^2}{\partial t^2}\right)S_{xx}-2\lambda_1 S_{yx}\frac{\partial u}{\partial y}-2\lambda_2\left(\frac{\partial S_{yx}}{\partial t}\frac{\partial u}{\partial y}+S_{yx}\frac{\partial^2 u}{\partial y \partial t}\right)=-2\mu\lambda_3\left(\frac{\partial u}{\partial y}\right)^2, \tag{5.10}$$

$$\left(1+\lambda_1\frac{\partial}{\partial t}+\lambda_2\frac{\partial^2}{\partial t^2}\right)S_{xy}-\lambda_1 S_{yy}\frac{\partial u}{\partial y}-\lambda_2\left(\frac{\partial S_{yx}}{\partial t}\frac{\partial u}{\partial y}+S_{yy}\frac{\partial^2 u}{\partial y \partial t}\right)=\mu\left(1+\lambda_3\frac{\partial}{\partial t}\right)\frac{\partial u}{\partial y}, \tag{5.11}$$

$$\left(1+\lambda_1\frac{\partial}{\partial t}+\lambda_2\frac{\partial^2}{\partial t^2}\right)S_{xz}-\lambda_1 S_{yz}\frac{\partial u}{\partial y}-\lambda_2\left(\frac{\partial S_{yz}}{\partial t}\frac{\partial u}{\partial y}+S_{yz}\frac{\partial^2 u}{\partial y \partial t}\right)=0, \tag{5.12}$$

$$\left(1+\lambda_1\frac{\partial}{\partial t}+\lambda_2\frac{\partial^2}{\partial t^2}\right)S_{yy}=0, \tag{5.13}$$

$$\left(1+\lambda_1\frac{\partial}{\partial t}+\lambda_2\frac{\partial^2}{\partial t^2}\right)S_{yz}=0, \tag{5.14}$$

and

$$\left(1+\lambda_1\frac{\partial}{\partial t}+\lambda_2\frac{\partial^2}{\partial t^2}\right)S_{zz}=0. \tag{5.15}$$

Having in mind the initial conditions of form

$$\boldsymbol{S}(y,0)=\frac{\partial \boldsymbol{S}(y,0)}{\partial t}=0, \tag{5.16}$$

Eqs. (5.12)-(5.15) becomes

$$S_{yy}=S_{yz}=S_{zz}=S_{xz}=0. \tag{5.17}$$

5.4 Statement of the Problem

Let us consider an incompressible, laminar and unsteady Burgers fluid lies between two plates that are parallel to each other at a distance d apart. Porous medium is taken into consideration. The flow is considered along $x-$axis. Initially the plate is at rest. After some time $t>0$, we have considered two cases: (i) constantly accelerating flow, and (ii) sine oscillation motion of the velocity. Moreover, the fluid above the plate is slowly displaced by shear. Introducing, the velocity field given by Eq. $(5.6)_a$ into Eq. (5.10) and (5.11) and since $\boldsymbol{V}(0,y)=0$ and $\boldsymbol{S}(y,0)=0,\ 0\le y\le d$, then

$$\left(1+\lambda_1\frac{\partial}{\partial t}+\lambda_2\frac{\partial^2}{\partial t^2}\right)\tau(\mathrm{y},\mathrm{t})=\mu\left(1+\lambda_3\frac{\partial}{\partial t}\right)\frac{\partial u}{\partial y}, \tag{5.18}$$

and

$$\left(1+\lambda_1\ \frac{\partial}{\partial t}+\lambda_2\frac{\partial^2}{\partial t^2}\right)\sigma_x-2\lambda_1\tau\frac{\partial u}{\partial y}-2\lambda_2\left(\frac{\partial\tau}{\partial t}\frac{\partial u}{\partial y}+\tau\frac{\partial^2 u}{\partial y\partial t}\right)=-2\mu\lambda_3\left(\frac{\partial u}{\partial y}\right)^2, \quad (5.19)$$

where $\tau(y,t)=S_{xy}(y,t)$ and $\sigma_x = S_{xx}$ are the non-zero tangential stress. Linear momentum equilibrium (5.2), without body forces can be expressed in component form as

$$\rho\frac{\partial u}{\partial t}=-\frac{\partial p}{\partial x}+\frac{\partial\tau(y,t)}{\partial y}+R_x, \quad (5.20)$$

$$0=-\frac{\partial p}{\partial y}, \quad (5.21)$$

and

$$0=-\frac{\partial p}{\partial z}, \qquad \Rightarrow p \neq p(y,z) \quad (5.22)$$

where $R_x(y,t)$, the Darcy resistance along $x-$ axis that satisfy the relation [20]:

$$\left(1+\lambda_1\frac{\partial}{\partial t}+\lambda_2\frac{\partial^2}{\partial t^2}\right)R_x(y,t)=-\frac{\mu\varphi}{k}\left(1+\lambda_3\frac{\partial}{\partial t}\right)u(y,t), \quad (5.23)$$

Eliminating $\tau(y,t)$ among Eqs. (5.18) and (5.20) and using Eq. (5.23), to get the linear third order differential equation of Burgers fluid when constant pressure is applied in the flow direction, the problem is governed by

$$\left(1+\lambda_1\ \frac{\partial}{\partial t}+\lambda_2\frac{\partial^2}{\partial t^2}\right)\frac{\partial u(y,t)}{\partial t}=\nu\left(1+\lambda_3\frac{\partial}{\partial t}\right)\frac{\partial^2 u}{\partial y^2}-\frac{\nu\varphi}{k}\left(1+\lambda_3\frac{\partial}{\partial t}\right)u(y,t), \quad 0\le y\le d, \ \ t>0, \quad (5.24)$$

in which $\nu = \mu/\rho$ is the kinematic viscosity.

The suitable initial restrictions are defined below:

I.C $$u(y,0) = 0, \quad \left.\frac{\partial u(y,t)}{\partial t}\right|_{t=0} = 0, \quad \left.\frac{\partial^2 u(y,t)}{\partial t^2}\right|_{t=0}; \quad 0 \le y \le d, \tag{5.25}$$

and the boundary conditions are defined for two cases:

B.C $$u(0,t) = At, \; u(d,t) = 0; \; t > 0, \tag{5.26}$$

for the movement caused by the constantly accelerating bottom plate and

B.C $$u(0,t) = U\,sin(\omega t), \quad u(d,t) = 0; \; t > 0, \tag{5.27}$$

for the flow due to oscillation of the bottom plate, in which A is acceleration, U is the amplitude of velocity and ω the frequency of oscillations.

5.5 Solution of the Problem

5.5.1. Case I: Flow due to accelerating bottom plate

Dimensionless variables are defined to create the proposed model non-dimensional:

$$y^* = \frac{y}{d}, \quad t^* = \frac{t}{\sqrt[3]{A^2/\nu}}, \quad u^* = \frac{u}{\sqrt[3]{A\nu}}, \quad \tau^* = \frac{\tau}{\rho dA}, \quad \sigma_x^* = \frac{\sigma_x}{\rho dA}. \tag{5.28}$$

Using the dimensionless quantities from Eq. (5.28) into Eqs. (5.24)–(5.26) and removing the star notation, the non-dimensional initial and boundary value problem takes the following form

$$\left(1 + We\,\frac{\partial}{\partial t} + \lambda_2^* \frac{\partial^2}{\partial t^2}\right)\frac{\partial u(y,t)}{\partial t} = \frac{1}{Re}\left(1 + \lambda_3^* \frac{\partial}{\partial t}\right)\frac{\partial^2 u(y,t)}{\partial y^2} - K\left(1 + \lambda_3^* \frac{\partial}{\partial t}\right)u(y,t),$$
$$0 < y < 1, \; t > 0, \tag{5.29}$$

and the non-dimensional initial and boundary conditions are given below

I.C $$u(y,0) = \frac{\partial u(y,t)}{\partial t}\Big|_{t=0} = 0, \quad \frac{\partial^2 u(y,t)}{\partial t^2}\Big|_{t=0} = 0, \text{ for } 0 \le y \le 1; \tag{5.30}$$

and

B.C $$u(0,t) = t, \quad u(1,t) = 0, \quad \text{for} \quad t > 0. \tag{5.31}$$

Here, in Eq. (5.29), K is the porosity parameter, Re is the Reynolds number and We is the Weissenberg number given below;

$$Re = \frac{\eta d}{\nu}, \quad We = \lambda_1 \frac{\eta}{d}, \quad K = \frac{\phi \nu \sqrt[3]{\nu}}{k \sqrt[3]{A^2}}, \qquad \lambda_2^* = \lambda_2 \frac{U^2}{d^2}, \qquad \lambda_3^* = \lambda_3 \frac{\eta}{d}, \tag{5.32}$$

where the characteristic velocity is given by $\eta = d \sqrt[3]{A^2/\nu}$ is. Dimensionless forms of the Eq. (5.18) and (5.19) are given below

$$\left(1 + We \frac{\partial}{\partial t} + \lambda_2^* \frac{\partial^2}{\partial t^2}\right) \tau(y,t) = \frac{1}{Re}\left(1 + \lambda_3^* \frac{\partial}{\partial t}\right) \frac{\partial u(y,t)}{\partial y}, \tag{5.33}$$

and

$$\left(1 + We \frac{\partial}{\partial t} + \lambda_2^* \frac{\partial^2}{\partial t^2}\right) \sigma_x(y,t) = 2\beta\, \tau(y,t) \frac{\partial u(y,t)}{\partial y} - 2\lambda_2^* \left(\frac{\partial \tau}{\partial t} \frac{\partial u}{\partial y} + \tau \frac{\partial^2 u}{\partial y \partial t}\right) - 2\mu\lambda_3^* \left(\frac{\partial u}{\partial y}\right)^2, \tag{5.34}$$

where the constant $\beta = \lambda_1 \sqrt[3]{A\nu}/d$. The initial conditions that correspond to this are:

$$\tau(y,0) = \left.\frac{\partial \tau(y,t)}{\partial t}\right|_{t=0} = 0, \quad 0 \le y \le 1, \tag{5.35}$$

and

$$\sigma_x(y,0) = \left.\frac{\partial \sigma_x(y,t)}{\partial t}\right|_{t=0} = 0, \qquad 0 \le y \le 1. \tag{5.36}$$

Multiplying Eq. (5.29) by $sin(\lambda_n y)$, where $\lambda_n = n\pi$, integrating the result with respect to y between zero and one and having in mind the boundary restrictions (5.31), it follows that

$$Re\,\lambda_2^* \frac{\partial^3 u_{Fn}(t)}{\partial t^3} + Re\,We \frac{\partial^2 u_{Fn}(t)}{\partial t^2} + (Re + \lambda_3^* \mu_n^2) \frac{\partial u_{Fn}(t)}{\partial t} + \mu_n^2\, u_{Fn}(t) = \left(1 + \lambda_3^* \frac{\partial}{\partial t}\right) \lambda_n\, t;$$

$$t > 0, \tag{5.37}$$

with the initial conditions:

$$u_{Fn}(0) = \left.\frac{du_{Fn}(t)}{dt}\right|_{t=0} = \left.\frac{\partial^2 u_{Fn}(t)}{\partial t^2}\right|_{t=0} = 0\,; \quad n = 1, 2, 3\,\ldots., \tag{5.38}$$

where $u_{Fn}(t)$ is FFST of $u(y,t)$.

The solution of the Eq. (5.37) by using initial conditions (5.38), is given below:

$$u_{Fn}(t) = \frac{\lambda_n(\mu_n^2(\mathrm{r}_{3n} + \mathrm{r}_{1n}) + Re\,\mathrm{r}_{1n}\mathrm{r}_{3n})}{(\mathrm{r}_{3n} - \mathrm{r}_{2n})(\mathrm{r}_{2n} - \mathrm{r}_{1n})}\, e^{r_{2n}t} - \frac{\lambda_n(\mu_n^2(\mathrm{r}_{3n} + \mathrm{r}_{2n}) + Re\,\mathrm{r}_{2n}\mathrm{r}_{3n})}{(\mathrm{r}_{2n} - \mathrm{r}_{1n})(\mathrm{r}_{3n} - \mathrm{r}_{1n})}\, e^{r_{1n}t}$$

$$+ \frac{\lambda_n(\mu_n^2(\mathrm{r}_{2n} + \mathrm{r}_{1n}) + Re\,\mathrm{r}_{2n}\mathrm{r}_{1n})}{(\mathrm{r}_{3n} - \mathrm{r}_{2n})(\mathrm{r}_{3n} - \mathrm{r}_{1n})}\, e^{r_{3n}t} + \frac{\lambda_n}{\mu_n^2}\left(t - \frac{Re}{\mu_n^2}\right), \tag{5.39}$$

where

$$\mathrm{r}_{1n} = -\frac{We}{3\lambda_2^*} - \frac{2^{1/3}\left((-Re^2We^2)/\lambda_2^* + 3Re(Re + \lambda_3^*\mu_n^2)\right)}{3ReA} + \frac{A}{32^{1/3}Re\lambda_2^*}, \qquad (a)$$

$$\mathrm{r}_{2n} = -\frac{We}{3\lambda_2^*} + \frac{\left(1 + i\sqrt{3}\right)\left((-Re^2We^2)/\lambda_2^* + 3Re(Re + \lambda_3^*\mu_n^2)\right)}{3 \times 2^{2/3}ReA} - \frac{\left(1 - i\sqrt{3}\right)A}{6 \times 2^{1/3}Re\lambda_2^*}, \qquad (b)$$

$$r_{3n} = -\frac{We}{3\lambda_2^*} + \frac{\left(1 - i\sqrt{3}\right)\left((-Re^2We^2)/\lambda_2^* + 3Re(Re + \lambda_3^*\mu_n^2)\right)}{3 \times 2^{2/3}ReA} - \frac{\left(1 + i\sqrt{3}\right)A}{6 \times 2^{1/3}Re\lambda_2^*}, \qquad (c)$$

are roots of above Eq. (5.39), in which $\mu_n^2 = \lambda_n^2 + K\,Re$ and

$$\mathrm{A} = -2\mathrm{Re}^3\mathrm{We}^3 + 9\mathrm{Re}^3\mathrm{We}\lambda_2^* - 27\mathrm{Re}^2{\lambda_2^*}^2\mu_n^2 + 9\mathrm{Re}^2\mathrm{We}\lambda_2^*\,\lambda_3^*\mu_n^2\,\sqrt[\frac{1}{3}]{(-2\mathrm{Re}^3\mathrm{We}^3 + 9\mathrm{Re}^3\mathrm{We}\lambda_2^*}$$

$$+\sqrt{-27\mathrm{Re}^2{\lambda_2^*}^2\mu^2 + 9\mathrm{ZRe}^2\mathrm{We}\lambda_2^*\lambda_3^*\mu_n^2)^2 + 4(-\mathrm{Re}^2\mathrm{We}^2 + 3\mathrm{Re}\lambda_2^*(\mathrm{Re} + \lambda_3^*\mu_n^2))^3}^{1/3}. \qquad (d)$$

By applying inverse FFST to Eq. (5.39), the following velocity profile is obtained:

$$u(y,t) = 2\sum_{n=1}^{\infty}\{t - (Re/\,\mu_n^2)$$
$$- [(\mu_n^2(\mathrm{r}_{3n} + \mathrm{r}_{1n}) + Re\;\mathrm{r}_{1n}\mathrm{r}_{3n})(\mathrm{r}_{3n} - \mathrm{r}_{1n})\,e^{r_{2n}t}][(\mu_n^2\;(\mathrm{r}_{3n} - \mathrm{r}_{2n})$$

$$\times (\mathrm{r}_{2n} - \mathrm{r}_{1n})\;\;(\mathrm{r}_{3n} - \mathrm{r}_{1n})] - [\;(\,\mu_n^2\;(\,\mathrm{r}_{3n} + \mathrm{r}_{2n}\,) + \;Re\,\mathrm{r}_{2n}\;\,\mathrm{r}_{3n})\;(\mathrm{r}_{3n} - \mathrm{r}_{2n})\;\,e^{\,r_{1n}t}\,]$$

$$\times [\mu_n^2(\mathrm{r}_{3n}-\mathrm{r}_{2n})(\mathrm{r}_{2n}-\mathrm{r}_{1n})(\mathrm{r}_{3n}-\mathrm{r}_{1n})] + [(\mu_n^2(\mathrm{r}_{2n}+\mathrm{r}_{1n}) + Re\ \mathrm{r}_{1n}\mathrm{r}_{2n})(\mathrm{r}_{2n}-\mathrm{r}_{1n})$$

$$\times\ e^{r_{3n}t})]\lambda_n \sin(\lambda_n y) / \mu_n^2\}/ [\mu_n^2(\mathrm{r}_{3n}-\mathrm{r}_{2n})(\mathrm{r}_{2n}-\mathrm{r}_{1n})(\mathrm{r}_{3n}-\mathrm{r}_{1n})], \tag{5.40}$$

or equivalently

$$u(y,t) = (1-\mathrm{y})\mathrm{t} - 2\ \mathrm{t}\,\mathrm{K}\ \mathrm{Re}\sum_{n=1}^{\infty}\frac{\sin(\lambda_n y)}{\lambda_n\mu_n^2} + 2\sum_{n=1}^{\infty}\{1$$

$$-\frac{(\mu_n^2(\mathrm{r}_{3n}+\mathrm{r}_{1n})+Re\ \mathrm{r}_{1n}\mathrm{r}_{3n})(\mathrm{r}_{3n}-\mathrm{r}_{1n})e^{r_{2n}t}}{\mu_n^2(\mathrm{r}_{3n}-\mathrm{r}_{2n})(\mathrm{r}_{2n}-\mathrm{r}_{1n})(\mathrm{r}_{3n}-\mathrm{r}_{1n})} + \frac{-(\mu_n^2(\mathrm{r}_{3n}+\mathrm{r}_{2n})+Re\ \mathrm{r}_{2n}\mathrm{r}_{3n})(\mathrm{r}_{3n}-\mathrm{r}_{2n})e^{r_{1n}t}}{\mu_n^2(\mathrm{r}_{3n}-\mathrm{r}_{2n})(\mathrm{r}_{2n}-\mathrm{r}_{1n})(\mathrm{r}_{3n}-\mathrm{r}_{1n})}$$

$$+\frac{(\mu_n^2(\mathrm{r}_{2n}+\mathrm{r}_{1n})+Re\ \mathrm{r}_{1n}\mathrm{r}_{2n})(\mathrm{r}_{2n}-\mathrm{r}_{1n})e^{r_{3n}t}}{\mu_n^2(\mathrm{r}_{3n}-\mathrm{r}_{2n})(\mathrm{r}_{2n}-\mathrm{r}_{1n})(\mathrm{r}_{3n}-\mathrm{r}_{1n})}\Big\}\frac{\lambda_n\sin(\lambda_n y)}{\mu_n^2}. \tag{5.41}$$

Introducing $u(y,t)$ from Eq. (5.41) into Eq. (5.33) and integrating the result by keeping in mind the initial condition Eq. (5.35), its result that:

$$\tau(y,t) = -t/Re + (We/Re)[1-\exp(-t/(\lambda_2^* + We)] - 2K\sum_{n=1}^{\infty}\{t - (We - (\lambda_n^2/K\ \mu_n^2)$$

$$\times\ [1-\exp(-t/(\lambda_2^* + We)]\cos(\lambda_n y)/\mu_n^2 - 2/\lambda_2^*\sum_{n=1}^{\infty}\{[\mu_n^2(\mathrm{r}_{3n}+\mathrm{r}_{1n})$$

$$+Re\ \mathrm{r}_{1n}\mathrm{r}_{3n}(\mathrm{r}_{3n} - \mathrm{r}_{1n})e^{r_{2n}t}]/(r_{2n}^2\lambda_2^* + We\ r_{2n} + 1) + [(\mu_n^2(\mathrm{r}_{3n}+\mathrm{r}_{2n})$$

$$+Re\ \ \mathrm{r}_{2n}\mathrm{r}_{3n})\ (\mathrm{r}_{3n}-\mathrm{r}_{2n})e^{r_{1n}t}\ ]/\ (\ r_{1n}^2\lambda_2^*+We\ r_{1n}+1)-[\mu_n^2(\mathrm{r}_{2n}+\mathrm{r}_{1n})$$

$$+Re\ \mathrm{r}_{1n}\mathrm{r}_{2n}\ (\mathrm{r}_{2n}-\mathrm{r}_{1n})e^{r_{3n}t}]\ \ /\ \ (\ r_{3n}^2\ \lambda_2^*+We\ r_{3n}+1)\ \lambda_n^2\ \ \cos\ \ (\lambda_n y)\}$$

$$/[(\ \mathrm{r}_{3n}-\mathrm{r}_{2n})\ (\ \mathrm{r}_{2n}-\mathrm{r}_{1n})(\ \mathrm{r}_{3n}-\mathrm{r}_{1n}\ )\ \mu_n^4]+\ \ 2/Re\ \ \ \exp\ \ (-t/\ (\lambda_2^*+\ \ We\ )$$

$$+\sum_{n=1}^{\infty}\left\{\begin{pmatrix}[(\mu_n^2(\mathrm{r}_{3n}+\mathrm{r}_{1n})+Re\ \mathrm{r}_{1n}\mathrm{r}_{3n})(\mathrm{r}_{3n}-\mathrm{r}_{1n})(r_{1n}^2\ \lambda_2^*+Wer_{3n}+1)(r_{1n}^2\lambda_2^*+Wer_{1n}+1)]\\ -[(\mu_n^2(\mathrm{r}_{3n}+\mathrm{r}_{2n})+Re\ \mathrm{r}_{2n}\mathrm{r}_{3n})(\mathrm{r}_{3n}-\mathrm{r}_{2n})(r_{2n}^2\lambda_2^*+Wer_{3n}+1)(r_{2n}^2\lambda_2^*+Wer_{2n}+1)]\\ +[(\mu_n^2(\mathrm{r}_{2n}+\mathrm{r}_{1n})+(Re\ \mathrm{r}_{1n}\mathrm{r}_{2n})(\mathrm{r}_{2n}-\mathrm{r}_{1n})(r_{3n}^2\lambda_2^*+Wer_{2n}+1)(r_{3n}^2\lambda_2^*+Wer_{3n}+1)]\\ /[(\mathrm{r}_{3n}-\mathrm{r}_{2n})(\mathrm{r}_{2n}-\mathrm{r}_{1n})(\mathrm{r}_{3n}-\mathrm{r}_{1n})(r_{1n}^2\lambda_2^*+Wer_{1n}+1)(r_{2n}^2\lambda_2^*+Wer_{2n}+1)\end{pmatrix}\right.$$

$$\left.\times\ (r_{3n}^2\lambda_2^*+Wer_{3n}+1)]\ \lambda_n^2\cos(\lambda_n y)/\mu_n^4\right\},$$

(5.42)

5.5.2 Special cases

(i) By taking $K \to 0$, above Eq. (5.41) becomes

$$u(y,t)=(1-\mathrm{y})\ \mathrm{t}+2\ \sum_{n=1}^{\infty}\left\{1-\frac{(\lambda_n^2(\mathrm{r}_{6n}+\mathrm{r}_{4n})+Re\ \mathrm{r}_{4n}\mathrm{r}_{6n})(\mathrm{r}_{6n}-\mathrm{r}_{4n})e^{r_{5n}t}}{\lambda_n^2(\mathrm{r}_{6n}-\mathrm{r}_{5n})\ (\mathrm{r}_{5n}-\mathrm{r}_{4n})\ \ (\mathrm{r}_{6n}-\mathrm{r}_{4n})}\right.$$
$$+\frac{-(\lambda_n^2\ (\mathrm{r}_{6n}+\mathrm{r}_{5n})\ \ +Re\ \ \mathrm{r}_{5n}\ \mathrm{r}_{6n})\ (\mathrm{r}_{6n}\ -\mathrm{r}_{5n})\ \ e^{\,r_{4n}t}}{\lambda_n^2\ \ (\mathrm{r}_{6n}-\mathrm{r}_{5n})\ (\mathrm{r}_{5n}-\mathrm{r}_{4n})\ \ (\mathrm{r}_{6n}-\mathrm{r}_{4n})}$$
$$\left.+\frac{(\lambda_n^2(\mathrm{r}_{5n}+\mathrm{r}_{4n})+Re\ \mathrm{r}_{4n}\mathrm{r}_{5n})(r_{5n}-\mathrm{r}_{4n}\ )\ e^{r_{6n}t}}{\lambda_n^2(\mathrm{r}_{6n}-\mathrm{r}_{5n})\ (\mathrm{r}_{5n}-\mathrm{r}_{4n})\ \ (\mathrm{r}_{6n}-\mathrm{r}_{4n})}\right\}\frac{\lambda_n\sin(\lambda_n^2 y)}{\lambda_n^2},$$

(5.43)

where r_{4n}, $r_{5n}and\ \ r_{6n}$ are the roots of above equation and defined below

$$\mathrm{r}_{4n} = -\frac{We}{3\lambda_2^*} - \frac{2^{1/3}\left((-Re^2We^2)/\lambda_2^* + 3Re(Re + \lambda_3^*\lambda_n^2)\right)}{3ReA} + \frac{A}{32^{1/3}Re\lambda_2^*}, \qquad (e)$$

$$\mathrm{r}_{5n} = -\frac{We}{3\lambda_2^*} + \frac{\left(1 + i\sqrt{3}\right)\left((-Re^2We^2)/\lambda_2^* + 3Re(Re + \lambda_3^*\lambda_n^2)\right)}{3 \times 2^{2/3}ReA} - \frac{\left(1 - i\sqrt{3}\right)A}{6 \times 2^{1/3}Re\lambda_2^*}, \qquad (f)$$

$$\mathrm{r}_{6n} = -\frac{W}{3\lambda_2^*} + \frac{\left(1 - i\sqrt{3}\right)\left((-Re^2We^2)/\lambda_2^* + 3Re(Re + \lambda_3^*\lambda_n^2)\right)}{3 \times 2^{2/3}ReA} - \frac{\left(1 + i\sqrt{3}\right)A}{6 \times 2^{1/3}Re\lambda_2^*}, \qquad (g)$$

in which

$$\mathrm{A} = -2\mathrm{Re}^3\mathrm{We}^3 + 9\mathrm{Re}^3\mathrm{We}\lambda_2^* - 27\mathrm{Re}^2{\lambda_2^*}^2\lambda_n^2 + 9\mathrm{Re}^2\mathrm{We}\lambda_2^*\,\lambda_3^*\lambda_n^2\sqrt[\frac{1}{3}]{(-2\mathrm{Re}^3\mathrm{We}^3 + 9\mathrm{Re}^3\mathrm{We}\lambda_2^*} + \sqrt{-27\mathrm{Re}^2{\lambda_2^*}^2\lambda_n^2 + 9\mathrm{ZRe}^2\mathrm{We}\lambda_2^*\lambda_3^*\lambda_n^2)^2 + 4(-\mathrm{Re}^2\mathrm{We}^2 + 3\mathrm{Re}\lambda_2^*(\mathrm{Re} + \lambda_3^*\lambda_n^2))^3}^{1/3}, \qquad (h)$$

(ii) Taking $\lambda_2^* \to 0$ in Eqs. (5.41), We obtain similar solutions that relate to incompressible Oldroyd-B fluid executing same motions as

$$u_{OB}(y,t) = (1 - y)t - 2tKRe\sum_{n=1}^{\infty}\frac{\sin(\lambda_n y)}{\lambda_n\mu_n^2} - 2Re\sum_{n=1}^{\infty}\{1 + \frac{(\mu_n^2 + Re\ r_{7n})\,e^{r_{8n}t} + (\mu_n^2 + Re\ r_{8n})\,e^{r_{7n}t}}{Re(r_{8n} - r_{7n})}\}\frac{\lambda_n \sin(\lambda_n y)}{\mu_n^4}, \qquad (5.44)$$

where $r_{7n}, r_{8n} = [-1 - \mu_n^2\lambda_3^*/Re + \sqrt{-4We\,\mu_n^2 + (1 + \mu^2\lambda_3^*/Re)^2}]/(2\mathrm{We})$.

(iii) Taking $\lambda_2^* \to 0$ and $\lambda_3 \to 0$ in Equations (5.41), we obtain similar solutions that relate to incompressible Maxwell fluid executing identical motions

$$u_M(y,t) = (1 - y)t - 2tKRe \sum_{n=0}^{\infty} \frac{\sin(\lambda_n y)}{\lambda_n \mu_n^2} - 2Re \sum_{n=1}^{\infty} \{1 + \frac{(\mu_n^2 + Re\ r_{9n})\, e^{r_{10n}t} + (\mu_n^2 + Re\ r_{10n})\, e^{r_{9n}t}}{Re(r_{10n} - r_{9n})}\} \frac{\lambda_n \sin(\lambda_n y)}{\mu_n^4}, \quad (5.45)$$

Where $r_{9n}, r_{10n} = [-1 \pm \sqrt{1 - 4We\mu_n^2/Re}]\,/(2We)$.

(iv) Taking $We \to 0$, $\lambda_2 \to 0$ and $\lambda_3 \to 0$ in Eq. (5.41), we obtain similar solutions that relate to incompressible Newtonian fluids executing identical motions ([17], Eq. (29)) i.e;

$$u_N(y,t) = (1 - y)t - 2tKRe \sum_{n=1}^{\infty} \frac{\sin(\lambda_n y)}{\lambda_n \mu_n^2} - 2Re \sum_{n=1}^{\infty} \frac{\lambda_n \sin(\lambda_n y)}{\mu_n^2} \left[1 - \exp(-\frac{\mu_n^2}{Re} t)\right], \quad (5.46)$$

(v) By taking $We \to 0$, $\lambda_2^* \to 0$and $\lambda_3^* \to 0$ into Eq. (5.42), the similar solution for Newtonian fluid is retrieved for the tangential stress in the following form:

$$\tau_N(y,t) = -\frac{t}{Re} - 2tK \sum_{n=0}^{\infty} \frac{\cos(\lambda_n y)}{\mu_n^2} - 2 \sum_{n=0}^{\infty} \frac{\cos(\lambda_n y)}{\mu_n^4} \left[1 - \exp\left(-\frac{\mu_n^2}{Re} t\right)\right]. \quad (5.47)$$

Moreover, the long-time solutions adequately represent the fluid motion at large values of time t:

$$\mathrm{u_{Lt}(y,t)} = (1 - \mathrm{y})\mathrm{t} - 2\mathrm{Re} \sum_{n=1}^{\infty} \left(t\, K + \frac{\lambda_n^2}{\mu_n^2}\right) \frac{\sin(\lambda_n y)}{\lambda n \mu_n^2}, \quad (5.47a)$$

And

$$\tau_{Lt}(y,t) = -\frac{(-t+We)}{Re} - 2K\sum_{n=1}^{\infty}\left(t - We + \frac{\lambda_n^2}{\mu_n^2}\right)\frac{\cos(\lambda_n y)}{\mu_n^2}. \quad (5.47b)$$

5.5.3 Case II: Flow due to oscillatory motion of the bottom plate:

Let us consider following non-dimensional variables:

$$y^* = \frac{y}{d}, \quad t^* = \frac{t\,U}{d}, \quad u^* = \frac{u}{U}, \quad \tau^* = \frac{\tau}{\rho\,U^2}, \quad \sigma_x^* = \frac{\sigma_x}{\rho\,U^2}, \quad \omega^* = \frac{\omega\,d}{U}. \quad (5.48)$$

Introducing Eq. (5.48), into Eqs. (5.24)-(5.25) and (5.27), the dimensionless problem obtained same as Eq. (5.29) and (5.30) after removing the star notation in which:

$$Re = \frac{\eta d}{v}, \quad We = \lambda_1\frac{\eta}{d}, \quad K = \frac{\phi v\sqrt[3]{v}}{k\sqrt[3]{A^2}}, \quad \lambda_2^* = \lambda_2\frac{U^2}{d^2}, \quad \lambda_3^* = \lambda_3\frac{\eta}{d}, \quad (5.49)$$

While the boundary restrictions are given below

$$u(0,t) = sin(\omega t);\ t > 0, \quad (5.50)$$

and

$$u(1,t) = 0;\ \ t > 0. \quad (5.51)$$

Again, apply FFST to Eq. (5.29) and bear in mind the restrictions (5.50) and (5.51), we obtain:

$$Re\lambda_2^* \frac{\partial^3 u_{Fn}(t)}{\partial t^3} + ReWe \frac{\partial^2 u_{Fn}(t)}{\partial t^2} + (Re + \lambda_3^* \mu_n^2) \frac{\partial u_{Fn}(t)}{\partial t} + \mu_n^2 u_{Fn}(t)$$

$$= \lambda_n \sin(\omega t) + \lambda_n \lambda_3^* \omega \cos(\omega t);\ t > 0. \tag{5.52}$$

The solution of the Eq. (5.52) using the initial conditions (5.38) is given in following form:

$$\begin{aligned} u_{Fn}(\mathrm{t}) = [\eta_1 \cos(\omega \mathrm{t}) + \eta_2 \sin(\omega \mathrm{t})]\lambda_n + [\eta_2 \ (r_{3n}^2 - r_{2n}^2)\omega - \eta_1(r_{3n}r_{2n} - \omega^2) \\ + e^{r_{1n}t}] - [\eta_2(r_{1n}^2 - r_{3n}^2)\omega + \eta_1(r_{3n}r_{1n} - \omega^2) \ e^{r_{2n}t}] + [\eta_2(r_{2n}^2 - r_{1n}^2)\omega \\ - \eta_1(r_{1n}r_{2n} - \omega^2) \ e^{r_{1n}t}]/[\ (r_{3n} - r_{2n}) \ (r_{2n} - r_{1n}) \ (r_{3n} - r_{1n}) \ ]\lambda_n, \end{aligned} \tag{5.53}$$

where $\eta_1 = (d_n + \omega\lambda_3^* a_n)/(d_n^2 + a_n^2)$, $\eta_2 = (a_n - \omega\lambda_3^* d_n)/(d_n^2 + a_n^2)$

$$d_n = \omega^3 Re\lambda_2^* - \omega(Re + \lambda_3^* \mu_n^2), \quad \text{and} \quad a_n = \mu_n^2 - WeRe\omega^2 \tag{5.54}$$

Now by applying the inverse FFST to Eq. (5.53), the result is that the dimensionless velocity field $u_s(y,t)$ can written as

$$u_s(y,t) = u_{sp}(y,t) + u_{st}(y,t), \tag{5.55}$$

in which

$$u_{sp}(y,t) = 2\sum_{n=1}^{\infty}(\eta_1 \cos(\omega \mathrm{t}) + \eta_2 \sin(\omega \mathrm{t}))\, \lambda_n \sin(\lambda_n y), \tag{5.56}$$

and

$$u_{st}(y,t) = 2\sum_{n=1}^{\infty}\{[\eta_2(r_{3n} + r_{2n})\omega - \eta_1(r_{3n}r_{2n} - \omega^2)e^{r_{1n}t}](r_{3n} - r_{2n}) - [\eta_2(r_{1n} + r_{3n})\omega$$

$$+\eta_1(r_{3n}r_{1n}-\omega^2)e^{r_{2n}t}](r_{3n}-r_{1n})+[\eta_2(r_{2n}+r_{1n})\omega-\eta_1(r_{1n}r_{2n}-\omega^2)e^{r_{1n}t}]$$

$$\times(r_{2n}-r_{1n})/\left[(r_{3n}-r_{2n})(r_{2n}-r_{1n})(r_{3n}-r_{1n})\right]\}\lambda_n\sin(\lambda_n y), \tag{5.57}$$

here $u_{sp}(y,t)$ is the permanent and $u_{st}(y,t)$ is the transient solution.

Moreover, Eq. (5.56) can also be written as

$$u_{sp}(y,t)=(1-\mathrm{y})\sin(\omega\mathrm{t})+2\sum_{n=1}^{\infty}\{(\eta_2(\mathrm{Re}(\mathrm{We}\omega^2-\mathrm{K})-\ \mathrm{a}_n)\sin(\omega\mathrm{t})$$

$$+\ \eta_1\ \cos(\ \omega\ \mathrm{t})\ )\ \ \lambda_n^2)\}\sin(\lambda_n y). \tag{5.58}$$

Generalized form of $u_{sp}(y,t)$ can be written as:

$$u_{sp}\ (y,t)=-\mathrm{Im}\left\{\frac{1}{(1+\mathrm{i}\omega\lambda_3^*)\delta}e^{-\delta y+i\omega t}\right\};\ \delta=\sqrt{\frac{(-\lambda_2^*\omega^2-\mathrm{i}\omega\mathrm{We})\mathrm{i}\omega+\mathrm{K}(1+\mathrm{i}\omega)}{(1+\mathrm{i}\omega\lambda_3^*)}}, \tag{5.59}$$

where “Im” denotes the imaginary component.

Also, the expression for shear stress $\tau_s(y,t)$ can be written in the following form

$$\tau_s(y,t)=\tau_{sp}(y,t)+\tau_{st}(y,t), \tag{5.60}$$

where

$$\tau_{sp}(y,t) = [(1/\ [(1-\omega^2\lambda_2^*)^2 - (\omega\, We)^2\ ])(2(1-\omega^2\lambda_2^*)^2)/\, Re)\sum_{n=1}^{\infty}[\lambda_n^3\ \eta_2 cos(\,\lambda_n y)$$
$$+(We\omega/Re) - 2We\omega\lambda_n\sum_{n=1}^{\infty}\eta_1 Re(We\omega^2 - K) - a_n)\cos(\lambda_n y)]\ \cos[\omega\, t]$$
$$+[(\ 2/Re\ We\omega)\sum_{n=1}^{\infty}\lambda_n^3\,\eta_2\cos(\lambda_n y) - (\,1-\omega^2\lambda_2^*)[\,1/\ [(1-\omega^2\lambda_2^*)^2$$
$$-(\omega\, We)^2]\ )\,(2\,(1-\omega^2\ \ \lambda_2^*)^2)/\, Re)\sum_{n=1}^{\infty}\ [\lambda_n^3\ \ \eta_2 cos(\,\lambda_n y)$$
$$+(We\omega/Re) - 2We\omega\lambda_n\sum_{n=1}^{\infty}\eta_1 Re(We\omega^2 - K) - a_n)\cos(\lambda_n y)]\ \mathrm{s}\,in[\omega t]\,,$$

(5.61)

and

$$\tau_{st}(y,t) = \frac{2}{Re}\sum_{n=1}^{\infty}\left\{\frac{(1+\lambda_3^* r_{1n})[\eta_2(r_{3n}+r_{2n})\omega - \eta_1(r_{3n}r_{2n}-\omega^2)e^{r_{1n}t}]}{(r_{3n}\ -\ r_{1n})(r_{2n}\ -\ r_{1n})(r_{1n}^2 + Wer_{1n}+1)}\right.$$
$$-\ \ (1+\lambda_3^* r_{2n}\,)\frac{[\ \eta_2(r_{1n}+r_{3n})\omega + \eta_1(r_{3n}\ \ r_{1n}-\omega^2)\ \ e^{r_{2n}t}]}{(r_{3n}\ -\ r_{2n})(r_{2n}\ -\ r_{1n})(r_{2n}^2 + Wer_{2n}+1)}$$
$$\left.+(1+\lambda_3^* r_{3n}\,)\frac{[\eta_2(r_{2n}+r_{1n})\quad \omega - \eta_1\ \ (r_{1n}r_{2n}-\omega^2)\ \ e^{r_{3n}t}]}{(r_{3n}\ -\ r_{2n}\ \ )(r_{3n}\ -\ r_{1n})(r_{3n}^2 + We\, r_{3n}+1)}\right\}$$
$$\times\ \lambda_n^2\cos\ \ (\lambda_n y) - \frac{2}{Re}\,\mathrm{Exp}\left[-\frac{We}{\lambda_2^*}t\right]$$
$$\times\sum_{n=1}^{\infty}\left\{(1+\lambda_3^* r_{1n})\frac{[\eta_2(r_{3n}+r_{2n})\ \ \omega - \eta_1(r_{3n}r_{2n}-\omega^2)e^{r_{1n}t}]}{(r_{3n}\ -\ r_{1n})(r_{2n}\ -\ r_{1n})(r_{1n}^2 + Wer_{1n}+1)}\right.$$
$$-(1+\lambda_3^* r_{2n}\,)\frac{[\ \ \eta_2(r_{1n}+r_{3n})\omega + \eta_1(r_{3n}r_{1n}-\omega^2\,)\ \ e^{r_{2n}t}]}{(r_{3n}\ -\ r_{2n})(r_{2n}\ -\ r_{1n})(r_{2n}^2 + Wer_{2n}+1)}$$
$$\left.+(1+\lambda_3^* r_{3n}\,)\ \ \frac{[\eta_2(r_{2n}+r_{1n})\omega - \eta_1(r_{1n}r_{2n}-\omega^2)e^{r_{3n}t}]}{(r_{3n}\ -\ r_{2n})(r_{3n}\ -\ r_{1n})(r_{3n}^2 + Wer_{3n}+1)}\right\}$$
$$\times\ \lambda_n^2\cos(\lambda_n y) - \mathrm{Exp}\left[-\frac{We}{\lambda_2^*}t\right]\left\{\frac{\omega\, We - \omega^2\lambda_2^* + 1}{\left((\omega\, We)^2 - \left(\omega^2\lambda_2^* + 1\,\right)^2\right)Re}\right\}$$
$$-2\sum_{n=1}^{\infty}\frac{\lambda_n^2 + \left(\omega^2\lambda_2^* + 1\,\right)b_n}{[d_n^2 + a_n^2]\left((\omega\, We)^2 - \left(\omega^2\lambda_2^* + 1\,\right)^2\right)},$$

(5.62)

where b_n = (μ_n^2 $- ReWe\omega^2$)(Weω^2 − K) − Reω^2.

Generalized form of $\tau_{sp}(y,t)$ can be written as.

$$\tau_s(y,t) = \mathrm{Im}\left\{\frac{1}{(1-\lambda_2^*\omega^2-\mathrm{i}\omega\mathrm{We})} e^{-\delta\, y+i\omega t}\right\};\ \delta = \sqrt{\frac{(-\lambda_2^*\omega^2-\mathrm{i}\omega\mathrm{We})\mathrm{i}\omega+\mathrm{K}(1+\mathrm{i}\omega)}{(1+\mathrm{i}\omega\lambda_3^*)}}, \qquad (5.63)$$

is readily obtained in the same manner as for $u_{sp}(y,t)$.

5.5.4 Special cases

(i) Similarly, without porous medium Eqs. (5.58) and (5.57) take the simpler form as define below

$$u_{sp}(y,t) = (1-\mathrm{y})\sin(\omega\mathrm{t}) + 2\sum_{n=1}^{\infty}\{(\eta_2(\mathrm{Re}(\mathrm{We}\omega^2) - \mathrm{a}_n)\sin(\omega\mathrm{t}) + \eta_1\cos(\omega\ \mathrm{t})\ \lambda_n^2)\}\frac{\sin(\lambda_n y)}{\lambda_n}, \qquad (5.64)$$

and

$$u_{st}(y,t) = 2\sum_{n=1}^{\infty}\{(\lambda_n^2 - WeRe\omega^2) - \omega\lambda_3^* d_n)/(d_n^2 + (\lambda_n^2 - WeRe\omega^2)^2\,[(r_{6n}+r_{5n})\omega(r_{6n} - r_{5n}) - (r_{4n}+r_{6n})\omega(r_{6n}-r_{4n}) + (r_{5n} + r_{4n})\omega(r_{5n}-r_{4n})] - (d_n + \omega\lambda_3^*(\lambda_n^2 - WeRe\omega^2)/(d_n^2 + (\lambda_n^2 - WeRe\omega^2)^2)[(r_{3n}r_{2n} - \omega^2)e^{r_{4n}t}\ (r_{6n} - r_{5n}) + (r_{6n}r_{4n} - \omega^2)e^{r_{5n}t} \times (r_{6n} - r_{4n}) - (r_{4n}r_{5n} - \omega^2)e^{r_{6n}t}(r_{5n} - r_{4n})]/[(r_{6n} - r_{5n})(r_{5n} - r_{4n})(r_{6n} - r_{4n})]\} \times \lambda_n \sin(\lambda_n y), \qquad (5.65)$$

where r_{4n}, $r_{5n} and\ r_{6n}$ are the roots defined below

$$\mathrm{r}_{4n} = -\frac{We}{3\lambda_2^*} - \frac{2^{1/3}\left((-Re^2We^2)/\lambda_2^* + 3Re(Re + \lambda_3^*\lambda_n^2)\right)}{3ReA} + \frac{A}{32^{1/3}Re\lambda_2^*}, \qquad (e)$$

$$\mathrm{r}_{5n} = -\frac{We}{3\lambda_2^*} + \frac{\left(1 + i\sqrt{3}\right)\left((-Re^2We^2)/\lambda_2^* + 3Re(Re + \lambda_3^*\lambda_n^2)\right)}{3 \times 2^{2/3}ReA} - \frac{\left(1 - i\sqrt{3}\right)A}{6 \times 2^{1/3}Re\lambda_2^*}, \qquad (f)$$

$$\mathrm{r}_{6n} = -\frac{W}{3\lambda_2^*} + \frac{\left(1 - i\sqrt{3}\right)\left((-Re^2We^2)/\lambda_2^* + 3Re(Re + \lambda_3^*\lambda_n^2)\right)}{3 \times 2^{2/3}ReA} - \frac{\left(1 + i\sqrt{3}\right)A}{6 \times 2^{1/3}Re\lambda_2^*}, \qquad (g)$$

in which

$$\mathrm{A} = -2\mathrm{Re}^3\mathrm{We}^3 + 9\mathrm{Re}^3\mathrm{We}\lambda_2^* - 27\mathrm{Re}^2{\lambda_2^*}^2\lambda_n^2 + 9\mathrm{Re}^2\mathrm{We}\lambda_2^*\,\lambda_3^*\lambda_n^2\sqrt[\frac{1}{3}]{(-2\mathrm{Re}^3\mathrm{We}^3 + 9\mathrm{Re}^3\mathrm{We}\lambda_2^*} + \sqrt{-27\mathrm{Re}^2{\lambda_2^*}^2\lambda_n^2 + 9\mathrm{ZRe}^2\mathrm{We}\lambda_2^*\lambda_3^*\lambda_n^2)^2 + 4(-\mathrm{Re}^2\mathrm{We}^2 + 3\mathrm{Re}\lambda_2^*(\mathrm{Re} + \lambda_3^*\lambda_n^2))^3}^{1/3}, \qquad (h)$$

(i) Taking $\lambda_2^* \to 0$ in the Eqs. (5.56), (5.57), (5.61) and (5.62), we recover the similar solutions for Oldoryd-B fluid as follows

$$u_{OBsp}\,(y,t) = \frac{\lambda_3\, a_n + (Re + \lambda_3^*\,\mu^2)}{a_n^2 + \omega^2(Re + \lambda_3^*\,\mu^2)^2}\left(\cos(\omega\, t) + \frac{\omega(Re + \lambda_3\,\mu^2)}{a_n}\,\sin(\omega\, t)\right). \qquad (5.66)$$

(i) Taking $\lambda_2^* \to 0$ and $\lambda_3^* \to 0$ in the equalities (5.56) and (5.57) and (5.61) and (5.62), we recover the similar solutions for Maxwell fluid fluid in the following form

$$u_{Msp}\,(y,t) = (1 - y)\sin(\omega t) + 2Re\sum_{n=1}^{\infty}\{\,(a_n(\mathrm{We}\omega^2 - \mathrm{K}) - \mathrm{Re}\omega^2)$$

$$\times \sin(\omega t) - \omega\lambda_n^2\cos(\omega t))\,Sin(\lambda_n y)/\,\lambda_n\}/(a_n^2 + (\omega Re)^2), \qquad (5.67)$$

$$u_{Mst}(y,t) = 2\omega \sum_{n=1}^{\infty} \left\{ \frac{\left((a_n + Re\, r_{11n}) e^{\, r_{12n} t} - (a_n + Re\, r_{12n}) e^{r_{11n} t} \right)}{(r_{2n} - r_{1n}) \mu_n^4} \right\} \lambda_n Sin(\lambda_n y), \quad (5.68)$$

$$\tau_{sp}(y,t) = \frac{(\omega We\, cos(\omega t) - \sin(\omega t))}{[(\omega Re)^2 + 1] Re} + 2 \sum_{n=1}^{\infty} \left\{ \frac{\left(b_n - We\, \omega^2 \lambda_n^2\right) \sin(\omega t) - \omega \left(b_n We + \lambda_n^2\right) \cos(\omega t)}{\left[a_n^2 + (\omega Re)^2\right] [(\omega We)^2 + 1]} \right\} \cos(\lambda_n y), \quad (5.69)$$

and

$$\tau_{st}(y,t) = \frac{2\omega}{We} \sum_{n=1}^{\infty} \left\{ \frac{(a_n + Rer_{2n})(Wer_{12n} + 1) e^{\, r_{11n} t} - (a_n + Rer_{11n})(Wer_{11n} + 1) e^{\, r_{12n} t}}{(Wer_{12n} + 1)(r_{12n} - r_{1n})(Wer_{11n} + 1)[a_n^2 + (\omega Re)^2]} \right\} \lambda_n^2 \cos(\lambda_n y)$$

$$- \frac{2\omega}{We} e^{\left(-\frac{t}{We}\right)} \sum_{n=1}^{\infty} \left\{ \frac{(a_n + Rer_{12n})\ (Wer_{12n} + 1) e^{\, r_{11n} t} - \ (a_n + Rer_{11n})\ (Wer_{11n} + 1)\ e^{\, r_{12n} t}}{(Wer_{12n} + 1)(r_{12n} - r_{11n})(Wer_{11n} + 1)(a_n^2 + \ (\omega Re)^2)} \right\}$$

$$\times\ \lambda_n^2 \cos(\lambda_n\, y) - e^{\left(-\frac{t}{We}\right)} \left\{ \frac{\omega\, We}{(\omega\, We)^2 + 1) Re} - 2\omega \sum_{n=1}^{\infty} \frac{\left(\lambda_n^2 + We\, b_n\right)}{((\omega\, We)^2 + 1)[a_n^2 + (\omega\, Re)^2]} \right\} \cos(\lambda_n y), \quad (5.70)$$

where

$r_{11n},\, r_{12n} = \left[-1 \pm \sqrt{1 - 4We\mu_n^2/Re}\right]/2We$, and b_n=((μ$_n^2$ − $ReWe\omega^2$)(Weω^2−K) − Re ω^2).

(ii) Taking $\lambda_2^* \to 0$, $\lambda_3^* \to 0$ and We → 0 in the Eqs. (5.56), (5.57), (5.61) and (5.62), we recover the similar solutions for viscous fluid given below

$$u_{Nsp}(y,t) = (1 - y)\ \sin(\omega t) - \ 2\, Re\ \sum_{n=1}^{\infty} \left\{ \frac{\left(K\mu_n^2 + Re\omega^2\right) \sin(\omega t) + \omega \lambda_n^2 \cos(\omega t)}{\left(\lambda_n^2 + KRe\right)^2 + (\omega Re)^2} \right\} \frac{\sin(\lambda_n y)}{\lambda_n}, \quad (5.71)$$

$$u_{Nst}(y,t) = 2\omega Re \sum_{n=1}^{\infty} \left\{ \frac{\lambda_n \sin(\omega t)}{\left(\lambda_n^2 + KRe\right)^2 + (\omega Re)^2} e^{\left[-\left(\frac{\lambda_n^2}{Re} + K\right)t\right]} \right\}, \tag{5.72}$$

$$\tau_{Nsp}(y,t) = -\frac{t}{Re}\sin(\omega t) - 2\sum_{n=1}^{\infty} \left\{ \frac{\left(K\mu_n^2 + Re\omega^2\right)\sin(\omega t) + \omega\lambda_n^2 \cos(\omega t)}{\left(\lambda_n^2 + KRe\right)^2 + (\omega Re)^2} \right\} \cos(\lambda_n y), \tag{5.73}$$

and

$$\tau_{Nst}(y,t) = 2\omega \sum_{n=1}^{\infty} \left\{ \frac{\lambda_n \cos(\omega t)}{\left(\lambda_n^2 + KRe\right)^2 + (\omega Re)^2} e^{\left[-\left(\frac{\lambda_n^2}{Re} + K\right)t\right]} \right\}. \tag{5.74}$$

5.6 Results and Discussions

In this chapter, we present the solutions for laminar, unsteady, incompressible Burgers fluid with porous medium that lies between two horizontal parallel plates at a distance d apart. We consider a constant pressure so that the motion in the fluid is produced due to either constantly accelerating bottom plate or sinusoidal oscillations of the same plate, respectively. Finite Fourier Sine Transform (FFST) is used to find the exact analytical solutions for the velocity profile and the corresponding tangential stress. Starting solutions are presented for the sine oscillation of the boundary, depending on the initial and boundary conditions as sum of permanent (steady-state) and transient solutions. To shed light upon certain physical aspects of the achieved outcomes through different parameters, the graphical illustration of velocity field and shear stress is made. Furthermore, in order to see the effect of porosity parameter, a comparison of velocity field and associated tangential stress for these flows with and without porous medium is given. The similar solutions when $\lambda_3^* \to 0$, $\lambda_3^* \to 0$ and $\lambda_2^* \to 0$, and $\lambda_3^* \to 0$, $\lambda_2^* \to 0$ and $We \to 0$, corresponding to Oldoryd-B fluid, Maxwell fluid and Newtonian fluid, respectively are also discussed through graphs. The numerical results for the velocity field and corresponding shear stress are plotted in Figures 5.2-5.8 and Figure 5.9-5.11, respectively. We investigate these findings regarding variation of various values of time and the physical parameters of the flow.

Figures 5.2-5.4 show the velocity profiles in regard of constantly accelerating flows. Figures 5.2 and 5.3 are plotted for different values of rheological parameter of Burgers fluid when $\omega = \frac{\pi}{12}$, $Re = 100$, $We = 0.7$ and $\lambda_3^* = 0.05$ for two different values of time t, with and without porous medium. It can be seen that velocity is increasing function of Burgers parameter and amplitude of velocity is larger when time is increasing. Moreover, velocity profile approaches to zero more faster as compared to the case $K = 0$ (without porous medium). Figure 5.4 gives a comparison between the profiles of Burgers fluid, Oldoryd_B fluid when $\lambda_2^* \to 0$, Maxwell fluid when $\lambda_2^* \to 0$ and $\lambda_3^* \to 0$ and Newtonian fluid when $We \to 0$, $\lambda_2^* \to 0$ and $\lambda_3^* \to 0$ with and without porous medium. Here, we have seen that the amplitude of Burgers velocity is smaller than the Newtonian velocity for both with and without porous medium.

Figure 5.5-5.8 display the steady-state velocity profiles for the sine oscillation of the bottom plate, with and without porous medium. In Figure 5.5 and 5.6 equivalence the effect of different forms of component of velocity $u_{sp}(y,t)$ given by Eqs. (5.58) and (5.59) for two different times when $\omega = 5, K = 0.8\ and\ 0, We = 0.7, \lambda_2^* = 0.8$ and λ_3^* = 0.6 is provided. The features of Burgers parameter λ_2^* can be observed via Figure 5.7 and 5.8. It can be seen that the amplitude of velocity is larger for the case of Newtonian fluid when compared with different values of Burgers parameter λ_2^*, when $\omega = 5, K = 0.8, Re = 100, We = 0.7, \lambda_3^* = 0.5,$ for two different values of time. We can also see that in connection with time, velocity increases. Figure 5.8 provides the time variations of the mid plane when $y = 0.5$ for steady-state velocity for $K = 0,$ and $K = 0.8$ and four different values of Burgers' parameter. Furthermore, the amplitude of oscillation is larger when there is no porous medium while compared with the case with porous medium effects when $K = 0.8$.

Figures 5.9 and 5.10 display the equivalence effect of two different form of shear stress given by Eqs. (5.62) and (5.63) with and without porous medium when $\omega = 5, Re = 100, We = 0.7, \lambda_3^* = 0.6, \lambda_2^* = 0.8$ to check their correctness graphically. Figure 5.11 shows the time variations of the mid plane when $y = 0.5$ for steady-state shear stress with and without porous medium. It is clear that the oscillation's amplitude is decreasing by increasing Burgers parameter and also oscillations' amplitude is smaller without porous medium effects.

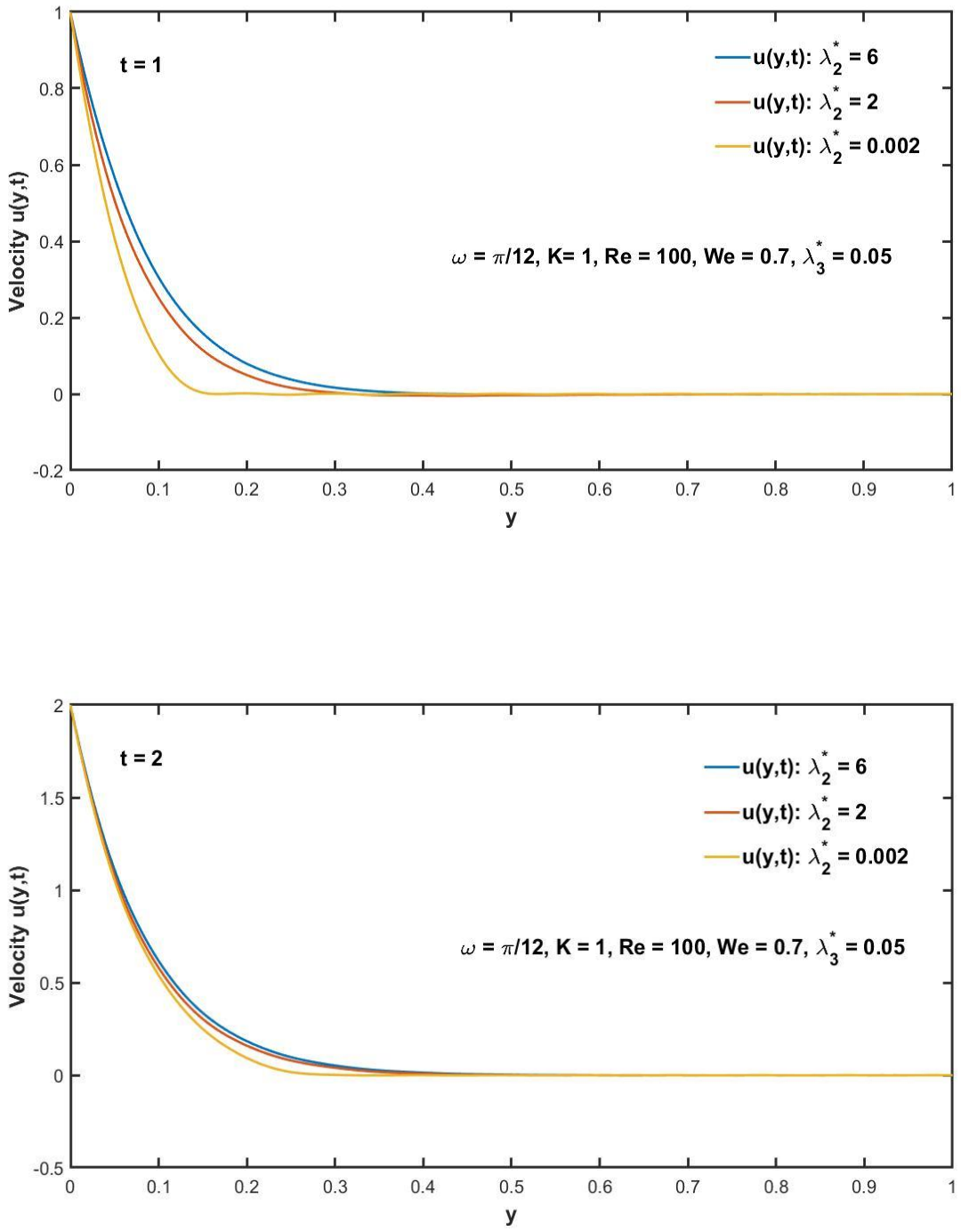

Figure 5.2: Velocity profiles $u(y,t)$ for various values of Burgers parameter with porous effects.

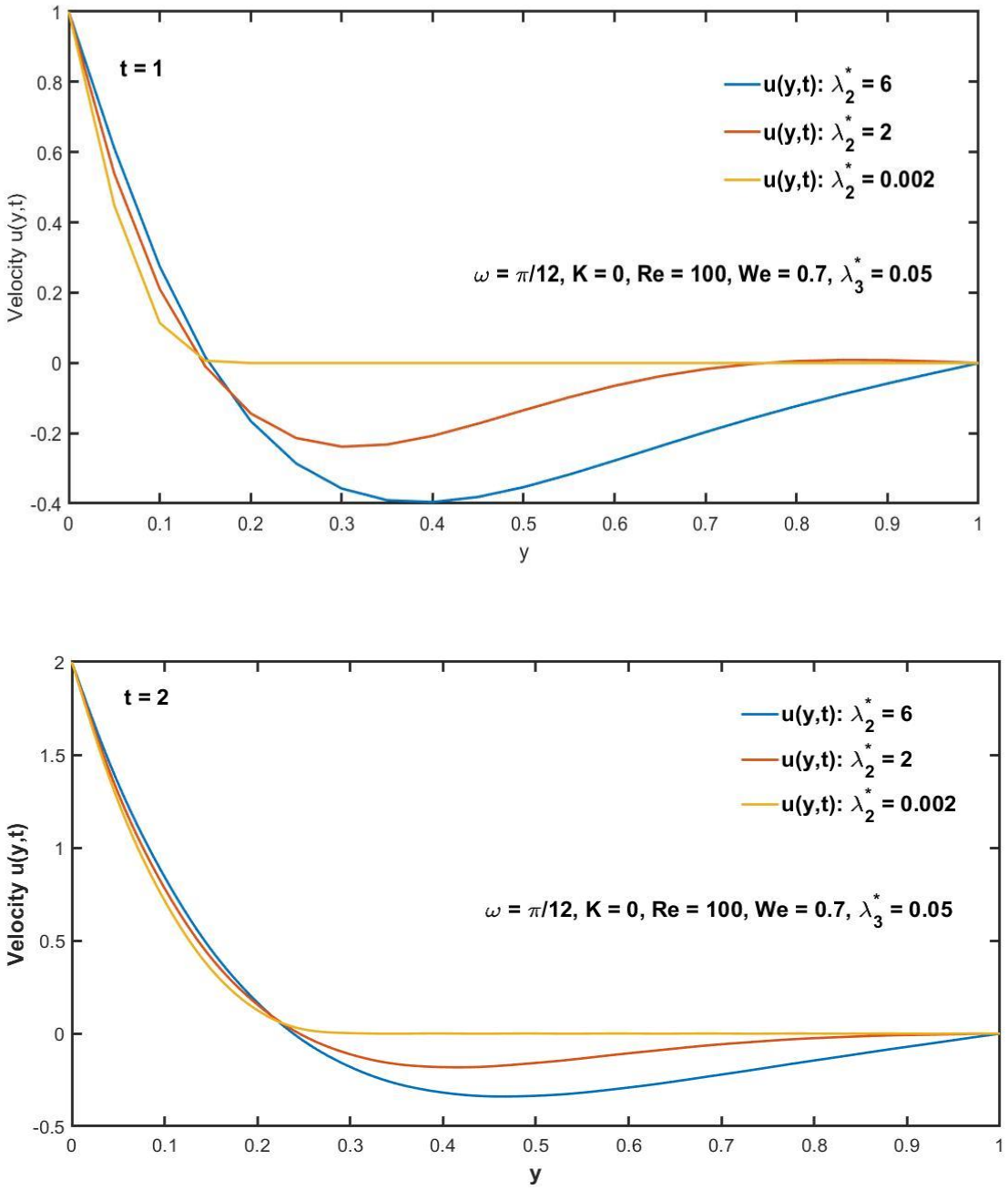

Figure 5.3: Velocity profile $u(y,t)$ for various values of Burgers parameter without porous effects.

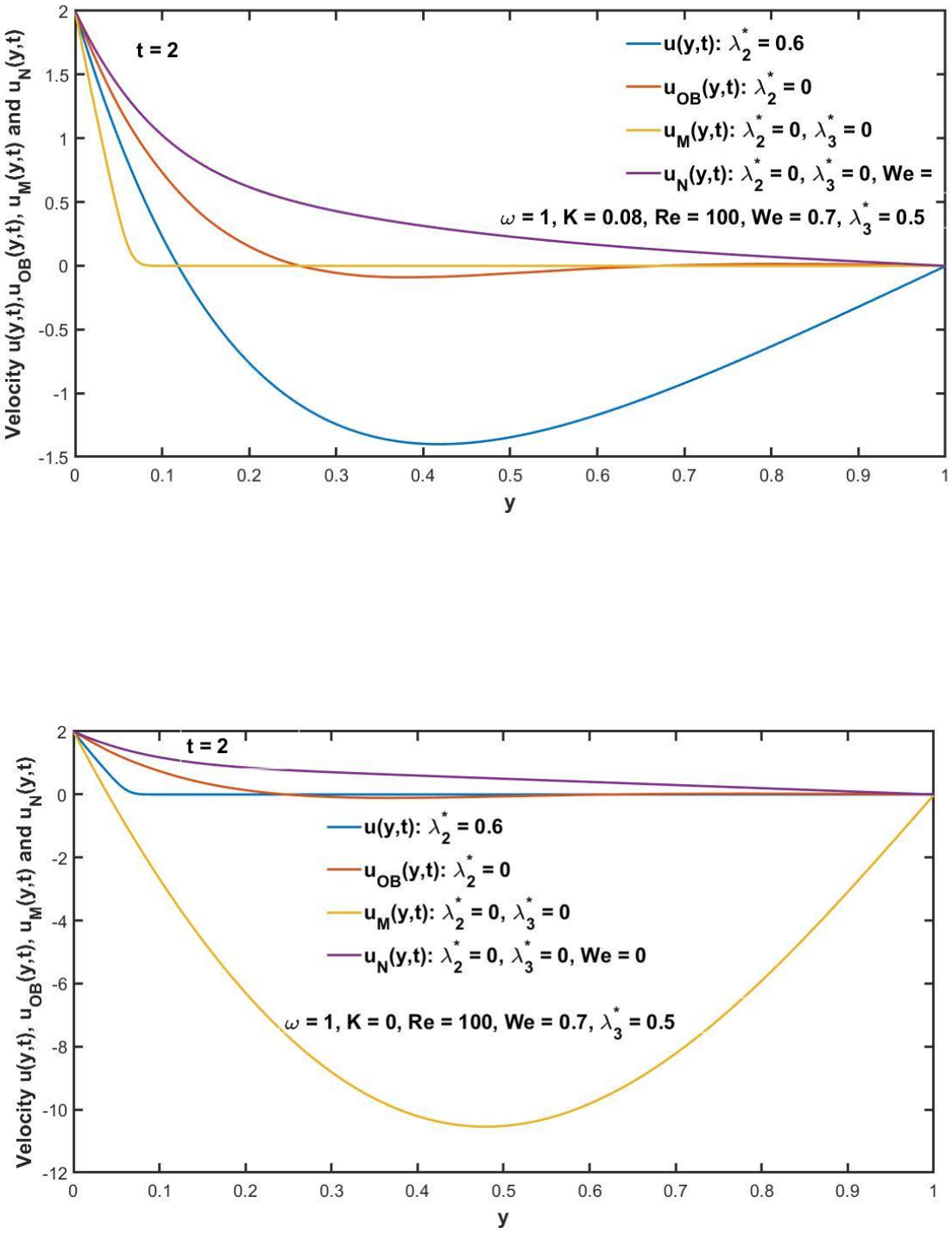

Figure 5.4: A comparison of the profiles of velocity with or without porous effects, respectively.

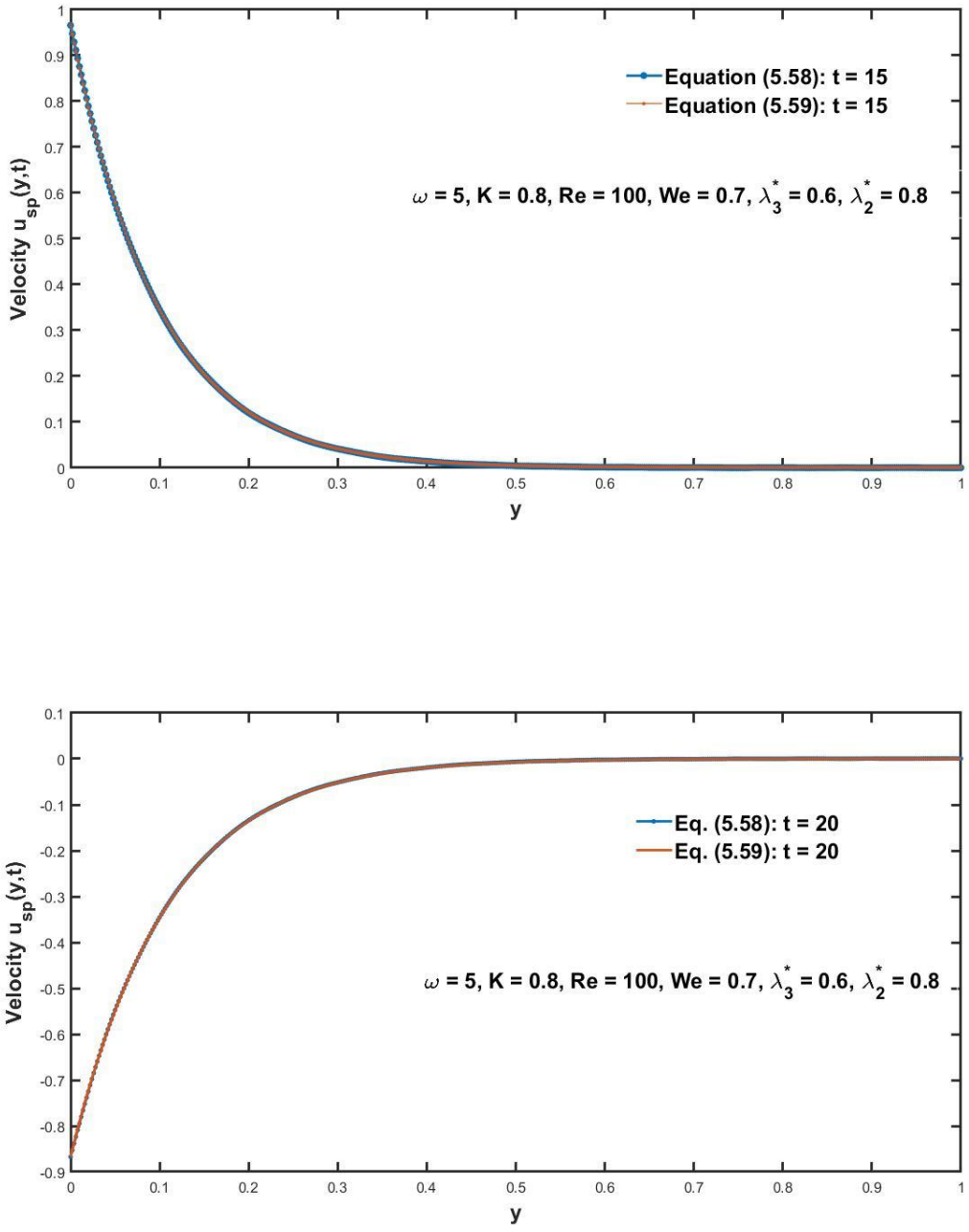

Figure 5.5: The steady-state component's profiles $u_{sp}(y,t)$ with porous effects.

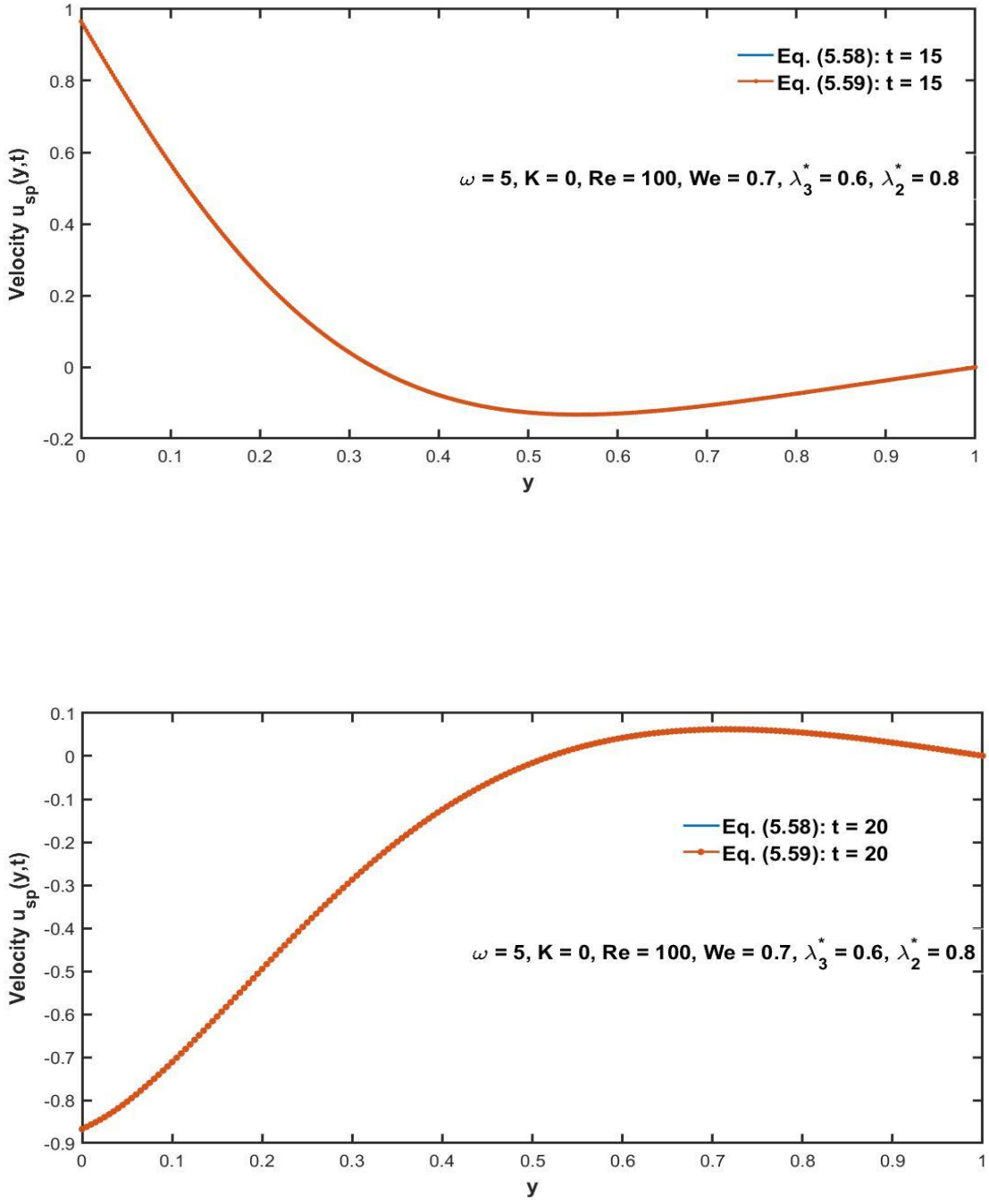

Figure 5.6: The steady-state component's profiles $u_{sp}(y,t)$ without porous effect.

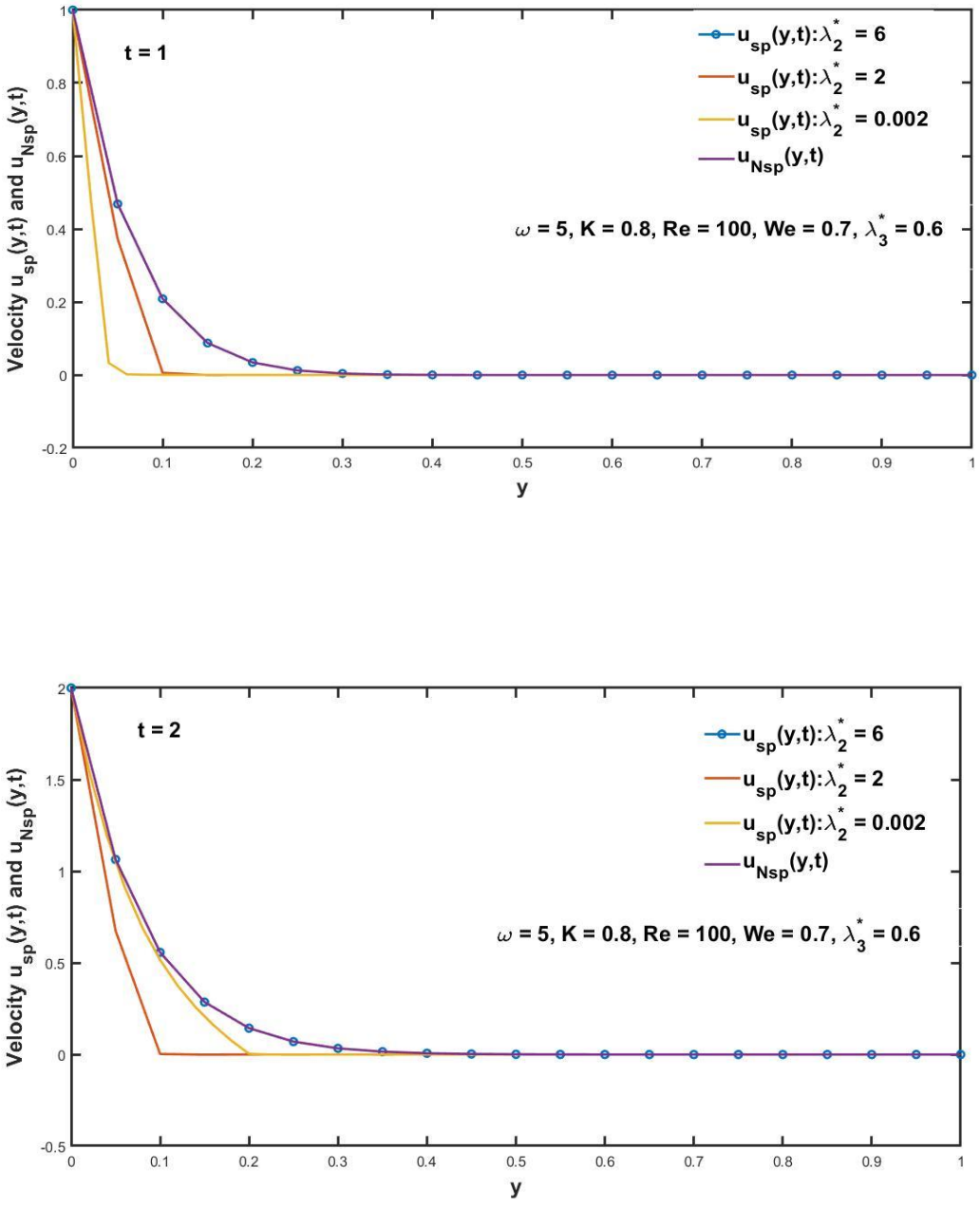

Figure 5.7: The steady-state component's profiles $u_{sp}(y,t)$ and $u_{Nsp}(y,t)$.

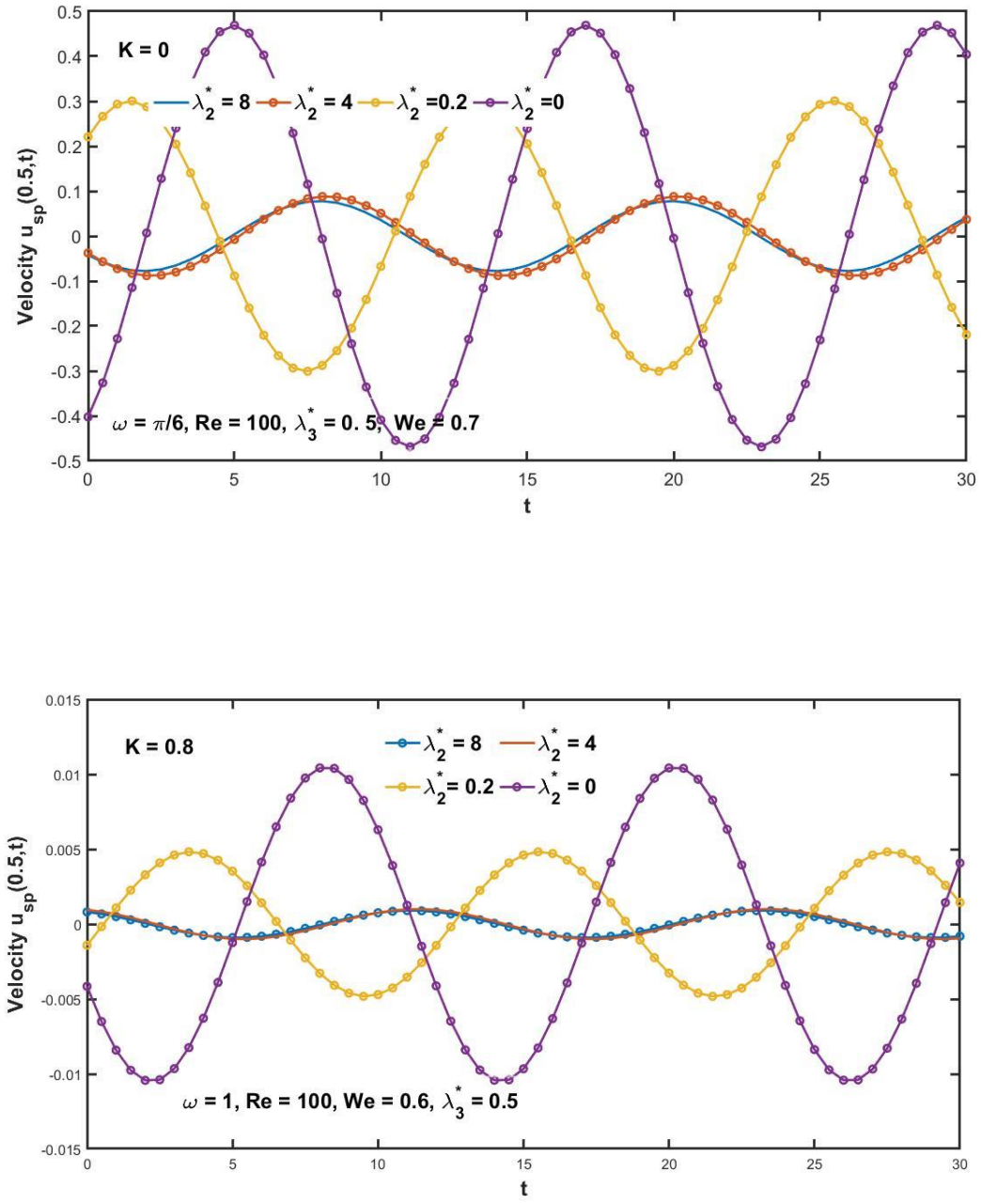

Figure 5.8: Time series steady-state component without and with porous effects.

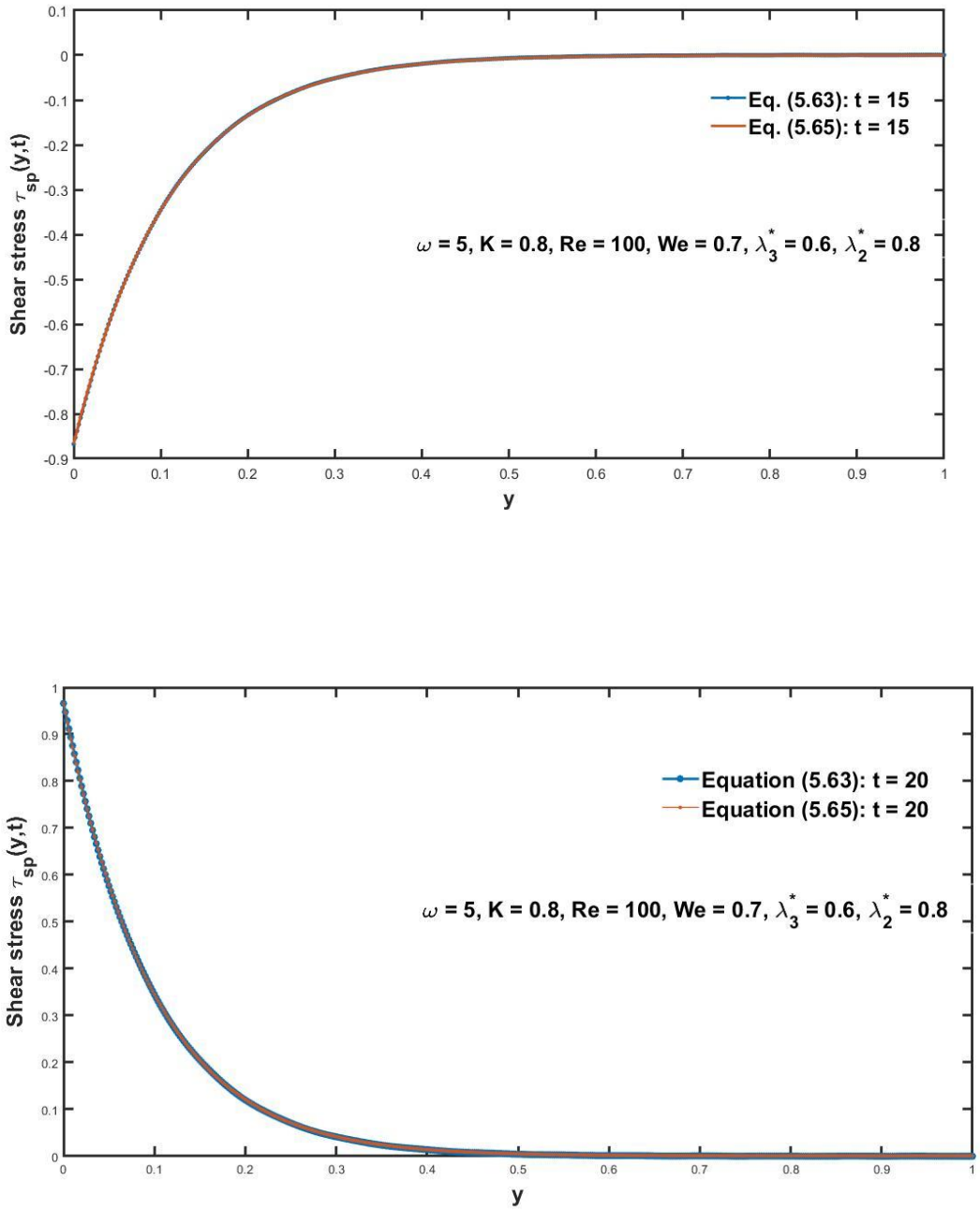

Figure 5.9: The steady-state component's profiles of shear stress $u_{sp}(y,t)$ with porous effects.

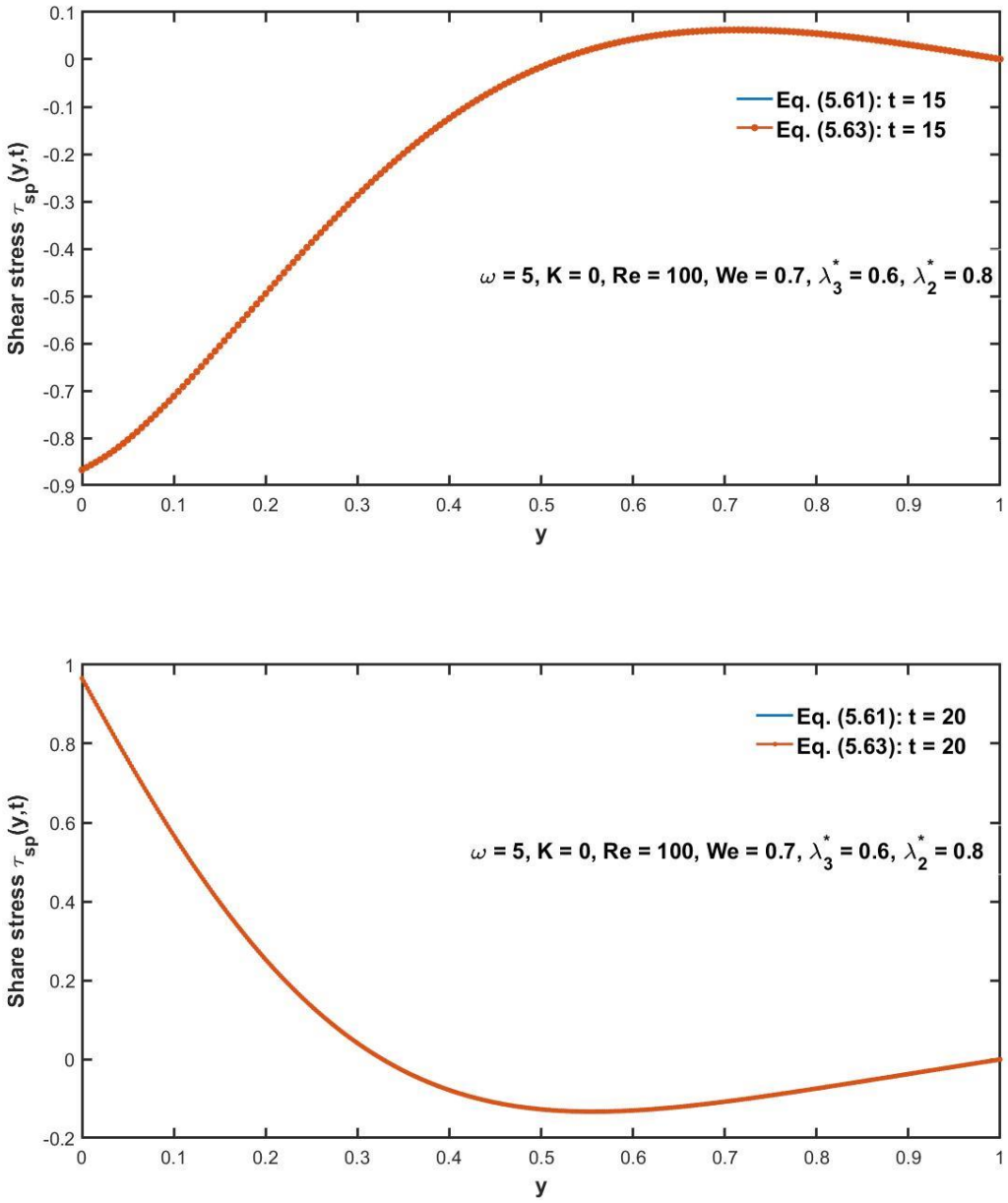

Figure 5.10: The steady-state component's profiles of shear stress $u_{sp}(y,t)$ without a porous effect.

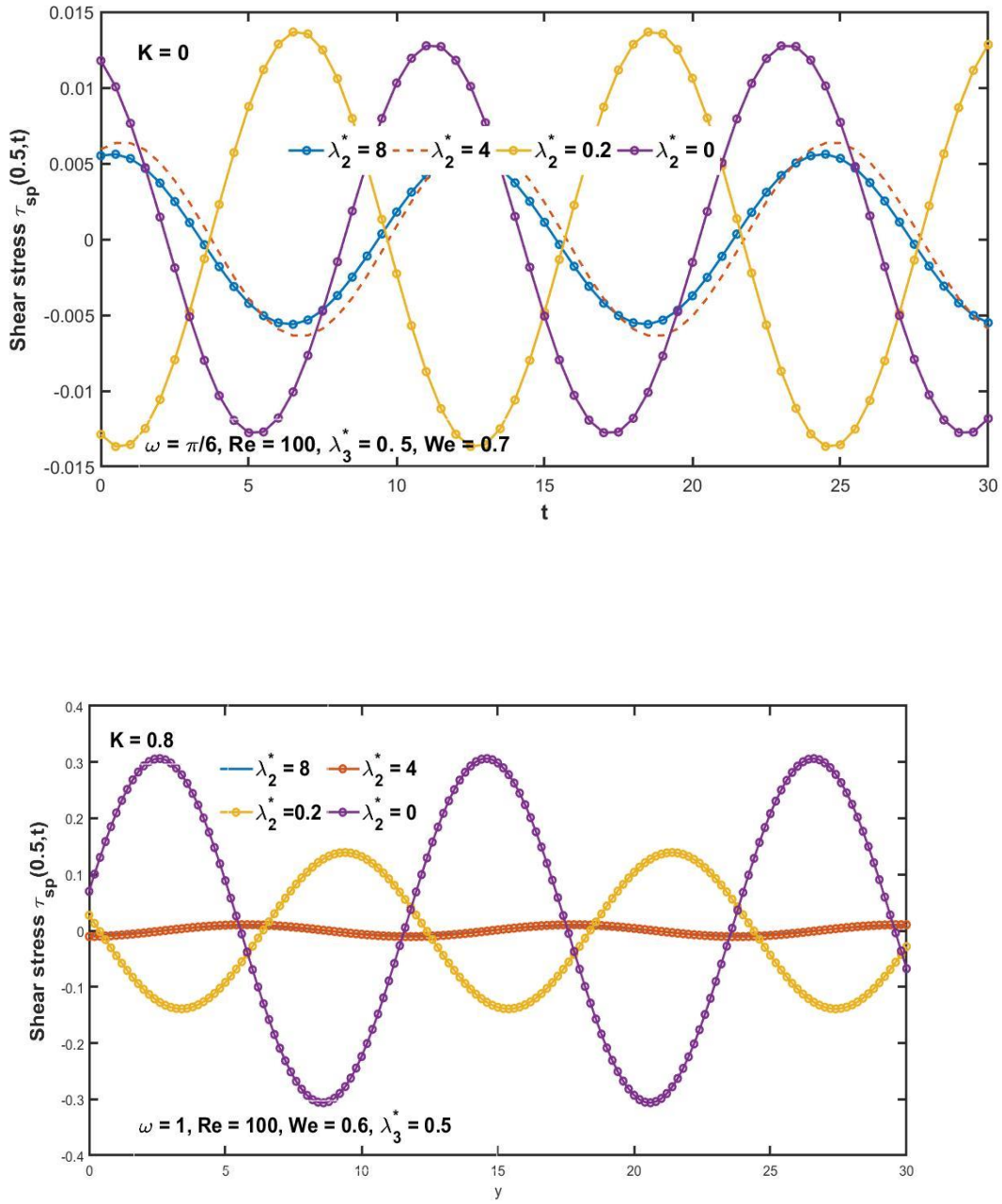

Figure 5.11: Time variation of mid plane of steady-state component $\tau_{sp}(0.5, t)$ without and with porous effects.

CHAPTER 6

CONCLUSION AND FUTURE WORK

We present the main findings, when we have contributed, and ideas for future work based on this study. This thesis has focused to initiate exact analytical solutions for constantly accelerating flow of the bottom plate and sine oscillation of the same boundary of a non-Newtonian fluid. The unsteady flows of an incompressible Maxwell (chapter four) and further work of chapter four is extended to Burgers fluid (chapter five) with porous medium effects were considered. The Burgers fluid model is a rate type fluid model which can predict the relaxation and retardation time phenomena. Moreover, the Burgers fluid model includes Oldoryd-B model, Maxwell model and Newtonian models, as special cases. As a result of these facts, the velocity profile's analytical expression and the associated shear stress for constantly accelerating or sine oscillation of the bottom plate have been determined by means of integral transform. The starting solutions for the oscillation of the boundary were written as sum of permanent and transient solutions and they depict the motion of non_Newtonian fluid for small and large times. Furthermore, these solutions are also important for those who want to eliminate the transient part from their solutions and find the approximate time after which the fluid is moving according to permanent behavior. The graphical results for velocity fluid and the corresponding shear stress in the presence as well as in the absence of porous medium and a comparison between various rate type model and Newtonian model were model for different pertinent parameters of the interesting aspects of the obtained results. This section provides a summary of the findings and recommendations from the study that were discussed in the preceding chapters.

In chapter 4, we have displayed the analytical solutions for constantly accelerating or sine oscillation of the bottom plate of an incompressible UCM fluid. The Finite Fourier Sine Transformation (FFST) was used to tackle the second order governing equation to obtain the velocity for two different cases of the boundary. The solutions that are produced fulfil all of

the prescribed starting and boundary requirements. The solution for sine oscillation of the boundary was expressed as sum of steady-state (permanent) and transient solutions. The graphs have been made for both constantly accelerating and sine oscillation of the boundary. It can be seen in both cases that velocity is an increasing function of Weissenberg number and amplitude of velocity is larger for increasing time. Moreover, the amplitude of oscillation is larger for steady-state velocity without porous medium but for steady-state shear stress, amplitude of velocity is larger when porous medium is present.

Ultimately, we have examined in chapter 5, the constantly accelerating and sinusoidal oscillation flows of an incompressible, unsteady Burgers fluid with porous medium. Moreover, we have assumed that there is no body force and constant pressure is applied in the direction of flow. The solutions obtained for the sine oscillation of the boundary can be written as sum of steady-state (permanent) and transient solutions. FFST was used to find the exact analytical solutions. The graphical results were displayed to see the effects of various parameters of the flow due to either acceleration of the bottom plate or the sine oscillation of the same boundary. Furthermore, we have found the required times to reach the permanent or degradation of the temporary solutions using graphs. Here, we've observed that velocity is an increasing function of Burgers fluid parameter and by increasing time the magnitude of velocity is larger for both cases. Moreover, the amplitude of oscillations is larger for the velocity profile without porous medium, but we have seen the opposite effect for the steady-state shear stress, for different values of Burgers parameter.

In this thesis, we have displayed the significant solutions for constantly accelerating and sinusoidal oscillations of the boundary with technical relevance for some non-Newtonian fluid. Also, this work provides significant unsteadying of the transient behaviors of non-Newtonian fluids. Finite Fourier Sine transform is valid to solve the linear partial differential equations having Dirichlet boundary conditions and bounded domain. Further directions and possible extensions of the current energy equation to observe impacts of temperature on the Burgers parameter. The exact analytical solutions were obtained here when there is no physical force. However, the velocity field's analytical solutions as well as the temperature profile for a Burger fluid can be found in the occurrence of permeable media and bodily forces.

We anticipate that the current work will be valuable in the analysis of more intricate issues and provide a foundation for several scientific and industrial uses.

REFERENCES

[1] J. M. Burgers, "Mechanical considerations-model systems-phenomenological theories of relaxation and of viscosity." First rep. on visc. and plast. 1 (1935).

[2] R. Lee, and H. D. Markwick, The Mechanical Properties of Bituminous Ma- terials Under Constant Stress. Jour. Soc. Chem. Ind., Vol. 56, 1937. 5.

[3] W. R. Peltier, W. Patrick, and A. Y. David, "The viscosities of the Earth's mantle." Anelasticity in the Earth 4 (1981): 59-77. x. Peltier, Wu. Patrick, and David A. Yuen. "The viscosities of the Earth's mantle." Anela. in the Earth 4 (1981): 59-77.

[4] M. Khan, S. H. Ali, and H. Qi, On accelerated flows of a viscoelastic fluid with the fractional Burgers' model. Nonlinear Analysis: R. W. Appl, 2009 Aug 1; 10 (4): 2286-96.

[5] K. Maqbool, O. A. Bég, A. Sohail, and S. Idreesa, "Analytical solutions for wall slip effects on magneto hydrodynamic oscillatory rotating plate and channel flows in porous media using a fractional Burgers viscoelastic model." The Eur. Phy. Jour. Plus 131 (2016): 1-17.

[6] M. Hassan, M. Marin, A. Alsharif, and R. Ellahi. "Convective heat transfer flow of nanofluid in a porous medium over wavy surface." Phy. Let. A 382, no. 38 (2018): 2749-2753.

[7] M. Krishna, Veera, and J. A. Chamkha. "Hall and ion slip effects on MHD rotating flow of elastico-viscous fluid through porous medium." Int. Com. in H. and M. Tran. 113 (2020): 104494.

[8] R. Ellahi, M. Sadiq, Sait, N. Shehzad, and Z. Ayaz. "A hybrid investigation on numerical and analytical solutions of electro-magneto hydrodynamics flow of nanofluid through porous media with entropy generation." Int. J.s of Num. Met. for H. & Flu. Flo. 30, no. 2 (2020): 834-854.

[9] S. U. Haq, M. A. Khan, and N. A Shah. "Analysis of magneto hydrodynamics flow of a fractional viscous fluid through a porous medium." Chem. Jour. of phy. 56, no. 1 (2018): 261-269.

[10] Y. Shuai, L. Wang, and S. Zhang. "Conformable derivative: Application to non-Darcian flow in low-permeability porous media." App. Mat. Let. 79 (2018): 105-110.

[11] R. Nauman, A. U. Awan, E. U Haque, M. Abdullah, and M. Me. Rashidi. "Unsteady flow of a Burgers' fluid with Caputo fractional derivatives: A hybrid technique." A. Sha. Eng. Jour. 10, no. 2 (2019): 319-325.

[12] J. Maria, M. Tahir, M. Imran, D. Baleanu, A. Akgül, and M. A. Imran. "Unsteady flow of fractional Burgers' fluid in a rotating annulus region with power law kernel." Alex. Eng. Jour. 61, no. 1 (2022): 17-27.

[13] C. Fetecau, N. A. Ahammad, D. Vieru, and N. A. Shah. "Steady-State Solutions for Two Mixed Initial-Boundary Value Problems Which Describe Isothermal Motions of Burgers' Fluids: App." Mat. 10, no. 19 (2022): 3681.

[14] Y. Jiang, H. G. Sun, Y. Bai, and Y. Zhang. "MHD flow, radiation heat and mass transfer of fractional Burgers' fluid in porous medium with chemical reaction." Compu. & Mat. with App. 115 (2022): 68-79.

[15] F. Wang, A. Ahmed, M. N. Khan, T. Alqahtani, and S. Algarni. "Features of energy transfer in buoyancy-driven unsteady flow of Maxwell fluid via Cattaneo–Christov theory." Wa. in Rand. and C. Med. (2022): 1-15.

[16] K. Zheng, F. Wang, M. Kamran, R. Khan, A. S. Khan, S. Rehman, and A. Farooq. "On rate type fluid flow induced by rectified sine pulses." A. Mat. 7, no. 2 (2022): 1615-1627.

[17] C. Fetecau, S. Akhtar, and C. Moroşanu. "Porous and Magnetic Effects on Modified Stokes' Problems for Generalized Burgers' Fluids." Dy. 3, no. 4 (2023): 803-819.

[18] G. Ali, F. Ali, A. Khan, A. H. Ganie, and I. Khan. "A generalized magnetohydrodynamic two-phase free convection flow of dusty Casson fluid between parallel plates." Ca. Stud. in Therm. Eng. 29 (2022): 101657.

[19] F. Shahzad, W. Jamshed, Ta. Sajid, M. D. Shamshuddin, R. Safdar, S. O. Salawu, M. R. Eid, M. B. Hafeez, and M. Krawczuk. "Electromagnetic control and dynamics of generalized burgers' nanoliquid flow containing motile microorganisms with Cattaneo–Christov relations: Gal. fin. Elem. Mech.." Appli. Sci. 12, no. 17 (2022): 8636.

[20] C. Fetecau, A. Rauf, T. M. Qureshi, and D. Vieru. "Steady-state solutions for MHD motions of Burgers' fluids through porous media with differential expressions of shear on boundary and applications." Mat. 10, no. 22 (2022): 4228.

[21] F. Wang, S. N. Ali, I. Ahmad, H. Ahmad, K. M. Alam, and Phatiphat Thounthong. "Solution of Burgers' equation appears in fluid mechanics by multistage optimal homotopy asymptotic method." Ther. Sci. 26, no. 1 Part B (2022): 815-821.

[22] N. Raza, A. K. Khan, A. Ul. Awan, and K. A. Abro. "Dynamical aspects of transient electro-osmotic flow of Burgers' fluid with zeta potential in cylindrical tube." Non. Eng. 12, no. 1 (2023): 20220256.

[23] J. Qi, and Q. Zhu. "Further results about the non-traveling wave exact solutions of nonlinear Burgers equation with variable coefficients." Resul. in Phy. 46 (2023): 106285.

[24] K. Ahmad, and K. Bibi. "New exact solutions of Burgers' equation using power index method." Disc. Dy. in Nat. and Soci. (2022).

[25] D. V. Tanwar, and A. M. Wazwaz, "Lie symmetries and exact solutions of KdV–Burgers equation with dissipation in dusty plasma." Qual. Th. of Dy. Sys. 21, no. 4 (2022): 164.

[26] K. A. Koroche, "Numerical solution of in-viscid Burger equation in the application of physical phenomena: The comparison between three numerical methods." Int. Journal of Mat. and Mat. Sci. 2022 (2022).

[27] S. Kumar, and S. Rani. "Symmetries of optimal system, various closed-form solutions, and propagation of different wave profiles for the Boussinesq–Burgers system in ocean waves." Phy. of F. 34, no. 3 (2022).

[28] C. Fetecau, S. Akhtar, and C. Moroşanu. "Permanent Solutions for MHD Motions of Generalized Burgers' Fluids Adjacent to an Unbounded Plate Subjected to Oscillatory Shear Stresses." Sy. 15, no. 9 (2023): 1683.

[29] K. Shah, and T. Singh. "A solution of the Burger's equation arising in the longitudinal dispersion phenomenon in fluid flow through porous media by mixture of new integral transform and homotopy perturbation method." Jour. of Geosci. and En. Prot. 3, no. 04 (2015): 24.

[30] S. K. Mohanty, S. Kumar, A. N. Dev, M. K. Deka, D. V. Churikov, and O. V. Kravchenko. "An efficient technique of G′ G–expansion method for modified KdV and Burgers equations with variable coefficients." Resul. in Phy. 37 (2022): 105504.

[31] Khan, K. Fakhar, and S. Sharidan. "Magnetohydrodynamic rotating flow of a generalized Burgers' fluid in a porous medium with Hall current." Tranp. in Por. Med. 91 (2012): 49-58.

[32] F. Oz, R. K. Vuppala, K. Kara, and F. Gaitan. "Solving Burgers' equation with quantum computing." Qu. Inf. Proc. 21 (2022): 1-13.

[33] M. Li, O. Nikan, W. Qiu, and D. Xu. "An efficient localized meshless collocation method for the two-dimensional Burgers-type equation arising in fluid turbulent flows." Eng. Analy. with Bou. E. 144 (2022): 44-54.

[34] R. Adem, B. Muatjetjeja, and T. S. Moretlo. "An Extended (2+ 1)-dimensional Coupled Burgers System in Fluid Mechanics: Symmetry Reductions; Kudryashov Method; Conservation Laws." Int. Jour. of Theo. Phy. 62, no. 2 (2023): 38.

[35] V. Biesek, and Pedro Henrique de Almeida Konzen. "Burgers' pinns with implicit euler transfer learning." arXiv p. arXiv:2310.15343 (2023).

[36] N. H. Aljahdaly, S. A. El-Tantawy, A. M. Wazwaz, and H. A. Ashi. "Novel solutions to the undamped and damped KdV-Burgers-Kuramoto equations and modeling the dissipative nonlinear structures in nonlinear media." Rom. Rep. Phys 74 (2022): 102.

[37] V. K. Tamboli, and P. V. Tandel. "Solution of the time-fractional generalized Burger–Fisher equation using the fractional reduced differential transform method." Jour. of O. Eng. and Sci. 7, no. 4 (2022): 399-407.

[38] Rampf, U. Frisch, and O. Hahn. "Eye of the tyger: Early-time resonances and singularities in the inviscid Burgers equation." Phys. Re. F. 7, no. 10 (2022): 104610.

[39] S. Doley, A. V. Kumar, K. R. Singh, and L. Jino. "Study of time fractional Burgers' equation using Caputo, Caputo-Fabrizio and Atangana-Baleanu fractional derivatives." Eng. Let. 30, no. 3 (2022).

[40] S. Sehra, A. Noor, S. Ul Haq, S. U. Jan, I. Khan, and A. Mohamed. "Heat transfer of generalized second grade fluid with MHD, radiation and exponential heating using Caputo–Fabrizio fractional derivatives approach." Sci. Rep. 13, no. 1 (2023): 5220.

[41] X. Yin, Q. Liu, and Sh. Bai. "The multiple kink solutions and interaction mechanism with help of the coupled Burgers' equation." Ch. Jour. of Phys. 77 (2022): 335-349.

[42] Lara, F. Manrique, and E. Ferrer. "Accelerating high order discontinuous Galerkin solvers using neural networks: 1D Burgers' equation." Comp. & F. 235 (2022): 105274.

[43] M. Farah, W. Wael, Mohammed, and M. El-Morshedy. "The analytical solutions for stochastic fractional-space Burgers' equation." Jour. of Mat. 2022 (2022): 1-8.

[44] S. Savović, M. Ivanović, and R. Min. "A Comparative Study of the Explicit Finite Difference Method and Physics-Informed Neural Networks for Solving the Burgers' Equation." Ax. 12, no. 10 (2023): 982.

[45] S. Ramya, K. Krishnakumar, and R. Ilangovane. "Exact solutions of time fractional generalized Burgers–Fisher equation using exp and exponential rational function methods." Int. Jour. of Dy. and Cont. (2023): 1-11.

[46] M. Alotaibi, Rasool Shah, Kamsing Nonlaopon, Sherif ME Ismaeel, and Samir A. El-Tantawy. "Investigation of the Time-Fractional Generalized Burgers–Fisher Equation via Novel Techniques." Sy. 15, no. 1 (2022): 108.

[47] K. Ali, M. Hussain, and M. Mah. Baig. "Analytical solution of magnetohydrodynamics generalized Burger's fluid embedded with porosity." Int. Jour. of Adv. and App. Sci. 4, no. 7 (2017): 80-89.

[48] S. Kr. Mohanty, O. V. Kravchenko, and A. N. Dev. "Exact traveling wave solutions of the Schamel Burgers' equation by using generalized-improved and generalized G′ G expansion methods." Res. in Phys. 33 (2022): 105124.

[49] H. Schlichting, Boundary Layer Theory; McGraw-Hill: NY, USA, 1960.

[50] Y. Wang, "Exact solutions of the unsteady Navier-Stokes equations." App. Mech. Re. ;(United States) 42, no. CONF-8901202- (1989).

[51] Y. Wang, “Exact solutions of the steady-state Navier-Stokes equations." A. Re. of F. Mech. 23, no. 1 (1991): 159-177.

[52] M. Emin. "On the unsteady unidirectional flows generated by impulsive motion of a boundary or sudden application of a pressure gradient." Inter. Jour. of non-lin. mech. 37, no. 6 (2002): 1091-1106.

[53] K. R. Rajagopal, "A note on unsteady unidirectional flows of a non-Newtonian fluid." Inter. Jour. of Non-Lin. Mec. 17, no. 5-6 (1982): 369-373.

[54] M. Siddiqui, T. Hayat, and S. Asghar. "Periodic flows of a non-Newtonian fluid between two parallel plates." Inter. Jour. of non-lin. mec. 34, no. 5 (1999): 895-899.

[55] W. S. P. Li, and Moli Zhao. "Analytical study of oscillatory flow of Maxwell fluid through a rectangular tube." Phys. of F. 31, no. 6 (2019).

[56] S. X. S. Wang, and M. Zhao. "Oscillatory flow of Maxwell fluid in a tube of isosceles right triangular cross section." Phys. of F. 31, no. 12 (2019).

[57] W. T. P. Wenxiao, and X. Mingyu. "A note on unsteady flows of a viscoelastic fluid with the fractional Maxwell model between two parallel plates." Inter. Jour. of Non-Lin. Mec. 38, no. 5 (2003): 645-650.

[58] Q. Haitao, and X. Mingyu, "Unsteady flow of viscoelastic fluid with fractional Maxwell model in a channel." Mech. Res. Com. 34, no. 2 (2007): 210-212.

[59] S. Rabia, M. Imran, M. Tahir, N. Sadiq, and M. A. Imran. "MHD flow of Burgers’ fluid under the effect of pressure gradient through a porous material pipe." P. U. Jour. of Mat. 50, no. 4 (2020).

[60] K. Al-Hadhrami, L. Elliot, M. D. Ingham, and X. Wen. "progression of liquids through even channels of permeable materials and got speed articulations regarding the Reynolds number." Inter. Jour. of en. Res. 27 (2003): 875-889.

[61] Cimpean, I. Pop, D. B. Ingham, and J. H. Merkin. "Fully developed mixed convection flow between inclined parallel plates filled with a porous medium." Trans. in por. Med. 77 (2009): 87-102.

[62] K. D. Ch, P. V. Satyanarayana, and A. Sudhakaraiah. "Effects of radiation and free convection currents on unsteady Couette flow between two vertical parallel plates with constant heat flux and heat source through porous medium." Inter. Jour. of Eng. Res. 2, no. 2 (2013): 113-118.

[63] M. E. I. Pažanin, and M. Radulović. "On the Darcy–Brinkman–Boussinesq flow in a thin channel with irregularities." Transport in Porous Media 131, no. 2 (2020): 633-660.

[64] Wolfgang, "Darcy, Forchheimer, Brinkman and Richards: classical hydromechanical equations and their significance in the light of the TPM." Archive of App. Mech. (2020): 1-21.

[65] Fetecau, and M. Narahari. "General solutions for hydromagnetic flow of viscous fluids between horizontal parallel plates through porous medium." Jour. of Eng. Mec. 146, no. 6 (2020): 04020053.

[66] Constantin, and M. Agop. "Exact solutions for oscillating motions of some fluids with power-law dependence of viscosity on the pressure." Annals of the Academy of Romanian Scientists: Ser. on Mat. and its App. 12 (2020): 295-311.

[67] G. Ahmad, M. Imran, C. Fetecau, and D. Vieru. "First exact solutions for mixed boundary value problems concerning the motions of fluids with exponential dependence of viscosity on pressure." AIP Adv. 10, no. 6 (2020).

[68] K. Satish, V. Průša, and K. R. Rajagopal. "On Maxwell fluids with relaxation time and viscosity depending on the pressure." International Jour. of Non-Lin. Mec. 46, no. 6 (2011): 819-827.

[69] M. Khan, R. Malik, and A. Anjum. "Exact solutions of MHD second Stokes flow of generalized Burgers fluid." App. Mat. and Mec. 36 (2015): 211-224.

[70] K. D. Housiadas, "An exact analytical solution for viscoelastic fluids with pressure-dependent viscosity." Jour. of Non-New. F. Mech. 223 (2015): 147-156.

[71] M. E. Shashi, Transmission pipeline calculations and simulations manual. G. Prof. Pub., 2014.

[72] Olesiak, and S. Zbigniew, "A Tribute to Ian Naismith Sneddon: 1919-2000." Jour. of Therm. Str. 25, no. 3 (2002): 207-213.

[73] Kotha, M. A. Kumari, M. V. S. Rao, K. Alnefaie, I. Khan, and M. Andualem, "Magnetization for burgers' fluid subject to convective heating and heterogeneous-homogeneous reactions." Mat. Pro. in Eng. (2022): 1-15.

[74] F. Constantin, R. Ellahi, and S. M. Sait. "Mathematical analysis of Maxwell fluid flow through a porous plate channel induced by a constantly accelerating or oscillating wall." Mat. 9, no. 1 (2021): 90